

ADDIS ABABA UNIVERSITY
ADDIS ABABA INSTITUTE OF TECHNOLOGY
SCHOOL OF CIVIL AND ENVIRONMENTAL
ENGINEERING



Analysis of Steel Frames Under Seismic Loads
Accounting for Imperfections

A Thesis in Structural Engineering

By Mekuriaw Mihrete

October 2019

Addis Ababa

A Thesis

Submitted in Partial Fulfillment of the Requirements for the Degree of Master of Science

UNDERTAKING

I certify that research work titled “**Analysis of Steel Frames Under Seismic Loads Accounting for Imperfections**” is my own work. The work has not been presented elsewhere for assessment. Where material has been used from other sources it has been properly acknowledged/referred.

Mekuriaw Mihrete

ABSTRACT

The study presented here is focused on the seismic analysis of moment-resisting steel frames accounting for imperfections. Geometrical and material nonlinear effects are considered in the modeling of steel frames. The objectives of this research are to identify the main parameters affecting the response of moment-resisting steel frames under seismic actions. The effects of modeling problems and their accuracy in analyzing isolated imperfect columns and a simple imperfect steel portal frame were also examined by varying the number of elements per member.

Two types of seismic analyses have been carried out by OpenSees for the steel frames considered in this research, these are nonlinear static and nonlinear dynamic analysis. Force-based distributed plasticity approaches were used for modeling of beam-column elements and fiber sections were assumed for modeling steel sections. Initial sway imperfections, residual stresses, and geometric nonlinear effects were considered for the global analysis of frames.

The effects of lateral load distributions on the results of nonlinear static analysis have also been investigated by considering three different patterns of lateral load distribution: linear, modal and triangular.

The results of the pushover analysis for the frames under consideration show that the lateral load distribution patterns have a greater effect than the magnitude of the loads applied to the structure. The effects of imperfections for moment-resisting sway frames are less than that of the second-order effects.

Three verification examples are performed to demonstrate the capability of the OpenSees program in solving nonlinear problems in comparison with experimental results. These examples were analyzed by both OpenSees and SeismoStruct and the results were presented against experimental results.

The second-order elastic analysis results for isolated columns show that the number of elements needed per member to model the cantilever column is lower than the pin ended column. A simple portal frame analyzed by modeling imperfections directly to the frame geometry and by replacing imperfections to equivalent lateral loads has no considerable difference between the results from these types of modeling imperfections.

ACKNOWLEDGMENTS

First and foremost, I would like to thank the Almighty God for being with me throughout the progress of this research.

My deepest gratitude shall be extended to my advisor Dr.-Ing. Bedilu Habte, for his unreserved guidance, support and continual supervision throughout the study. His guidance, motivation, and advice have been a great asset in my progress in writing this thesis.

I am also very grateful to my family, for their support, their advice and their patience throughout my years as a student at Addis Ababa institute of Technology (AAiT). I am also indebted to my friends and teachers who made these years at AAiT unforgettable.

I would also like to thank the Ethiopian Roads Authority (ERA) for sponsoring me to study this program at AAiT.

TABLE OF CONTENTS

UNDERTAKING	II
ABSTRACT.....	III
ACKNOWLEDGMENTS	IV
TABLE OF CONTENTS	V
LIST OF TABLES	VIII
LIST OF FIGURES	IX
LIST OF ABBREVIATIONS & SYMBOLS	XI
CHAPTER 1 INTRODUCTION	1
1.1 Background.....	1
1.2 Statement of the Problem.....	2
1.3 Significance of the Research	3
1.4 Objective of the Study	3
1.4.1 General Objective	3
1.4.2 Specific Objectives	3
1.5 Scope of the Study	3
1.6 Organization of the Thesis.....	4
CHAPTER 2 LITERATURE REVIEW	6
2.1 General.....	6
2.2 Literature Review	6
2.3 Code Provisions for Seismic Analysis of Steel Frames.....	11
2.3.1 Moment Resisting Steel Frames (MRFs)	13
2.4 Types of Seismic Analysis of Steel Frames	16
2.4.1 Linear Static Analysis.....	17
2.4.2 Nonlinear Static or Pushover Analysis	18
2.4.3 Non-Linear Dynamic or Nonlinear Time History Analysis	21
2.5 Imperfections in Steel Frames	22
2.5.1 Equivalent Sway Imperfections.....	24
2.5.2 Initial Bow Imperfections	26

2.5.3	Analytical Solutions of Initial Imperfections for Single Columns	29
2.5.4	Residual Stresses	31
2.5.5	Accidental Torsional Effects	32
CHAPTER 3	MATERIALS & ANALYSIS METHODS	33
3.1	General.....	33
3.2	Geometry of the Analyzed Frame.....	33
3.2.1	Loading Conditions	35
3.2.2	Characteristics of Selected Ground Motion Records.....	38
3.3	Analysis Methods	41
3.4	Description of SeismoStruct and OpenSees	41
3.4.1	Introduction to SeismoStruct	41
3.4.2	Introduction to OpenSees	42
3.5	Modeling and Analysis Procedures of the Frame by OpenSees.....	47
3.5.1	Definitions of the Material Model	47
3.5.2	Modeling of Sections	48
3.5.3	Modeling of Elements.....	50
3.5.4	Definition of Loads in OpenSees.....	53
3.5.5	Analysis Procedures.....	54
CHAPTER 4	RESULTS AND DISCUSSION	56
4.1	Verifications of Single Column Imperfections.....	56
4.2	Verification of Portal Frame Imperfections.....	58
4.3	Linear Elastic Analysis Results	60
4.4	Nonlinear Analysis Results of Frames	62
4.4.1	Pushover Analysis Results of Plane Frames.....	62
4.4.2	Pushover Analysis Results of 3D Frame	64
4.4.3	Imperfections and Second-order Effects in Pushover Analysis Results.....	65
4.4.4	Nonlinear Dynamic Analysis Results of Plane Frames.....	67
CHAPTER 5	CONCLUSIONS & RECOMMENDATIONS.....	73
5.1	Conclusions.....	73

5.2	Recommendations.....	74
REFERENCES	75
APPENDIX A TABLES AND EQUATIONS	79
APPENDIX B SOFTWARE VERIFICATION	81
APPENDIX C OPENSEES SCRIPT FOR PLANE FRAMES	85
APPENDIX D OPENSEES SCRIPT FOR SPACE FRAMES	103

LIST OF TABLES

Table 2-1 Behavior Factors for MRFs.....	12
Table 3-1 Sections Used for Modeling the Frame.....	33
Table 3-2 Characteristics Values of Vertical Permanent & Live Loads [24].....	35
Table 3-3 Seismic Weight of the Building	36
Table 3-4:Overstrength Factor for MRFs	38
Table 3-5 Characteristics of Selected Ground Motions.....	39
Table 3-6 Some of OpenSees Commands and Available Options[16].....	46
Table 4-1 Analysis Results for Cantilever Column.....	56
Table 4-2 Pin Ended Column	58
Table 4-3 Second-Order Elastic Analysis of Imperfect Portal Frame.....	59
Table 4-4 Fundamental Periods per Mode of Vibration.....	60
Table 4-5 Lateral Load Patterns for Plane Frames	61
Table 4-6 Distribution of Lateral Loads for 3D Frame	61
Table 4-7 Stability Coefficients in X direction.....	61
Table 4-8 Stability Coefficients in Y direction.....	61
Table 4-9 Equivalent Imperfection Loads Per Floor	62
Table 4-10 Maximum Roof Displacements for 2D Analysis	67
Table A--5-1: Recommended Values of Parameters for Type 1 Elastic Response Spectra [4].....	79
Table B-5-2 Material properties of Lehman et al.1998 column.....	81
Table B-5-3: Material Properties of Vecchio and Emara Frame.....	83
Table B-5-4 Elemental Forces	84
Table B-5-5 Nodal Displacements.....	84

LIST OF FIGURES

Figure 2-1: Plastic Hinge Behavior in MRFs	13
Figure 2-2: Lateral Load distribution patterns for pushover analysis.....	20
Figure 2-3: Initial sway imperfection for a cantilever column	25
Figure 2-4: Equivalent Sway Imperfections in Framed Structures	26
Figure 2-5: Replacement of Initial Sway Imperfections by Equivalent Lateral Loads	26
Figure 2-6: Replacement of Initial Bow Imperfections by Equivalent Lateral Loads	27
Figure 2-7: Classification of Imperfections.....	28
Figure 2-8: Axially loaded pin ended column with initial bow imperfection	29
Figure 2-9: Initial sway imperfection for a Cantilever Column	30
Figure 2-10: Portal frame with initial sway imperfection	31
Figure 2-11: Residual Stress Pattern Recommended by ECCS [29].....	32
Figure 3-1: Typical Plan of the building.....	34
Figure 3-2: Elevation of the frame in the x-direction	34
Figure 3-3: a) 3D Model of the Frame by SeismoStruct[35] b) Elevation in y.....	35
Figure 3-4: Elastic and Design Response Spectrum for Horizontal Component of Ground Motion.....	38
Figure 3-5: Original Accelerograms	40
Figure 3-6: Matched Accelerograms	40
Figure 3-7: The mean matched Spectrum and the Target Spectrum	41
Figure 3-8: The OpenSees Interface	43
Figure 3-9: Main Abstractions in OpenSees.....	43
Figure 3-10: OpenSees Software Packages for FEM Analysis [40].....	45
Figure 3-11: Stress-Strain Relationship of Steel01 in OpenSees	47
Figure 3-12: Hysteretic Behavior of Steel02 Material with Isotropic Hardening[39].....	48
Figure 3-13: Section Discretization	49
Figure 3-14: Notation on Quadrilateral Patch for Section Discretization[42].....	50
Figure 3-15: Distributed Plasticity Fiber Element.....	51
Figure 3-16: Local Coordinates for Beams and Columns	53
Figure 3-17: Flowchart for Frame Analysis	55
Figure 4-1: Geometry of Imperfect Cantilever Column	56
Figure 4-2: Axially Loaded Pin Ended Imperfect Column	57
Figure 4-3: Variation of Transversal Displacements for Pin Ended Column.....	58

Figure 4-4: Configuration of Typical Portal Frame.....	59
Figure 4-5: Second order Nonlinear Analysis of Imperfect Portal Frame.....	59
Figure 4-6: Effects of Lateral Load Patterns in Pushover X	63
Figure 4-7: Effects of Lateral Load Patterns in Pushover Y	63
Figure 4-8: Effects of Lateral Load Pattern on 3D Pushover X	64
Figure 4-9: Effects of Lateral Load pattern on 3D Pushover Y	64
Figure 4-10: Second order effects and Initial Imperfections on Plane Frame X direction	65
Figure 4-11: Second-Order Effects and Imperfections on Plane Frame Y Direction.....	65
Figure 4-12: Second-Order Effects and Imperfections for 3D Frame X direction.....	66
Figure 4-13: Second-Order Effects and Imperfections for 3D Frame Y direction.....	66
Figure 4-14: Displacement Responses of the Roof	70
Figure 4-15: Inter Story Drift Comparison	72
Figure B-5-1: Geometry and loading condition (a) section properties (b) of the column	81
Figure B-5-2: Force deformation relationship of the column tested by Lehman	82
Figure B-5-3: Details of Vecchio and Emara Frame[45]	83
Figure B-5-4: Base shear vs top story displacement of Vecchio & Emara Frame	83
Figure B-5-5: Geometry (a) Node & Element Assignments (b) of Portal Frame	84

List of Abbreviations & Symbols

List of Abbreviations

AISC	American Institute of Steel Construction
AMD	Approximate Minimum Degree ordering algorithm
ATC	Applied Technology Council
BFGS	Broyden-Fletcher-Goldfarb-Shanno
CBFs, EBFs	Concentrically Braced Frames, Eccentrically Braced Frames
DCH, DCM, DCL	Ductility Class High, Medium, Low
ES EN 2015	Ethiopian Standard Euro Norm 2015
FEMA	Federal Emergency Management Agency
IPE, HEM	Parallel flanges European I section, European H section
MDOF	Multi Degree of Freedom
MRFs	Moment Resisting Frames
OpenSees	Open Systems for earthquake engineering simulation
PEER	Pacific Earthquake Engineering Research
RCM	Reverse Cuthill-McKee
SDOF	Single Degree of Freedom
SLS	Serviceability Limit State
SPD	System Positive Definite
ULS	Ultimate Limit State

List of Symbols

E	Young's modulus or modulus of elasticity
G	Shear modulus or modulus of rigidity
ν	Poisson's ratio
f_y, f_u	Yield strength, ultimate strength of Steel
b, h	Width, depth of a cross-section
t_w, t_f	Thickness of web, thickness of flange
V_{Ed}	Design vertical load
N_{Ed}	Design value of the axial force
$M_{Ed,y}$	Design moment about the y-axis
$M_{Ed,z}$	Design moment about the z-axis
$N_{pl, Rd}$	Design plastic axial load resistance
$V_{pl, Rd}$	Design Shear resistance
$W_{el,y}$	Elastic section modulus about the major axis
$W_{pl,y}$	Plastic section modulus about the major axis
P_{cr}	Critical buckling load
$\bar{\lambda}$	Non-dimensional slenderness
q	Behavior factor
a_g	Ground acceleration
T_1	Fundamental period of the structure
A	Cross-sectional area

I_y	Moments of inertia (second moment of area) about the major axis
I_z	Moments of inertia (second moment of area) about the minor axis
L_{cr}	Critical buckling length
i	Radius of gyration
λ_l	Slenderness value to determine the relative slenderness
χ	Reduction factor for flexural buckling
η	Damping correction factor
α	Imperfection factor
ϕ	Global initial sway imperfection
ϕ_0	Basic value for global initial sway imperfection
α_h	Reduction factor for height h applicable to columns
α_m	Reduction factor for the number of columns in a row
m	Number of columns in a row
e_0	Maximum amplitude of a member imperfection
θ	Second-order sensitivity coefficient
ξ	Damping ratio
α_{cr}	Critical load ratio for imperfections
P- δ	Second order effect of members
P- Δ	Second order effect of the system

CHAPTER 1 INTRODUCTION

1.1 Background

The main goal of seismic analysis is to estimate the response of either new or existing structure against ground motions that might occur during its lifetime. The prediction of seismic forces induced by such ground motions will enable to prevent the structure from collapse. Over the last few decades, steel structures have gained more attention over reinforced concrete structures. The increase in demand for the construction of steel structures relies on environmental sustainability, associated with better strength and ductility characteristics, as well as more rapid construction processes. The use of steel structures for construction is proven to be more attractive and adequate characteristics from a seismic-resistant viewpoint [1, 2]. A steel frame of beams and columns is much more common nowadays. Great adaptability is possible, allowing this form of construction to be used ranging from small, simple low-rise buildings to much more complicated multistory buildings.

However, the use of ductile materials alone can give no guarantee for the ductile design of structures. Detail design procedures are required to exploit the capacity of materials and the sequence of local or global structural failures should be examined.

The damage levels observed in steel structures after the Northridge and Kobe earthquakes initiated the development of research studies and experimental campaigns targeting the improvement of standards and recommendations for the seismic design of steel structures [3]. Seismic design of steel structures has become an increasing research trend, particularly since the early 90's.

According to the new seismic design code [4], the purposes of earthquake-resistance design are: (a) to prevent non-structural damage in minor earthquakes, which may occur frequently in a lifetime. (b) to prevent structural damage and minimize non-structural damage in moderate earthquakes which may occur occasionally. (c) to prevent collapsing or serious damage in major earthquakes which may occur rarely. Designs are explicitly done only under the third condition.

Steel frames were previously designed to carry gravity loads, including those from the non-load bearing unreinforced masonry walls. Although engineers often instinctively relied on the stiff cladding to resist lateral loads, beams were connected to columns in a manner that allowed for the development of some frame action. Requirements for wind and earthquake design only became mandated decades later.

1.2 Statement of the Problem

The primary concern of earthquake-resistant design is to evaluate and protect either new or existing structures from brittle failures. The structure has to serve without significant damage throughout its design life. The seismic analysis and design of steel structures are less common than reinforced concrete structures in Ethiopia. Seismic analysis of steel structures has gained more attention over reinforced concrete structures due to their high strength to weight ratios and their high ductility which makes them to be preferred in high seismic zones.

In some building codes, first-order elastic analysis is done globally to determine internal member design forces and inelasticity is introduced through the interaction equations to check the strength of every member separately. The global analysis by considering material and geometric nonlinearities with imperfections can eliminate this shortcoming.

A review of previous literature shows that, even though there are some works devoted to the seismic design of plane steel frames using advanced analysis, there are no such works dealing with the case of space steel frames. In this research, finite element analysis of both two-dimensional and three-dimensional steel moment-resisting frames under seismic loads accounting for imperfections was carried out.

The effects of imperfections and their modeling strategies are less studied and subjected to research. The building codes provide different allowances to take into account these effects on the analysis of structures. For example, the steel design code [5] suggests the method of initial bow imperfections and the method of using European buckling curves for analysis of imperfections. The American steel design code specification [6] establishes the direct analysis method (DM) as the standard stability analysis and design procedure.

1.3 Significance of the Research

This thesis contributes to a better understanding of the seismic behavior of current code-based analysis and design of steel moment-resisting frames by incorporating geometric and material nonlinearities and unavoidable imperfections. The purpose of this investigation is to determine the effect of nonlinear material behavior, geometric imperfections and residual stresses on the structural resistance of hot-rolled sections by using the finite element method. This research contributes to initiate different analysts to study the behavior of steel structures under seismic loads. OpenSees scripts were provided for both 2D&3D frames so that interested readers can refer these files to develop their models.

1.4 Objective of the Study

1.4.1 General Objective

The main objective of this research is the finite-element analysis of moment-resisting steel frames accounting for geometric and material nonlinearities, initial geometric imperfections and residual stresses.

1.4.2 Specific Objectives

- Identify the main parameters affecting the response of moment-resisting steel frames under seismic actions.
- Evaluate the influence of modeling issues and their precision for seismic analysis of moment-resisting steel frames.
- The effect of imperfections (material & geometry) on the behavior of steel moment-resisting frames under seismic actions has been investigated.

1.5 Scope of the Study

To narrow down the focus area, limitations have been made on this thesis. This study is limited to regular steel MRFs subjected to seismic loads. Other types of steel frames such as concentrically braced and eccentrically braced steel frames are not considered in this research. The types of frames considered in the study are regular both in plan and in

elevation, with uniform mass and stiffness distribution throughout the height of the structure.

Three-dimensional effects, such as member out-of-plane and/or torsional imperfections, are not considered in this study.

In plastic analysis of structures, there are two types of modeling of elements. These are concentrated plasticity (plastic hinge) approach and distributed plasticity (plastic zone) approach. However, concentrated plasticity modeling of elements is not studied. The force-based distributed plasticity approach is only considered in this study.

All frames were modeled by using line elements through centerline dimensions. The modeling of beam-column connections or panel zones is outside of the scope of this research. Two types of geometric imperfections can be modeled in structural analysis. These are initial bow imperfection for individual members, and the initial sway imperfection for the whole structure. The effect of initial bow imperfections for MRFs is less as compared to initial sway imperfections. However, their effect can be taken into account by performing second-order analysis and through the individual member check after running second-order analysis. It is preferable to model out-of-plumbness, or frame non-verticality, by modification of the frame geometry; however, in orthogonal frames, imperfections may be modeled through the use of equivalent horizontal notional loads, proportional to the gravity load, applied at each story level[5]. The global sway imperfections were introduced by incorporating equivalent notional loads into the MRFs.

1.6 Organization of the Thesis

This thesis is divided into five chapters and organized as follows.

Chapter 1 deals with the introduction and general background of the study, statement of the problem and objectives of the research.

Chapter 2 Discusses on the literature review and basic principles of seismic analysis and design of steel frames. A review of literature which includes the reviews of selected previous works on seismic analysis of steel frames including the consideration of the stability analysis of frames, the effects of initial geometric imperfections in the design of frame structures is presented in this chapter.

Chapter 3 is concerned about the materials, analysis methods and the types of finite element programs that were used in the study. This chapter also contains some of the procedures to be followed for modeling steel frames by the finite element program OpenSees.

Chapter 4 Based on the studies presented in chapters 2 and 3, the study presented in this chapter is focused on the results of different analyses and their discussions.

Chapter 5 presents the conclusions of this research and recommendations on future researches.

The Appendix of this document contains some tables, equations, verification examples and OpenSees scripts for modeling of frames under consideration.

CHAPTER 2 LITERATURE REVIEW

2.1 General

To provide a thorough review of the literature related to modeling of steel structures by considering all parameters would be difficult to address in this section. A review of some of the previous studies on the modeling of steel frames is presented in this section. This literature review focuses on recent contributions related to seismic analysis of steel frames and addresses some of the previous efforts made on the modeling of structures that are most closely related to this research's need.

2.2 Literature Review

In order to determine the load-carrying capacity of an actual structure, it is necessary to take into consideration parameters that affect analysis results. The reliability of steel structures depends on the variance of input imperfections which influence the evaluation of limit states of building structures. Imperfections are practically unavoidable, and they represent acceptable construction tolerances. The role of imperfections in the study and design of frame structures with slender members has always been known, but the manner in which analytical models interpret their influence on structural behavior varies due to their random nature. The attainment of limit states is generally a random phenomenon that is examined with probabilistic theories and numerical computation models in the field of reliability.

Kala [7] has performed a sensitivity analysis of two portal frames and has compared the influence of individual initial imperfections on the load-carrying capacities of such frames. Results of the sensitivity analyses of the load-carrying capacities of both frames show that the influence of initial bow imperfections compared to the influence of the initial sway imperfections is very small.

Bernal [8] has studied two-dimensional moment-resisting frames and has drawn the following conclusions a) dynamic instability cannot be prevented merely by limiting the maximum elastic story drifts under design lateral loads. b) the intensity of ground motion required to induce instability is well correlated with the shape of the controlling failure mechanism [8]. Bernal also proposed a rational method for checking the safety against

dynamic instability of two-dimensional buildings. This method was based on ensuring that a building's base shear capacity adequately exceeds an 'instability threshold' that, in turn, depends on the shape of its controlling failure mechanism.

MacRae and Roberto modified Bernal's studies into a more complex hysteretic response and both supported his findings, in particular, that the use of lateral drift as the only measure of damage may not in all cases be appropriate [9] and [10]. Roberto pointed out that the rate of damage accumulation also contributes significantly to the computed response of a model structure, in addition to P- Δ effects. Therefore, models need to be used that explicitly consider the level of damage in determining a system's seismic response[10].

Roberto pointed out that the rate of damage accumulation also contributes significantly to a model structure's calculated response, in addition to P- Δ effects. Therefore, models need to be used that explicitly consider the level of damage in determining a system's seismic response.

Jovasevic [11] has studied the seismic behavior of 10 dual concentrically braced plane frames. He has performed nonlinear static and dynamic time-history analyses. He concluded that lateral resistance of Dual-CBFs is suddenly decreased when brace in compression buckles. This decrease is immediately followed by an increase of lateral stiffness [11]. He has tried to show that hazard level and height are the most important parameters in seismic demand of the structure.

For a better understanding of structural collapse, Ibarra & Krawinkler [12] develop a methodology for evaluating the global collapse of the structure by considering both the P- Δ effect and stiffness and strength deterioration of structural components. To implement their methodology, they developed a hysteretic model that was capable of capturing basic strength as well as cyclic deterioration based on rules proposed by Mohshen Rhnama & Krawinkler [13]. Next, they have verified their model against experimental results obtained from tests of steel, plywood, and reinforced concrete components and then employed these models to calculate collapse capacities of SDOF systems and MDOF frame structures. They identified the main parameters that mostly affect collapse and assessed the sensitivity of collapse capacity to these parameters. It was concluded that

deterioration is an overriding consideration in the seismic response analysis of a structure when the structure is near the limit state of collapse.

The work of Ibarra & Krawinkler has been further extended by Dimitrios Lignos [14] and has modified the proposed model by Ibarra & Krawinkler [12] to better approximate the observed experimental behavior of steel components deteriorating in a local or lateral-torsional buckling mode. In addition [14] has provided a large database in which the modified model by Ibarra & Krawinkler [12] was calibrated against experimental results from hundreds of steel wide flange beams and columns, steel tubular sections, and RC beams and columns. Based on the statistical information provided by Dimitrios, empirical equations were proposed that associate deterioration modeling parameters with geometric and material properties of beams and columns. To this end, experimental and analytical case studies were performed and a good agreement was achieved between analytical predictions and experimental results. Thus, it was concluded that the collapse capacity of structures can be predicted with adequate level of accuracy, provided that the deterioration characteristics of critical components are adequately represented in the analytical models [15].

Yen-Cheng (Arthur) Lu [16] has performed monotonic and cyclic analysis of steel plane frames with different strengths and axial load levels. He pointed out that for the first half cycle of loading, the effects of initial residual stresses on the behavior of plane steel structures is identical to monotonic loading. However, their impact decreased progressively and it disappeared after several displacement cycles.

Villavarde [17] has reviewed and discussed the methodologies that are currently available to assess the collapse capacities of structures subjected to seismic ground motions. He assessed many analytical studies and the collapse assessment methodologies were based on the information obtained from: a) SDOF models b) Nonlinear Static Procedure c) Step-by-Step Finite Element Analyses d) Incremental Dynamic Analyses. He concluded that the current collapse assessment methods are not entirely satisfactory for predicting the collapse behavior of structures and reliable experimental studies should, therefore, be carried out to verify analytical results.

More recently, researchers focused on developing relationships between a ground motion intensity measure (IM) and the likelihood of collapse, referred to as the collapse fragility

curve, and the relationship between the same ground motion IM and the seismic hazard for the building referred to as the seismic hazard curve [15].

Steel MRFs are highly dependent on ductile inelastic behavior for earthquake resistance and are hence drift-sensitive. The evaluation of the elastic buckling method in relation to MRFs is therefore expected to give a fair idea of the role that the Direct Method may play in the seismic design of ductile earthquake-resistant systems [15].

Shayan & Rasmusen studied how the strength of steel frames varies with the number and magnitudes of eigenmodes. Initial geometric imperfections affect the nonlinear behavior of structures and may have a considerable influence on the ultimate strength. Thus, imperfections have to be modeled as a linear combination of scaled eigenmodes [18].

Various failures of steel beam-to-column connections were found after the 1994 Northridge earthquake. This resulted in a multi-year, multi-million-dollar research effort funded by FEMA, known as the SAC joint venture. The failures caused the design of seismic-resistant steel moment connections to be fundamentally rethought [19]. The FEMA-SAC Steel Project was launched to examine damage to moment-resistant welded steel frame buildings and to improve repair methods and new design strategies to mitigate such damage in future earthquakes.

Lee & Fouch [20], [21] carried out a series of analytical studies to forecast the quality of existing pre-Northridge buildings, compare them with Post-Northridge buildings and evaluate new seismic development provisions. The basic approach they adopted in all these studies was to: a) evaluate maximum story drift capacity using Incremental Dynamic Analysis b) find statistical drift demands using nonlinear dynamic analysis for 20 ground motions. c) measure the level of confidence for the output goals of Collapse Prevention (CP) or Immediate Occupancy (IO) using Demand to Capacity Ratio (DCR) and other statistical parameters to compensate for the uncertainty associated with the analyses.

However, Lee & Fouch observed that all post-Northridge buildings, built in compliance with the 1997 NEHRP18 guidelines, had a high level of confidence (> 90 percent) in achieving the quality goals of collapse prevention (CP) or Immediate Occupancy (IO).

Norin Filip-Vacarescu, Aurel Stratan & Dan Dubina [22] have carried out an experimental study for the calibration and implementation of a numerical model to determine the

performance of concentrically braced frames equipped with strain hardening friction dampers in the braces based on experimental results. It was concluded that the presence of dampers is efficient in reducing the seismic response of a building for earthquakes characterized by short corner periods.

Mathur has studied MRFs, which exhibit a ductile behavior and a high level of system overstrength and he has observed that the incorporation of imperfections and residual stresses into the steel frame model has no significant difference on seismic responses, and their only effect was to cause the instability to occur slightly earlier [15].

He has shown that the effects of residual stresses and initial imperfections do not aggravate the effect that cyclic strength degradation has on seismic stability.

Cyclic strength degradation at connections has a much greater impact on the seismic stability behavior of steel moment-resisting frames than residual stresses and initial imperfections do. Axial-flexural interaction checks at design-level forces showed very little variation between calculations based on first-order elastic analysis with no stiffness reduction and second-order elastic analysis with stiffness reduction.

Henriksson & Panarelli have performed a study on an initial bow imperfection for flexural buckling of steel members to evaluate the accuracy of the method with an initial bow imperfection both analytically and numerically. For columns, when comparing the method with initial bow imperfection to the method using buckling curves, most results were on the safe side considering both strong and weak buckling direction. Though, there were deviating results for the plastic analysis of both I and H cross-sections in weak buckling direction, where the results were unfavorable [23]. They have also done an optimization between these deviations regarding elastic analysis.

2.3 Code Provisions for Seismic Analysis of Steel Frames

The seismic design methodology of the steel seismic code [4] is targeted at guaranteeing global ductile behavior by enforcing that the yield of the dissipative elements occurs before the remaining members' damage and premature failure, in accordance with an approach to capacity design.

With regard to its main considerations, the code prescribes a requirement for no-collapse (to prevent local or global collapse) and a requirement for damage limitation (to prevent excessive damage from low-intensity earthquakes), prescribing different probabilities of occurrence for the seismic action associated with each requirement. The seismic action is defined in the code by using an elastic response range, considering two types of spectrum (types 1 and 2, referring to a seismic event of magnitude higher and lower than 5.5 respectively).

The seismic action is defined in the code through the use of an elastic response spectrum, with two spectrum types being considered (types 1 and 2, referring to a seismic event higher and lower than 5.5 in magnitude, respectively). Applicable methods of elastic analysis (equivalent method of lateral force or method of modal response spectrum) and behavioral variables (reference values reduced values) are considered a function of regularity of height and schedule.

According to the new seismic code [4], there are two design concepts of earthquake-resistant steel buildings

- Low-dissipative structural behavior and
- Dissipative structural behavior.

In the case of low-dissipative behavior, the effects of the action can be measured on the basis of an elastic global model which neglects the non-linear behavior, because a low dissipative structure does not meet the requirements for applying a plastic design for primarily static loading, and the behavior factor q is less than 2. Structures designed according to this definition belong to the DCL (Ductility Class Low) low dissipative structural class.

On the other hand, the ability of parts of the structure (dissipative zones) to undergo plastic deformations in the event of an earthquake is taken into consideration for the dissipative structural behavior. The behavior factor q may exceed 2 and depends on the type of structural scheme that is seismic-resistant Structures designed according to this concept may belong to the DCM (Ductility Class Medium) medium structural ductility class or the DCH (Ductility Class High) high ductility class. Both groups relate directly to the structure's increased capacity to dissipate energy by inelastic behavior [24].

Two fundamental seismic design levels are considered in the code [4] namely collapse prevention and damage limitation which essentially refer to ultimate and serviceability limit states, respectively. Collapse prevention corresponds to seismic action based on a recommended probability of exceedance of 10% in 50 years, or return period of 475 years, whereas damage limitation relates to a recommended probability of 10% in 10 years or return period of 95 years. Steel buildings may fall into one of the following structural types based on the behavior of their primary resisting structure under seismic actions [4].

- MRFs, are those in which the horizontal forces are mainly resisted by members acting in an essentially flexural manner.
- CBFs, are those in which the horizontal forces are mainly resisted by members subjected to axial forces.
- EBFs, are those in which the horizontal forces are mainly resisted by axially loaded members, but where the eccentricity of the layout is such that energy can be dissipated in seismic links by means of either cyclic bending or cyclic shear.

Table 2-1 Behavior Factors for MRFs

Type	Ductility Class	q	q_d
Non-dissipative	DCL (detailed to EC3)	1.5-2.0	1.5-2.0
MRFs	DCM	4.0	4.0
	DCH	$5 a_u / a_1$	$5 a_u / a_1$

2.3.1 Moment Resisting Steel Frames (MRFs)

The design of MRFs is based on a weak beam-strong column principle that emphasizes plastic hinges are formed in beams rather than columns (Figure 2-1). If plastic hinges develop in the beams rather than in the columns, structural frames can dissipate a larger amount of hysteretic energy. This beam-sway mechanism increases overall seismic resistance and prevents a multistory frame from forming a soft-story mechanism (column sway). This provides favorable performance, compared to strong beam-weak column behavior through which significant deformation and second-order effects may arise in addition to the likelihood of premature story collapse mechanisms[24]. The exception to this requirement for weak beam-strong column behavior is at the base of the ground floor columns where plastic hinges can form when there is no significant risk of soft-story plastic mechanisms.

MRFs usually have high ductility as reflected in the high reference q assigned in the seismic code[4] due to the spread of plasticity through flexural plastic hinges. However, they are sensitive to drift due to their inherent low stiffness and therefore lateral deformation effects should be carefully considered.

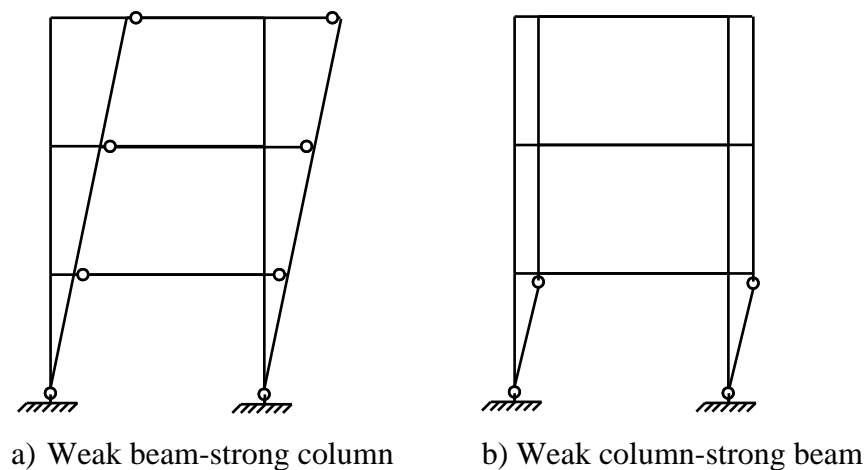


Figure 2-1: Plastic Hinge Behavior in MRFs

2.3.1.1 Capacity Design Requirements of MRFs

Typically, the 'weak beam-strong column' concept is needed, with plastic hinges at the base of the frame, at the top floor of multi-story frames and for single-story frames [4]. To obtain ductile plastic hinges in the beams, checks are made that the full plastic moment resistance and rotation is not reduced by coexisting compression and shear forces. To

satisfy this for each critical section, the applied moment (M_{Ed}) should not exceed the design plastic moment capacity, $M_{pl, Rd}$.

$$\frac{M_{Ed}}{M_{pl, Rd}} \leq 1.0 \quad (2-1)$$

The applied axial force N_{Ed} should not exceed 15% of the plastic axial capacity, $N_{pl, Rd}$.

$$\frac{N_{Ed}}{N_{pl, Rd}} \leq 0.15 \quad (2-2)$$

The shear force V_{Ed} due to the application of the plastic moments with opposite signs at the extremities of the beam should not exceed 50 percent of the design plastic shear resistance, $V_{pl, Rd}$ of the section

$$\frac{V_{Ed}}{V_{pl, Rd}} \leq 0.5 \quad (2-3)$$

in which $V_{Ed} = V_{Ed, G} + V_{Ed, M}$, where $V_{Ed, G}$ and $V_{Ed, M}$ are the shear forces due to the gravity and moment components on the beam, respectively.

According to Section 6.6.3 of [4], columns should be verified for the most unfavorable combination of bending moments M_{Ed} and axial forces N_{Ed} , based on the equation.

$$\begin{aligned} N_{Ed} &= N_{Ed, G} + 1.1 \times \gamma_{ov} \times \Omega \times N_{Ed, E} \\ M_{Ed} &= M_{Ed, G} + 1.1 \times \gamma_{ov} \times \Omega \times M_{Ed, E} \\ V_{Ed} &= V_{Ed, G} + 1.1 \times \gamma_{ov} \times \Omega \times V_{Ed, E} \end{aligned} \quad (2-4)$$

where Ω is the minimum overstrength in the connected beams ($\Omega_i = M_{pl, Rd} / M_{Ed, i}$).

The parameters $M_{Ed, G}$ and $M_{Ed, E}$ are the bending moments in the seismic design situation due to the gravity loads and lateral earthquake forces, respectively.

The most unfavorable shear force V_{Ed} of the column due to seismic combination actions must be less than 50 % of the ultimate shear resistance of the section. In columns where plastic hinges form, the resistance moment in those hinges shall be equal to $M_{pl, Rd}$. The beam overstrength parameter ($\Omega = M_{pl, Rd} / M_{Ed}$) as adopted in the code involves an approximation as it does not account accurately for the influence of gravity loads on the behavior [1].

Inelastic performance is integrated into the behavior factor for ultimate limit design, q to achieve a $S_{de}(T)$ acceleration model spectrum. To prevent inelastic or non-linear analysis,

linear spectral accelerations are typically separated by q , with the exception of some adjustment of $T < T_B$ to compensate for inherent properties, to minimize design forces.

2.3.1.2 Stability and Drift Considerations of MRFs

Deformation-related criteria are stipulated in the code for all building types but, as expected, due to their inherent flexibility, which often governs the design, they are particularly important in steel moment frames. The code stipulates two conditions relevant to deformation, namely ‘second-order effects’ and ‘inter-story drifts’ [4]. The former is associated with ultimate state whilst the latter is included as a damage limitation or serviceability condition. According to the code[4], if second-order (P- Δ) effects are not incorporated in the analysis, then they must be taken into account in the design process.

The code prescribes a simplified procedure to determine the sensitivity of the structure to P- Δ effects, by calculating a drift sensitivity coefficient, θ , for each story, as shown in Equation 2-6. Whilst the code does not allow θ to be higher than 0.3 which is the upper limit where instability is assumed to occur, if θ is lower than 0.1 then the influence of second-order effects can be ignored in the design, and if θ is between 0.1 and 0.2, then the influence of the P- Δ effects may be approximately accounted for by amplifying the seismic lateral forces by $\left(\frac{1}{1-\theta}\right)$. Second-order (P- Δ) effects are specified through an inter-story drift sensitivity coefficient (θ) given as follows [4].

$$\theta = \frac{P_{tot} d_r}{V_{tot} h} \quad (2-5)$$

Where P_{tot} and V_{tot} are the total cumulative gravity load and seismic shear, respectively, at the story under consideration; h is the story height and d_r is the design inter-story drift (product of elastic inter-story drift from analysis and q , i.e. $d_e \times q$).

For serviceability, d_r is limited in proportion to ‘ h ’ such that:

$$d_r \ v \leq \psi h \quad (2-6)$$

where ψ is suggested as 0.5%, 0.75% and 1% for brittle, ductile or non-interfering non-structural components, respectively, v is a reduction factor that accounts for the smaller more frequent earthquakes associated with serviceability, recommended as 0.4–0.5 depending on the importance class.

Evaluation of other codes, including US stipulations, suggests that drift-related requirements may be relatively more stringent or rigorous in the new seismic code[4], depending on the selected limit and the category of importance to be considered.

Consequently, direct application of the specific rules for moment frames in the code[4], followed by inter-story drift and second-order stability checks, often leads to a lateral overall capacity that is significantly different from that assumed in design. In particular, when large q factors are used and/or when the spectral design accelerations are not high, significant levels of lateral frame overstrength may be present. This overstrength is also a function of the design of gravity and spectral acceleration. Whereas the presence of overstrength reduces the ductility demand in dissipative zones, it also affects forces imposed on frame and foundation elements.

A rational application of capacity design necessitates a realistic assessment of lateral capacity after the satisfaction of all provisions, followed by a re-evaluation of global overstrength and the required q . Although high ' q ' factors are allowed for moment frames, in recognition of their ductility and energy dissipation capabilities, such a choice may in some cases be unnecessary and undesirable [1].

2.4 Types of Seismic Analysis of Steel Frames

In general, two types of analyses of structures are considered in seismic design these are: static and dynamic. The static analysis can further be divided into linear static and nonlinear static analysis. The dynamic analysis can also be subdivided into linear dynamic and nonlinear dynamic analysis. The linear static analysis is an approximation and simplification of the dynamic nature of the loads and it ignores the inelastic properties of materials. Therefore, the linear static analysis of structures for earthquake is less accurate than dynamic analysis because the nature of ground motion varies in time and cannot be predicted accurately as the ground motion may not be representative of the real behavior of the structure.

The linear dynamic analysis is not applied in this thesis and will therefore not be explained in this section.

2.4.1 Linear Static Analysis

Linear static analysis is the reference method to carry out structural analysis according to the new seismic code [4]. This type of analysis is based on decoupling the equations of motion of a dynamic multi-degree of freedom system or solving a system with N differential equations is replaced with solving N independent equations, which significantly simplifies the problem [24].

Decoupling the system of equations is possible due to the application of the principle of superposition of modal responses. Thus, to perform a modal response spectrum analysis it is necessary to determine the modes of vibration and the periods of vibration, solving the eigenvalue problem:

$$([k] - \omega_n^2 [m])\{\phi\}_n = \{0\} \quad (2-7)$$

where ω_n is the vibration circular frequency of mode “ n ”, and $\{\phi\}_n$ is the deformed shape in the “ n ” mode of vibration. Hence, for a structure having “ n ” dynamic degrees of freedom, “ n ” modes of vibration are determined. The fundamental mode of vibration corresponds to having the largest period of vibration T .

Although the modal response spectrum method is conventionally adopted in design, this type of analysis has two major limitations [24].

- The fact that the nature of the seismic action is dynamic action that varies in time. The results obtained using this method of analysis represent the envelope of response features namely, internal forces, displacements, etc., without providing any information about their time variation.
- The modal response spectrum method is elastic analyses. In reality, structures designed using the dissipative behavior principle should guarantee plastic ductile response under seismic action. However, the structural ductility is not directly checked, being fictitiously considered in a simplified manner through behavior factors q .
- The P- Δ effect cannot be explicitly accounted for in any linear method such as response spectrum method.

2.4.2 Nonlinear Static or Pushover Analysis

In the nonlinear static procedure, the structural model is subjected to an incremental lateral load whose distribution represents the inertia forces expected during ground shaking. The lateral load is applied until the imposed displacements reach the target displacement, which represents the displacement demand that the earthquake ground motions would impose on the structure. Once loaded to the target displacement, the demand parameters for the structural components are compared with the respective acceptance criteria for the desired performance state. System-level demand parameters, such as story drifts and base shears, may also be checked. The nonlinear static procedure is applicable to low-rise regular buildings, where the response is dominated by the fundamental sway mode of vibration. It is less suitable for taller, slender, or irregular buildings, where multiple vibration modes affect the behavior[25].

The concern of modern earthquake engineering aspect is the determination of the seismic performance of a structure after the first yielding. Static pushover analysis can provide an insight into the seismic structural demand imposed by the design ground motion, and can indicate the weak links, failure modes as well as the post-yield performance of the structure[26]. The pushover analysis is a static non-linear analysis under permanent vertical loads and gradually increasing lateral loads, which should approximately represent the earthquake-induced forces. It accounts for the plastic behavior of structural elements and geometrical nonlinearity occurring under seismic action.

Based on the nature of loads applied to the structure pushover analysis can be divided into;

- a) Monotonic Pushover Analysis; gradually increasing lateral loads with constant gravity loads.
- b) Cyclic pushover Analysis; reversal cyclic loading because the ground motion imposed into the structure is somewhat cyclic in nature.

The monotonic pushover analysis was carried out in this research

Based on the pattern of lateral loads, pushover analysis can be divided into Conventional, Modal, and Adaptive.

Conventional Pushover Analysis; load pattern based on the assumption that the structural response of a multi-degrees-of-freedom system can be represented as an equivalent single-

degree-of-freedom system, implying that the response can be calculated by a single vibration mode, and the shape (ϕ_n) of this mode remains constant throughout. The uniform load and inverted triangular load patterns can be the example of conventional load pattern. The frames analyzed in this research are regular where the seismic response is dominated by the first mode and conventional pushover analysis was therefore carried out.

Modal Pushover Analysis; When the seismic response is dominated by more than a single mode vibration, higher-order mode effects should be accounted for in the load pattern.

Adaptive Pushover Analysis; Note that the stiffness of a structure varies with its deformation level due to plasticity development and/or geometric non-linearity. A constant mode shape assumed by either the conventional pushover analysis or MPA cannot account for the influence due to this change. Based on the mode shapes and modal participation factors in each loading step of a pushover analysis, a more recent pushover analysis method proposes updating the load pattern in each loading step, leading to adaptive pushover analysis [27]. In adaptive pushover analysis, after defining an initial load vector, a looping is performed to compute the updated load pattern vector shape in each step of load or displacement increment. This implies that in each step of the increment, it is required to perform an eigenvalue analysis to obtain the mode shape(s) and the modal participation factor(s) based on the stiffness of the target structure at that load or displacement increment level [26].

2.4.2.1 Lateral Load Distribution for Non-Linear Static Analysis

The analysis results are sensitive to the selection of the control node and selection of lateral load pattern. The lateral load and its distribution patterns along the height of the structure should be determined before the stiffness and resistance design of a steel frame is performed. The calculation of base shear is carried out by selecting different base shear force coefficients for each model. To distribute shear forces in the elevation, the seismic design code [4] suggests two different patterns namely, load distribution proportional to mass (uniform pattern) and load distribution based on the first mode shape of the structure (modal pattern). Uniform load distribution, triangular load distribution (based on the height of the structure) and modal distribution were used in this research for pushover analysis, and the results of each distributions were compared.

- Uniform Lateral Load Pattern: The lateral force at any story is proportional to the mass at that story irrespective of its height.
- Triangular Lateral Load Pattern: The lateral load coefficients can be obtained by proportioning the height of the structure. The lateral load distribution coefficient, ϕ at any story i can be given as

$$\phi_i = \frac{h_i}{h} \quad (2-8)$$

Where h_i is the height of story i and h is the total height of the building.

- Modal Distribution of Lateral Loads: The lateral force at any story is proportional to the product of the amplitude of the elastic first mode and mass at that story

According to the steel design manual [24], for all triangular, uniform and modal cases, the lateral force distribution can be given as

$$F_i = m_i \phi_i \quad (2-9)$$

Where F_i and m_i are the lateral force and mass at story i , respectively, and ϕ_i is the amplitude of the normalized displacement for the elastic first mode at story i .

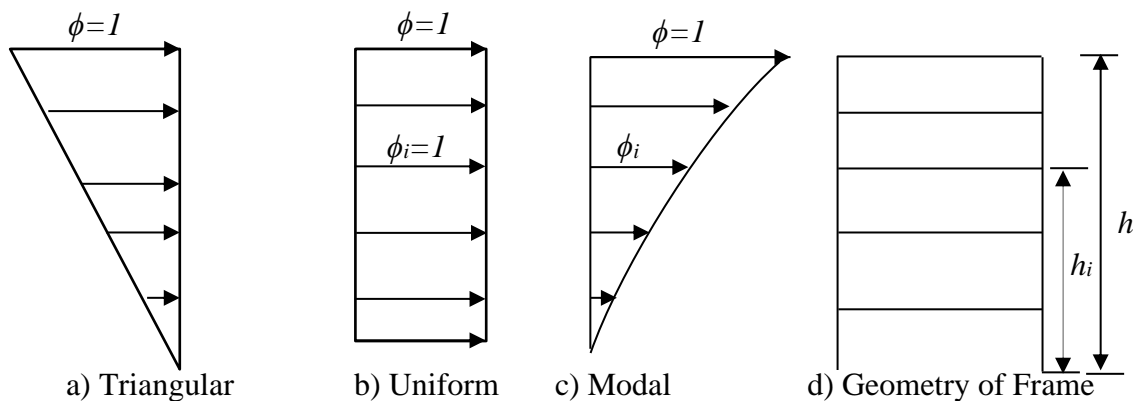


Figure 2-2: Lateral Load distribution patterns for pushover analysis

2.4.2.2 Target Displacement

ES EN 1998-1 [4] defines the target displacement as the seismic design displacement taken from the elastic response spectrum when considering an equivalent SDOF-system, i.e. an equivalent force-displacement relationship with a corresponding mass m^* . The method, as presented in the design code is also known as the N2-method developed at the

University of Ljubljana. The force F^* and displacement d^* of the equivalent system are determined by a transformation factor Γ .

$$m^* = m_i \times \Phi_i \quad (2-10)$$

$$\Gamma = \frac{m^*}{\sum (m_i \times \Phi_i^2)} \quad (2-11)$$

$$F^* = \frac{F_b}{\Gamma} \quad (2-12)$$

$$d^* = \frac{d_n}{\Gamma} \quad (2-13)$$

Where m_i is the lumped story mass, Φ_i is the normalized value of the mode shape at story i , F_b is the base shear force and d_n is the real displacement.

2.4.3 Non-Linear Dynamic or Nonlinear Time History Analysis

The nonlinear time history analysis (NTHA) method consists of applying spectrum compatible ground motions (natural or generated) to the structural model. If three ground motions are used, then the maximum value of the response quantities (forces, displacements, deformations, drifts, etc.) are used. If a minimum of seven ground motions are used, then the average response is used. The most important input parameters for the selection of the ground motion are the epicentral distance, the magnitude and the type of soil.

The main advantage of the NTHA method is that the structural model accurately simulates the damage pattern of the structure. The type of plastic mechanism (either partial or global) can be checked and directly measured, namely by monitoring if non-dissipative structural elements experience some plastic deformation, and comparing plastic deformation demand with the capacity for the dissipative elements allow [24].

2.4.3.1 Ground Motion Selection

According to the new code [4], different criteria have been established on the selection and scaling of ground motion records for the seismic analysis of buildings. The code stipulates that a minimum of three ground motion records should be used for a given group. In such a case, the structural response estimates should be taken based on the most unfavorable value observed for all the ground motions considered. However, if the suite

of earthquake records is composed of at least seven records, the structural response estimates can be considered to be equal to the average of the structural response quantities.

Additionally, the code prescribes that the mean of the zero-period spectral response acceleration values calculated from the individual time histories should not be smaller than the value of $\alpha_g S$ for the site under study, α_g being the design ground acceleration on rock and S the soil parameter.

Furthermore, in the range of periods between $0.2T_1$ and $2.0T_1$, where T_1 is the fundamental period of the structure in the direction in which the record will be applied, no value of the mean 5% damping elastic spectrum (calculated from the average between the response spectra of the considered ground motions), should be less than 90% of the corresponding value of the targeted 5% damping elastic response spectrum. Finally, the code establishes that, for 3D structural analysis, the seismic motion shall consist of three simultaneously acting ground motion records (two horizontal and one vertical earthquake directions). Moreover, the same ground motion record cannot be used simultaneously along both horizontal directions.

2.5 Imperfections in Steel Frames

Initial Imperfections are an unavoidable deviation from perfect geometry which is within the accepted practical tolerance of the particular applicable fabrication technology: for example, initial out-of-straightness (crookedness) of a member, initial out-of-plumb of a story, initial out-of-flatness of a plate, or initial denting or bulging of a shell. Imperfections of steel frames shall be accounted for the global analysis of structures[28].

In steel structures, irrespective of the care taken in their execution, there are always imperfections, such as lack of verticality and lack of linearity in members, residual stresses, eccentricities in joints, eccentricities of load, (clause 5.3.1(1))[29].

Actual steel structures have for several reasons geometric and structural imperfections. Geometric imperfections are due to both fabrication and erection, structural imperfections are due to fabrication errors e.g. welding or cold forming.

Accordingly, there are deviations between the nominal and the actual geometry of the structure as well as residual stresses in the material. These imperfections are responsible

for the introduction of additional secondary forces that must be taken into account in the global analysis and in the design of the structural elements. The influence of imperfections is generally eroding the carrying capacity of structures and should be considered in analysis. Geometrical imperfections are distinguished in two types, sway imperfections and bow imperfections.

Sway imperfections are considered in frame analysis, while bow imperfections are considered in individual columns, trusses or similar members. The two types of geometrical imperfections, as well as their magnitudes according to the steel building code[5], are illustrated in figures 2-5 and 2-6.

Sway imperfections may be ignored when the design horizontal forces are high due to the fact that the building must be provided with sufficient stiffness and strength to resist the horizontal loads. To restore equilibrium, equivalent forces must be also set in the supports. Sway imperfections must be always included in frame analysis unless the horizontal design forces are higher than 15% of the vertical one so that the effects of such imperfections are small. This is the case of frames subjected to high wind or seismic forces.

The type and amplitude of all imperfections are bounded by the tolerances specified in the building code standards. According to the steel design code[5], the imperfections should be incorporated in the analysis preferably in the form of equivalent geometric imperfections that include all imperfections (residual stresses, etc.) exclusively as geometrical imperfections, with values which reflect the possible effects of all types of imperfections (clause 5.3.1(2))[5]. Unless these effects are already included in the resistance formulae for member design, the following imperfections should be taken into account: i) global imperfections of the frame and ii) local imperfections of the members (clause 5.3.1(3))[5].

Imperfections for global analysis should be considered with the shape and direction that lead to the most adverse effects. So, the assumed shape of global and local imperfections may be derived from the elastic buckling mode of a structure in the plane of buckling considered (clauses 5.3.2(1)). Account should be taken of both in-plane and out-of-plane buckling including torsional buckling with symmetric and asymmetric buckling shapes (clause 5.3.2(2)).

For frames sensitive to buckling in a sway mode, the effect of imperfections should be allowed for in frame analysis by an equivalent imperfection in the form of an initial sway imperfection and individual bow imperfections of the members (clause 5.3.2(3)). The global initial sway imperfection corresponds to a lack of verticality of the structure, defined by an angle ϕ , given by (clause 5.3.2(3)a).

2.5.1 Equivalent Sway Imperfections

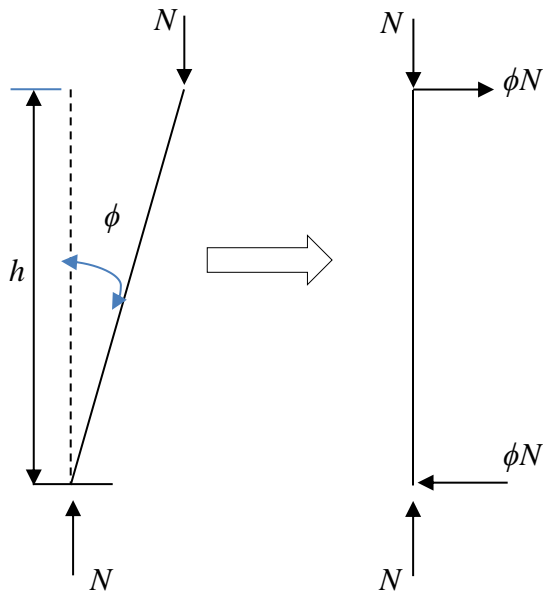
Structural system imperfections can be caused in different ways such as variability in the lengths of framing members, lack of verticality of columns and of horizontality of beams, errors in the location of foundations, errors in the placement of the connections and so on.

To simplify the modeling of imperfections, consider a cantilever column of height h with an out-of-plumb imperfection and subject to a vertical force N at the top (Figure 2-3). The additional bending moment M due to the lack of verticality, expressed by angle ϕ can be approximated at the fixed end as:

$$M = N[h \cdot \tan(\phi)] \quad (2-14)$$

Within the small displacement hypothesis (for small-angle ϕ , $\tan(\phi) = \phi$), the effect of this imperfection can be assimilated to that of a fictitious horizontal force F acting at the top of the column and causing the same bending moment at the base of the column. The magnitude of F is thus given by:

$$F = \frac{M}{h} = N\phi \quad (2-15)$$



a) Imperfect column b) Horizontal equivalent force

Figure 2-3: Initial sway imperfection for a cantilever column

Where the out of plumb angle ϕ can be determined from the following formula[5].

$$\phi = \phi_0 \alpha_h \alpha_m \quad (2-16)$$

Where ϕ_0 is the basic value: $\phi_0 = 1/200$, α_h is the reduction factor for height h applicable to columns and is given by

$$\alpha_h = \frac{2}{\sqrt{h}} \text{ but } \frac{2}{3} \leq \alpha_h \leq 1 \quad (2-17)$$

α_m is the reduction factor for the number of columns in a row and it is given by

$$\alpha_m = \sqrt{0.5 \left(1 + \frac{1}{m} \right)} \quad (2-18)$$

m is the number of columns in a row

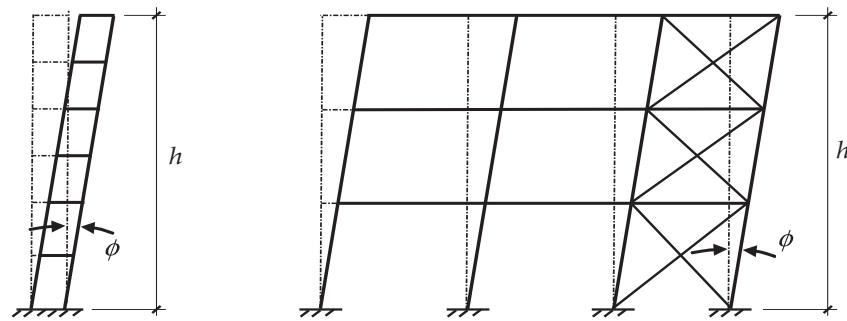


Figure 2-4: Equivalent Sway Imperfections in Framed Structures

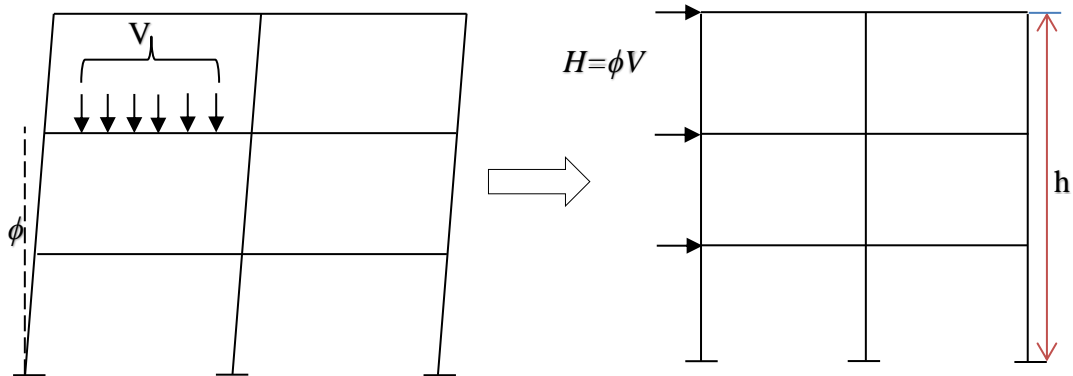


Figure 2-5: Replacement of Initial Sway Imperfections by Equivalent Lateral Loads

2.5.2 Initial Bow Imperfections

The initial out-of-straightness can be considered by means of a system of equivalent horizontal forces. Defining v_0 as the maximum out of straightness imperfection with respect to the ideal configuration, it is possible to obtain a system of uniformly distributed loads of a magnitude $8Nv_0/L^2$ that can generate a maximum bending moment equal to the moment that would be caused by imperfections in the presence of axial forces N . Relative initial local bow imperfections of members for flexural buckling is v_0/L where L is the member length.

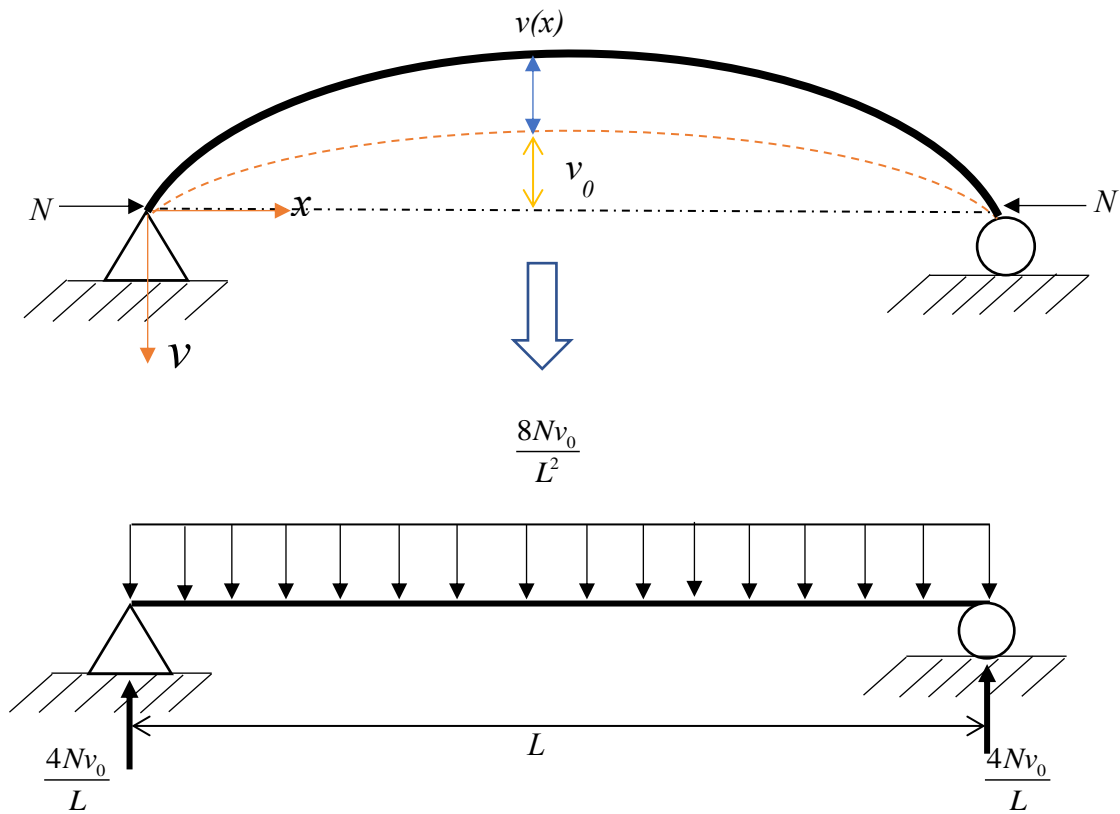


Figure 2-6: Replacement of Initial Bow Imperfections by Equivalent Lateral Loads

The value of $\frac{v_0}{L}$ can be taken from table 5.1 of the code [5] depending on the relevant buckling curve number and the type of analysis to be carried out. According to the code, the effects of initial out of straightness imperfections can be neglected if large lateral forces are applied to the structural system, for compression members in sway frames, the effects of imperfections can be neglected if:

$$N < 0.25N_{cr} \quad \text{or} \quad \bar{\lambda} < 0.5\sqrt{\frac{Af_y}{N}} \quad (2-19)$$

Where N is the axial force acting on the element and N_{cr} is the critical elastic buckling load for the member.

However, members for which inequality (2-19) is not satisfied shall be provided with bow imperfections.

The application of imperfections to the three-dimensional frames should be done independently, not simultaneously.

For practical members, initial bow and residual stress are unavoidable and must be considered in the buckling strength determination. The equivalent imperfection for these two sources of imperfections is given in the new steel code [5] they are called equivalent imperfections because value of these imperfections cannot be measured from the initial bow or crookedness of the member but it can be determined by a curve-fitting procedure against the buckling strength vs. slenderness curve. In other words, we can try different values of imperfections to obtain a curve giving a 5% lower bound curve to the experimental curve. We can calculate the imperfection using the available Perry Robertson constants. Generally, imperfections can be broadly categorized into mechanical, geometrical and material as shown in the chart below.

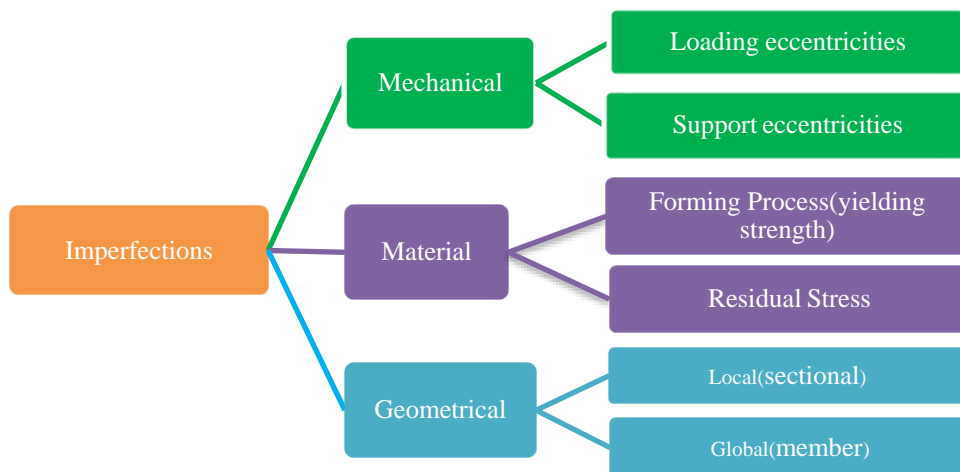


Figure 2-7: Classification of Imperfections

The material and geometrical imperfections were considered in this research, there are a number of approaches to consider the effects of geometric imperfections in advanced analysis of steel frames. The common approaches include: scaling of elastic buckling mode (EBM), equivalent horizontal forces method, reduction of member stiffness, and the direct modeling of initial geometric imperfections. The shape and magnitude of geometric imperfections may have a significant influence on the response of a structure, and hence need to be modeled accurately when determining the load-carrying capacity of a steel frame by advanced structural analysis.

2.5.3 Analytical Solutions of Initial Imperfections for Single Columns

Case a) Pin ended Column: Consider an axially loaded pin ended column with an initial bow imperfection of v_0 shaped as half-sine wave to determine the effect of initial geometrical imperfections (Figure 2-8).

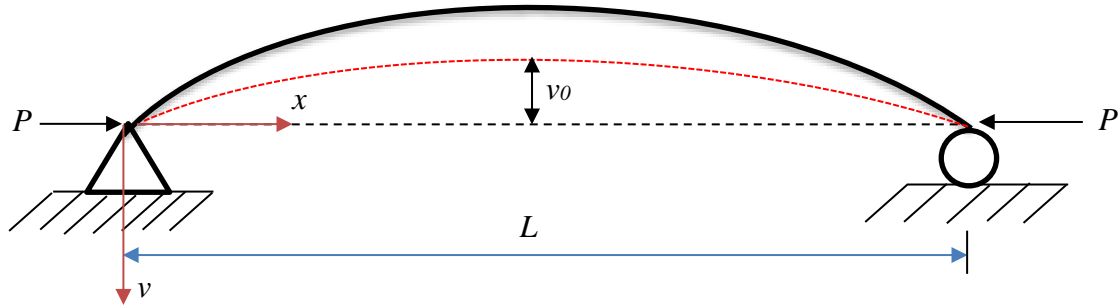


Figure 2-8: Axially loaded pin ended column with initial bow imperfection

The exact solution of the second-order moment and transversal displacement as a function of longitudinal distance x presented by [30] is given in the following equations.

$$M_{int} = -EI \frac{d^2v}{dx^2}, M_{ext} = P(v_i + v) \quad (2-20)$$

$$EI \frac{d^2v}{dx^2} + Pv = -Pv_i$$

$$v_i = v_0 \sin\left(\frac{\pi x}{L}\right) \quad (2-21)$$

After substitution and some rearrangement, the solution of the above ordinary differential equation becomes,

$$v = \frac{P}{P_{cr} - P} v_0 \sin\left(\frac{\pi x}{L}\right) \quad (2-22)$$

$$\text{where } P_{cr} = \frac{\pi^2 EI}{L^2}$$

The maximum total deflection at the middle of the column (at $x=L/2$) becomes then equal to

$$v_{tot} = v_i + v = \frac{P_{cr}}{P_{cr} - P} v_0 \quad (2-23)$$

$$M_{max} = v_{tot} \cdot P = \frac{P_{cr}}{P_{cr} - P} v_0 \cdot P \quad (2-24)$$

Case b) Cantilever Column: Figure 2-9 shows the cantilever column with initial sway imperfection v_0 subjected to axial load P and transversal load H at its free end.

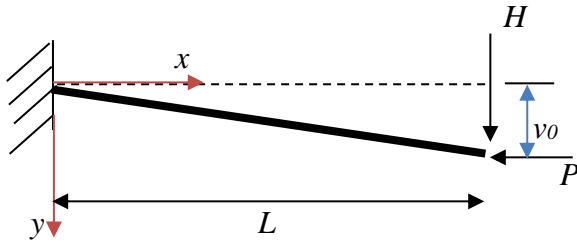


Figure 2-9: Initial sway imperfection for a Cantilever Column

Analytical solutions show that the maximum deflection occurs at the free end and the maximum moment occurs at the support [31].

$$y_{\max} = \left(v_0 + \frac{HL^3}{k^2 EI} \right) \left(\frac{\tan k}{k} - 1 \right) \quad (2-25)$$

$$M_{\max} = \frac{\tan k}{k} (HL + Pv_0) \quad (2-26)$$

Where k and v_0 are given as follows

$$k = \sqrt{\frac{PL^2}{EI}} \quad (2-27)$$

$$v_0 = \frac{L}{200}$$

For the case of sway frames, consider a portal frame with initial sway imperfection ($\phi=h/200$) and subjected to static loads as shown in (Figure 2-10).

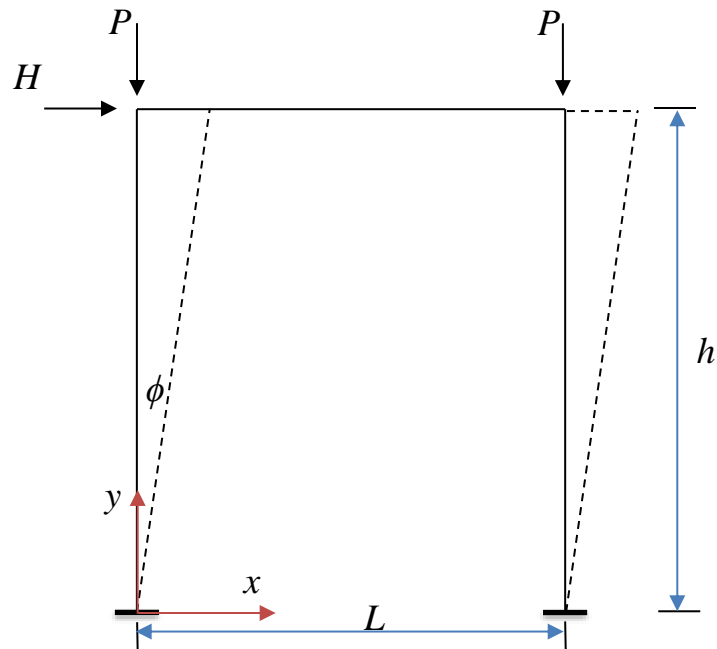


Figure 2-10: Portal frame with initial sway imperfection

The portal frame shown in Figure 2-10 is subjected to lateral load H and two concentrated downward loads P . The initial sway imperfection was considered as $h/200$ and this imperfection was applied to the frame into two different ways: This can be done either by modeling directly or by converting into an equivalent horizontal load applied at the top left end of the frame. The results for a given value of the loads, P & H and the frame geometry are presented in chapter 4.

2.5.4 Residual Stresses

In hot-rolled steel sections, residual stress exists as a result of uneven cooling rate after the rolling process creates a set of self-equilibrating initial stresses in the cross-section [32]. The faster cooling regions of the section, such as the flange tips are left in residual compression and the thicker, slower cooling regions, such as the corners are left in residual tension. Numerous researchers have studied the appropriate distribution of residual stress for I or H sections. However, many researchers used residual stress pattern recommended by [24]. Residual stresses develop due to differential cooling after hot rolling and any other kind of process involving heat (like welding and flame cutting, for example), shearing and cold forming and cold bending; despite being a self-equilibrated system, as illustrated in Figure 8 [33]. For an I section, these stresses change the load-deformation relationship for the cross-section as a whole.

The magnitude and distribution of residual stresses in a section not only depends on the type of manufacturing process (for example hot-rolled, welded or cold-formed sections), but also on the type of cross-section, the thickness of the section, cooling conditions, rolling temperature, straightening method, and steel properties. It is time-consuming and impractical to incorporate the exact residual stress distribution for all members into the analysis [34].

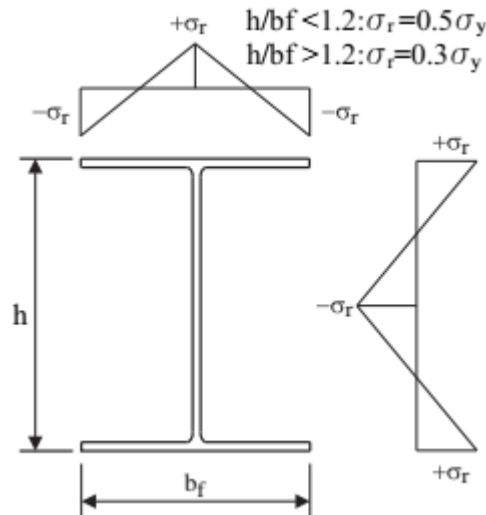


Figure 2-11: Residual Stress Pattern Recommended by ECCS [29]

2.5.5 Accidental Torsional Effects

In order to cover uncertainties in the location of masses and in the spatial variation of seismic motion the mass location will be displaced from the geometric mass center (K) by an accidental eccentricity, e_{ai} (Clause 4.3.2(1)P[4]).

$e_{ai} = +0.05L_i$ where L_i is the floor-dimension perpendicular to the direction of the seismic action of the i th floor.

The code gives guidelines for the effects of torsion. For structures with symmetrically distributed mass and stiffness that are modeled in two dimensions, the effects from accidental torsion are safeguarded by multiplying the acting design forces with a factor [4].

$$\delta = 1 + 1.2 \frac{X}{L_e} \quad (2-28)$$

where X is the distance from the mass center to the element in question, measured horizontally, and L_e is the distance between the two elements that resist horizontal forces and are the farthest from each other.

CHAPTER 3 MATERIALS & ANALYSIS METHODS

3.1 General

The material used in this study was structural steel S235 with a young's modulus corresponding to 210GPa. An average yield strength of 235 MPa and an ultimate strength of 360 MPa were assumed for this material (Table 3.1 of the code[5]) The partial factors for resistance of cross-sections and members were taken as $\gamma_{mo}=1$, $\gamma_{m1}=1$, $\gamma_{m2}=1.25$ and $\gamma_{ov}=1.25$. The finite element programs Opensees and SeismoStruct[35] were used for modeling the frame. The material inelasticity is distributed along the entire structural elements for both software. A lumped mass modeling strategy was adopted, in which masses were lumped at the nodal points according to its tributary area.

3.2 Geometry of the Analyzed Frame

The building under consideration is taken from [24] and is a six-story office building with a rectangular plan layout and an area of 31x24 m. The height of the first story is 4m and the height of other stories is 3.5m each (Figure 3-1). The columns are assumed as fixed on the ground.

European steel profiles were used for modeling the steel frame. HE sections were adopted for the columns and IPE sections were used for the beams. The choice of sections was mainly conditioned by the need to satisfy stability and drift limits.

Table 3-1 Sections Used for Modeling the Frame

Story	X-direction			Y- Direction	
	ExtCol	IntCol	All Beams	Beam on bays 2 and 3	Beam on bays 1and 4
6	HE600M	HE700M	IPE550	IPE550	IPE330
5	HE600M	HE700M	IPE550	IPE550	IPE330
4	HE600M	HE700M	IPE600	IPE600	IPE330
3	HE600M	HE700M	IPE600	IPE600	IPE330
2	HE600M	HE700M	IPE750x196	IPE750x196	IPE330
1	HE600M	HE700M	IPE750x196	IPE750x196	IPE330

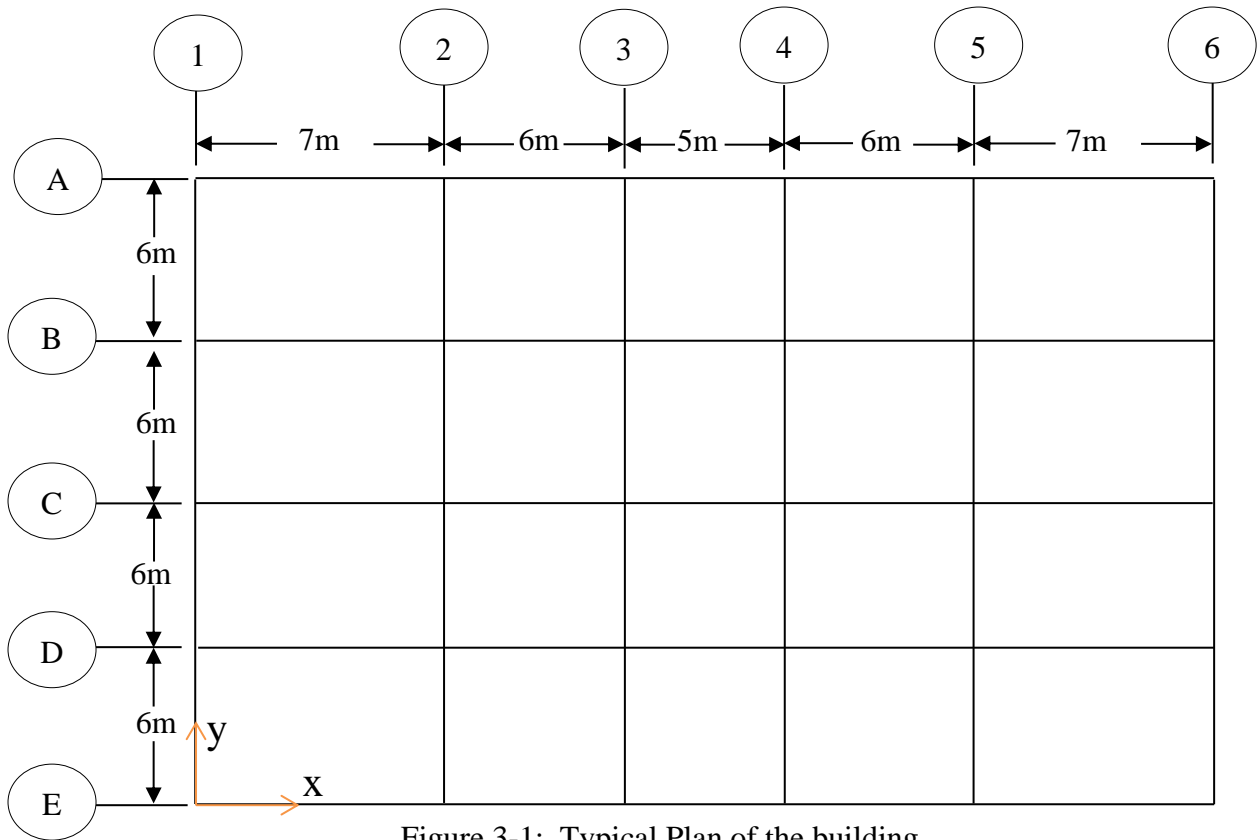


Figure 3-1: Typical Plan of the building

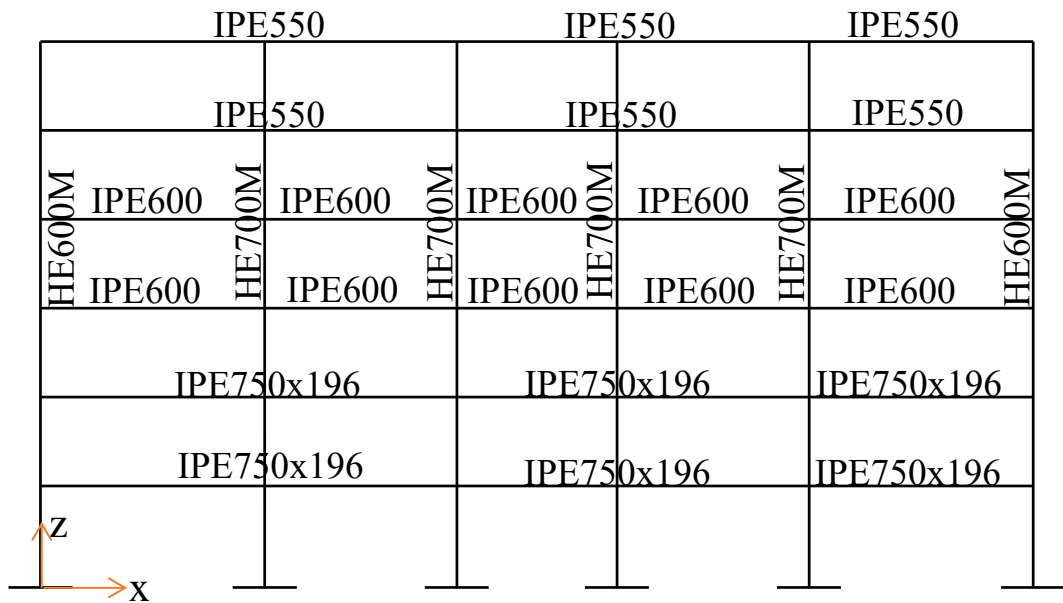


Figure 3-2: Elevation of the frame in the x-direction

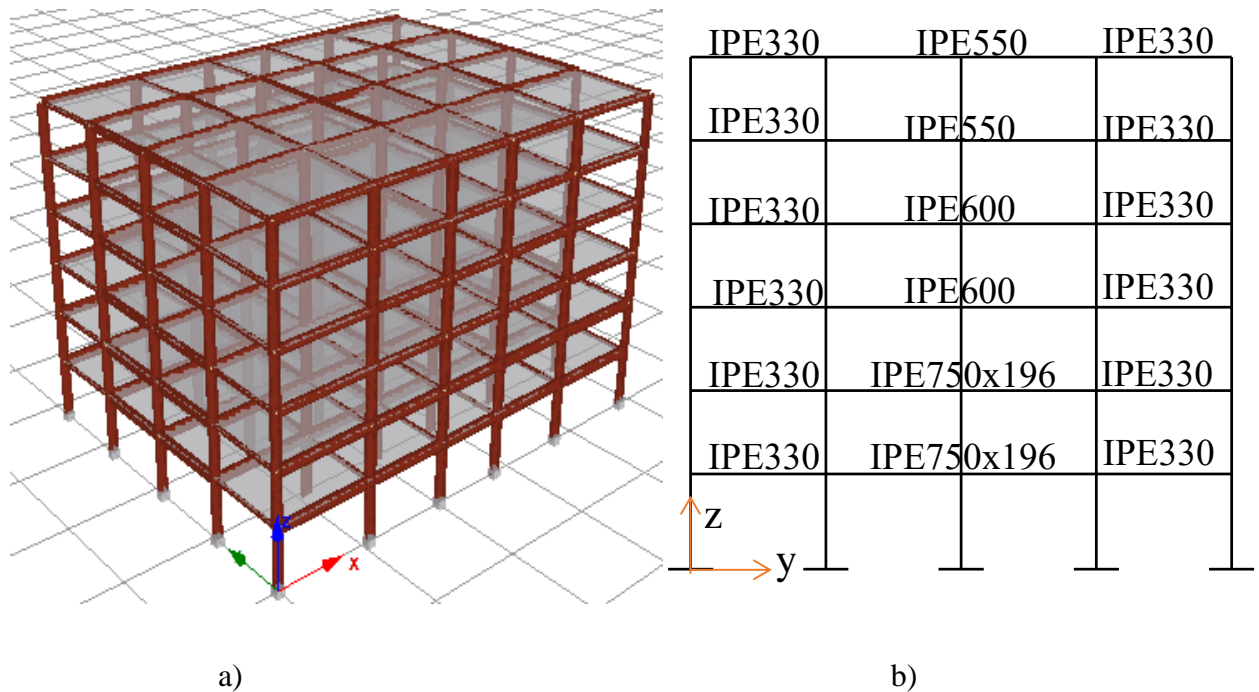


Figure 3-3: a) 3D Model of the Frame by SeismoStruct[35] b) Elevation in y

3.2.1 Loading Conditions

3.2.1.1 Gravity Load

The characteristic values of both permanent (G_k) and variable actions (Q_k), corresponding to office building Category B according to the new EBCS code [36] are given in(Table 3-2). The value for the slab weight includes the self-weight of profile steel sheeting, infill concrete, finishing floor elements and partition walls. Similarly, the weight of the stairwells includes the contribution of the flights, steps, and landings [24].

Table 3-2 Characteristics Values of Vertical Permanent & Live Loads [24]

Part	$G_k(kN/m^2)$	$Q_k(kN/m^2)$
Storey Slab	4.2	2
Roof Slab	3.6	0.5
Stairs	1.68	4
Claddings	2	-

The following load combinations are used to determine action effects [24].

$$\sum_{j \geq 1} G_{k,j} + A_{Ed} + \sum_{j \geq 1} \psi_{2,i} Q_{k,i} \quad (3-1)$$

$$\psi_{E,i} = \phi \cdot \psi_{2,i} \quad (3-2)$$

$$\psi_{E,i} = \phi \cdot \psi_{2,I} \quad (3-3)$$

Where $G_{k,j}$ is the characteristic value of permanent action j (the self-weight and all other dead loads), A_{Ed} is the design seismic action (corresponding to the reference return period multiplied by the importance factor).

Table 3-3 Seismic Weight of the Building

	Dead Load	Imposed Load	Seismic Mass
Story	Gk(kN)	Qk(kN)	(Tonnes)
6	3256.2	1356	365.1
5	3775.1	1608	409.41
4	3816.86	1608	413.67
3	3816.86	1608	413.67
2	4000.1	1608	432.34
1	4059.1	1608	438.36

3.2.1.2 Imperfection Loading

As it has already been discussed in chapter 2 frame imperfections can be due to material or geometry. Material imperfections have been considered by modeling the nonlinear material behavior associated with the profile dependent residual stresses.

Geometric imperfections (initial bow imperfections and initial sway imperfections) as their name implies are caused by the geometry of the structure. To include the effects of initial imperfections in structure analysis, they can be modeled directly. This can become difficult for structures of any significant size and/or complexity, and require several separate models to capture the most destabilizing effect on the structure. Initial bow imperfections are not explicitly modeled in this thesis but they are indirectly accounted for by performing second-order nonlinear analysis.

According to clause 5.3.2(4) of[5], the effects of global imperfections for buildings sensitive to buckling in a sway mode can be disregarded if the following condition is satisfied:

$$H_{Ed} \geq 0.15V_{Ed} \quad (3-4)$$

where H_{Ed} is the design value of the horizontal reaction at the bottom of the story to the horizontal loads. V_{Ed} is the total design vertical load on the structure on the bottom of the story.

An easier way to model the initial sway imperfections is to replace them with a system of horizontal loads of value ϕV_{ED} . Where V_{ED} is the vertical load on the column members of the frame. The lack of verticality of the columns, given by imperfection ϕ , can be replaced by equivalent horizontal forces, applied at the level of each floor and proportional to the vertical loads applied at that level. These forces are then added to the specified horizontal loads[5]. The equivalent horizontal load at each floor is given by $H_{Ed} = \phi V_{Ed}$ where V_{Ed} is the total design vertical load on each floor.

In this thesis, initial sway imperfections have been incorporated into the structure by a system of equivalent lateral loads for global analysis of the frame.

3.2.1.3 Earthquake Loading

The proposed office building is assumed to be located at the site corresponding to peak ground acceleration equal to $\alpha_{gR} = 0.25g$. In addition, soil type C, a type 1 spectral shape and importance factor II ($\gamma_1 = 1.0$) can be assumed for this site.

The horizontal elastic response spectrum can be plotted based on the above parameters and using the equations presented in appendix A. The design response spectrum is obtained by dividing the ordinates of elastic response spectrum by the behavior factor q . Figure 3-4 depicts both the resulting elastic and the design spectra. The lower bound factor for the design response spectrum was assumed equal to 0.2, as recommended in section 3.2.2.5 of the code [4].

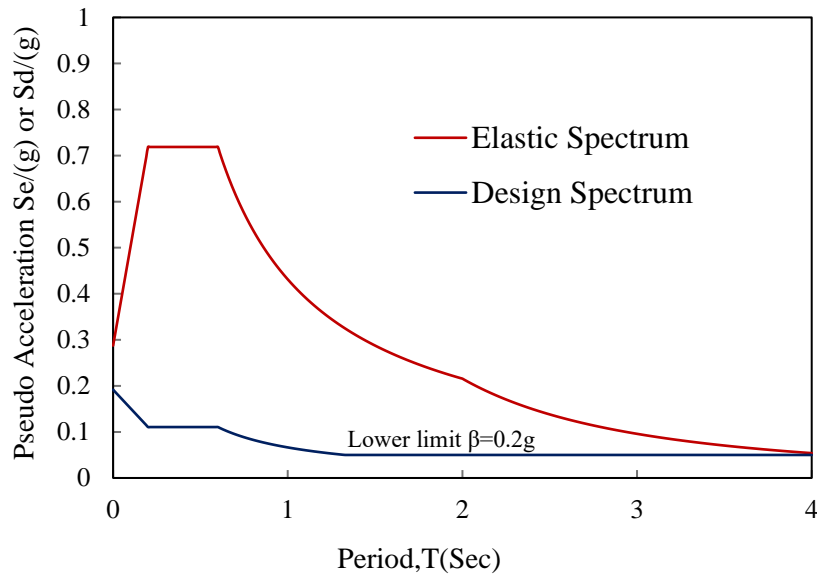


Figure 3-4: Elastic and Design Response Spectrum for Horizontal Component of Ground Motion

The behavior factor was chosen on the basis of the intended design concept, corresponding to DCH structures. For multiple MRFs, the behavior factor was chosen according to (table 6.2 section 5.2.2.2 of the seismic code)[4].

Table 3-4:Overstrength Factor for MRFs

Structural Type	Ductility Class	
	DCM	DCH
MRFs	4	5 α_u/α_1

$$q = \frac{\alpha_u}{\alpha_1} q_0 = 1.3(5) = 6.5 \quad (3-5)$$

For multistory, multi-bay frames or frame-equivalent dual structures: $\alpha_u/\alpha_1 = 1.3$.

3.2.2 Characteristics of Selected Ground Motion Records

The selection of ground motions from a given database is not straight forward however the following criteria have been considered in this research. Acceleration records were selected from the PEER NGA database. The set of seven ground motion records that represent a medium to high seismic hazard (MH) were selected from the database using the following criteria.

- Magnitude M from 6 to 7.5
- Distance from fault 10 km to 100km.
- Shear wave velocity V_s from 180 m/s to 360 m/s
- ES EN1998-1 Type 1 Soil C target spectrum with $PGA = 0.25 \text{ g}$

The characteristics of the selected seven ground motions is presented in Table 3-5.

Table 3-5 Characteristics of Selected Ground Motions

No.	Year	Earthquake Name	Station Name	Magnitude	PGA
1	1954	Northern Calif-03	Ferndale City Hall	6.50	0.163g
2	1979	Imperial Valley-06	Calexico Fire Station	6.53	0.277g
3	1980	Mammoth Lakes-01	Convict Creek	6.06	0.419g
4	1980	Victoria_ Mexico	Chihuahua	6.33	0.151g
5	1986	Chalfant Valley-02	Bishop - LADWP South St	6.19	0.249g
6	1987	Superstition Hills-02	Brawley Airport	6.54	0.144g
7	1992	Landers	Coolwater	7.28	0.284g

The selected acceleration records were matched to the target response spectrum using SeismoMatch so that the frequency content of records is manipulated to fit the elastic spectrum in the governing design code as shown in (Figure 3-6).

The mean response spectrum of the matched accelerograms for the seven ground motions was calculated by SeismoMatch and the resulting plot of the mean matched accelerograms against the previously defined target spectrum are reported in figure 3.7.

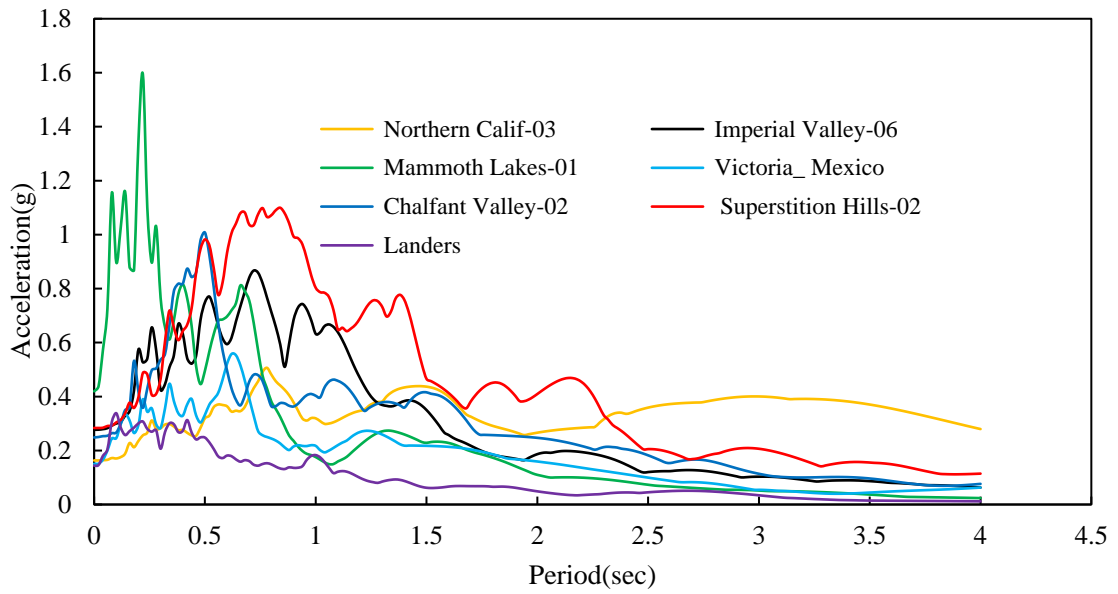


Figure 3-5: Original Accelerograms

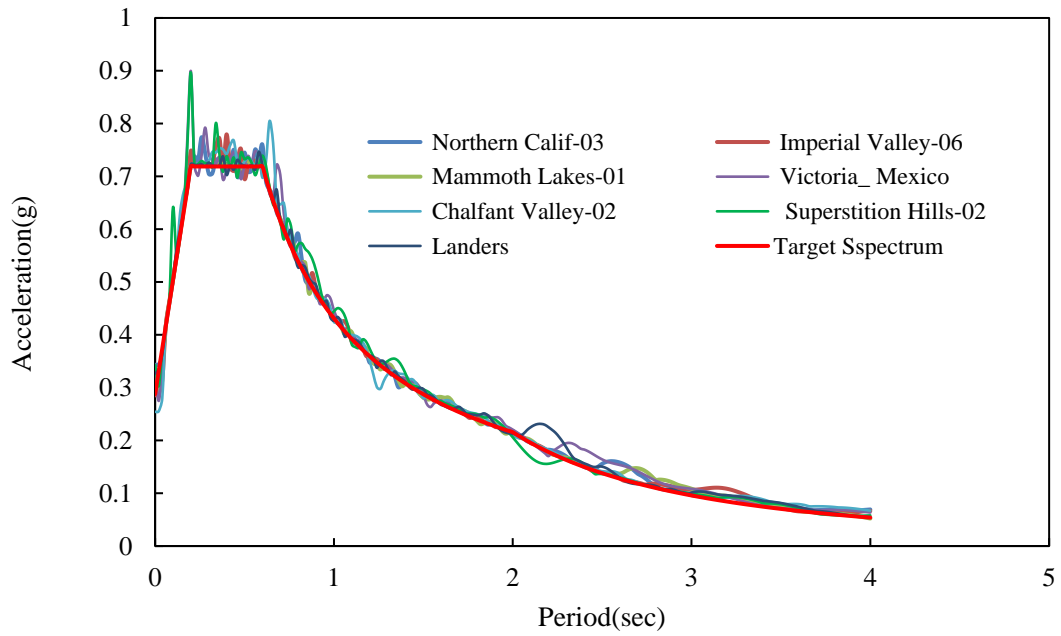


Figure 3-6: Matched Accelerograms

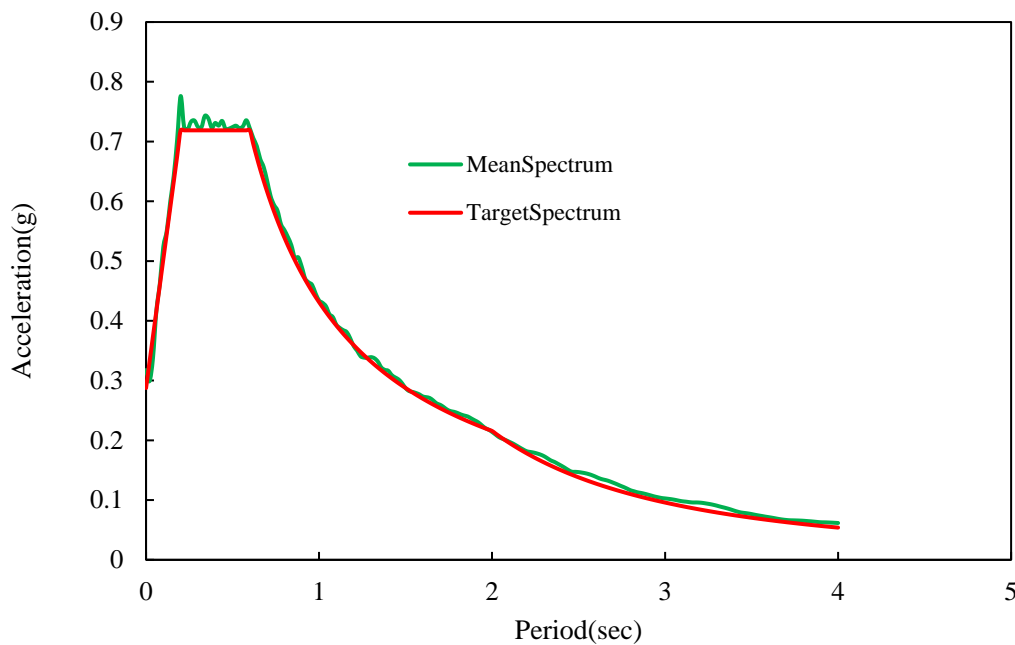


Figure 3-7: The mean matched Spectrum and the Target Spectrum

3.3 Analysis Methods

First, the mode of vibration and fundamental periods were determined from linear elastic analysis by ETABS[37], OpenSees[38] and SesmoStruct[35] for comparison purposes. Then the nonlinear analyses were carried out by the nonlinear finite element program OpenSees. The modeling and analysis procedures that have been carried out to the frame are described in the subsequent sections.

3.4 Description of SeismoStruct and OpenSees

3.4.1 Introduction to SeismoStruct

SeismoStruct is a finite element package capable of predicting the large displacement behavior of space frames under static or dynamic loading, taking into account both geometric nonlinearities and material inelasticity.

One of the most important features in this finite element program is that it requires no input or configuration files, programming scripts or any other time-consuming and complex text editing.

Columns and beams are modeled in SeismoStruct through a 2D&3D inelastic force-based frame elements (infrmFB) with 5 integration sections. The number of fibers used in section equilibrium computations is set to 250. All support nodes are considered as fully restrained against rotations and translations. A displacement-controlled pushover analysis has performed by SeismoStruct by maintaining gravity loads constant.

3.4.2 Introduction to OpenSees

OpenSees (Open System for Earthquake Engineering Simulation) is a finite element analysis framework for structural and geotechnical earthquake engineering simulation. OpenSees is being developed at the University of California Berkeley with support from the Pacific Earthquake Engineering Research Center (PEER) by Frank McKenna and Gregory L. Fenves[38]. OpenSees is an open-source software framework that can be downloaded by anyone. The framework itself is an interpreter of the Tool Command Language (TCL) programming language in combination with unique commands incorporating the finite element method and earthquake engineering. It is based on input scripts written in TCL together with different OpenSees commands.

Since it is mainly designed for research and academic purposes, it lacks a graphical interface (Figure 3-8). The program differs from commercialized software in the sense that the user manually creates every step throughout the assessment of analytical procedures. This makes it very difficult and time-consuming in creating large and complicated structural models. It is important to combine OpenSees with a visual pre and post-processor to handle complex problems and structures. The lack of a graphical user interface poses a challenge in using the tool, but on the other hand, it makes computation much quicker and is able to handle non-linear analysis with a variety of materials libraries. One of the most important aspects of this program is any user-defined materials or sections can be implemented into the model. Therefore, first-time use is a laborious process, but once that barrier has been reached, the framework offers tremendous opportunities for finite-element applications.

```
OpenSees -- Open System For Earthquake Engineering Simulation
Pacific Earthquake Engineering Research Center
Version 3.0.3 64-Bit

(c) Copyright 1999-2016 The Regents of the University of California
All Rights Reserved
(Copyright and Disclaimer @ http://www.berkeley.edu/OpenSees/copyright.html)

OpenSees >
```

Figure 3-8: The OpenSees Interface

3.4.2.1 Main Abstractions in OpenSees

The main abstractions in OpenSees can be described as shown in the following diagram and each class is described in the subsequent sections below[39].

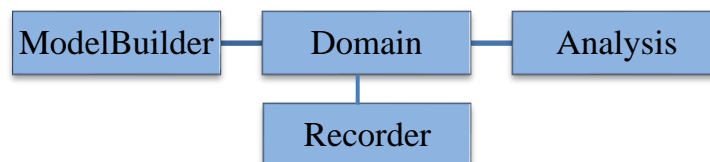


Figure 3-9: Main Abstractions in OpenSees

3.4.2.2 The OpenSees ModelBuilder

As in any finite-element analysis, the model builder constructs the first step of the analyst is to subdivide the body being studied into elements and nodes, define loads acting on the elements and nodes, and define constraints acting on the nodes. The ModelBuilder is the object in the program responsible for building the following objects in the model and adding them to the domain.

The ModelBuilder consists of the following:

Node, mass, material(nDmaterial command, uniaxialMaterial command), section, element, LoadPattern, TimeSeries, constraint.

3.4.2.3 *The OpenSees Domain Object*

The domain object is responsible for storing the objects created by the object ModelBuilder and providing access to these objects to the objects of Analysis and Recorder

3.4.2.4 *The OpenSees Analysis Object*

The analysis objects are responsible for carrying out the analysis. The analysis moves the model along from state at time t to state at time $t+dt$. This may vary from a simple linear static analysis to a transient (Transient Analysis, Variable Transient Analysis) non-linear analysis. In OpenSees each analysis object is composed of several component objects, which define the type of analysis of how the analysis is performed.

The Analysis component classes consist of the following:

ConstraintHandler determines how the constraint equations are enforced in the analysis and how it handles the boundary conditions/imposed displacements.

DOF_Numberer determines the mapping between equation numbers and degrees-of-freedom.

AnalysisModel defines what time of analysis is to be performed

Integrator determines the predictive step for time $t+dt$

SolutionAlgorithm determines the sequence of steps taken to solve the non-linear equation at the current time step.

SystemOfEqn/Solver within the solution algorithm, it specifies how to store and solve the system of equations in the analysis.

3.4.2.5 *The OpenSees Recorder Object*

The recorder commands are used to construct a Recorder object, which is used to monitor items of interest to the analyst at each commit (). The OpenSees Recorder object constitutes the following items that apply to all Node/Drift/Element recorders.

Node Recorder, Drift Recorder Element Recorder, Plot Recorder, Display Recorder.

The classes and their relationship are illustrated in Figure 3.9, which shows the class diagram using Rumbaugh notation [40].

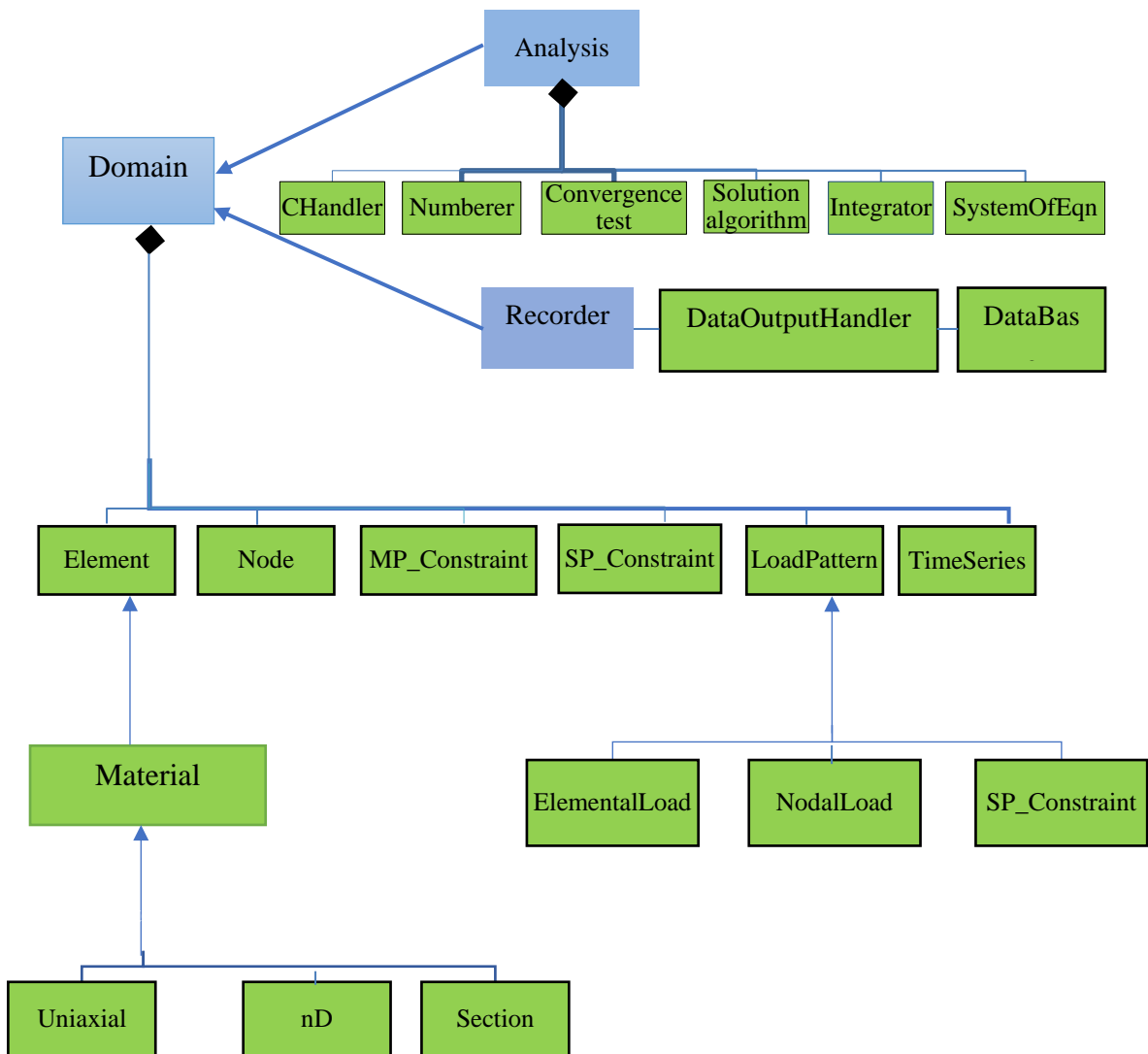


Figure 3-10: OpenSees Software Packages for FEM Analysis [40]

OpenSees provides a number of options for different analysis commands as listed in Table 3-6. The presence of these options is important to apply the most appropriate methods in each analysis command.

Table 3-6 Some of OpenSees Commands and Available Options[16]

Command	Available Options						
Constraints	Plain		Transformation		Lagrange Multipliers	Penalty	
Numberer	Plain		RCM		AMD		
System	Band General	Band SPD	Profile SPD	UmfPack	Sparse SPD	Sparse General	
Test	Norm Unbalance	Rel. Norm Unbalance	Norm Displacement Increment	Rel. Energy Increment	Energy Increment	Rel. Norm Displacement Increment	
Algorithm	Linear	Newton	Modified Newton	Newtown with Line Search	Krylov Newton	Broyden	BFGS
Integrator	Load Control	ArcLength Control	Min. Unbalanced Disp. Norm	Displacement Control	Central Difference	Hilber-Hughes-Taylor	Newmark
Analysis	Static		Transient		Variable Transient		

Further information about the software and its functionality can be obtained from the web page[39].

3.4.2.6 Why OpenSees is chosen for this Study

The software framework for simulating the seismic response of structural & geotechnical systems has been chosen to perform numerical analysis for the present thesis because it is an extremely powerful tool, which allows to use advanced constitutive material models. It is also possible to perform two dimensional and three-dimensional analysis. Another important aspect is the possibility of controlling every single part of the analysis in detail, unlike many finite element software that gives fewer parameter modification possibilities. The program OpenSees has been chosen for this study due to the following main reasons.

- It is an open-source finite element program that can easily be downloaded by registering from the website[39] for free. Since it is an opensource, it has a huge number of developers and contributors as compared to other commercial programs.
- It is capable of simulating both linear and nonlinear problems.
- It is powerful and computationally efficient, and it offers extensive tools for nonlinear structural analysis.
- It provides a wide range of materials, sections and elements library.
- It provides a library of various, analysis types & solution algorithms (for convergence issues).

3.5 Modeling and Analysis Procedures of the Frame by OpenSees

The procedures for the modeling and analysis of steel frames using OpenSees are described in the subsequent sections below.

3.5.1 Definitions of the Material Model

Analysis of structures depends on the constitutive relationship or stress-strain relation of the material. In OpenSees there are two types of uniaxial steel material models namely, Steel01 and Steel02.

Steel01 is a bilinear steel material with kinematic hardening and optional isotropic hardening described by a non-linear evolution equation. Figure 3-11 shows the stress-strain relationship for **Steel01** material defined by three parameters namely yield stress f_y , initial elasticity modulus E_0 and ratio between post yielding, E_{sh} and E_0 , b . i.e. strain hardening slope $E_{sh}=bE_0$

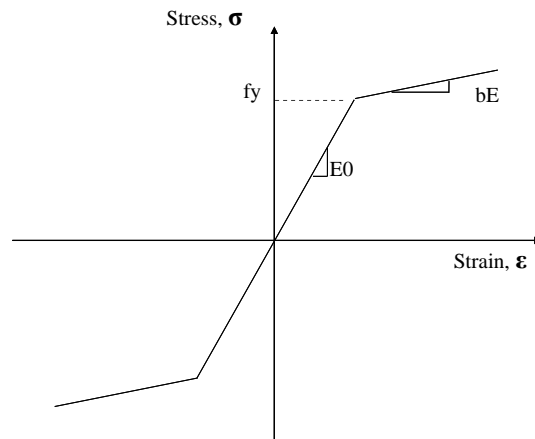


Figure 3-11: Stress-Strain Relationship of Steel01 in OpenSees

OpenSees Command: uniaxialMaterial Steel01 \$matTag \$Fy \$E0 \$b

Steel02 is a Giuffre-Menegotto-Pinto steel material with isotropic strain hardening [41]. The Steel02 material in OpenSees was considered in this study to represent the nonlinear transition from the elastic stage to the strain hardening stage (Figure 3-12).

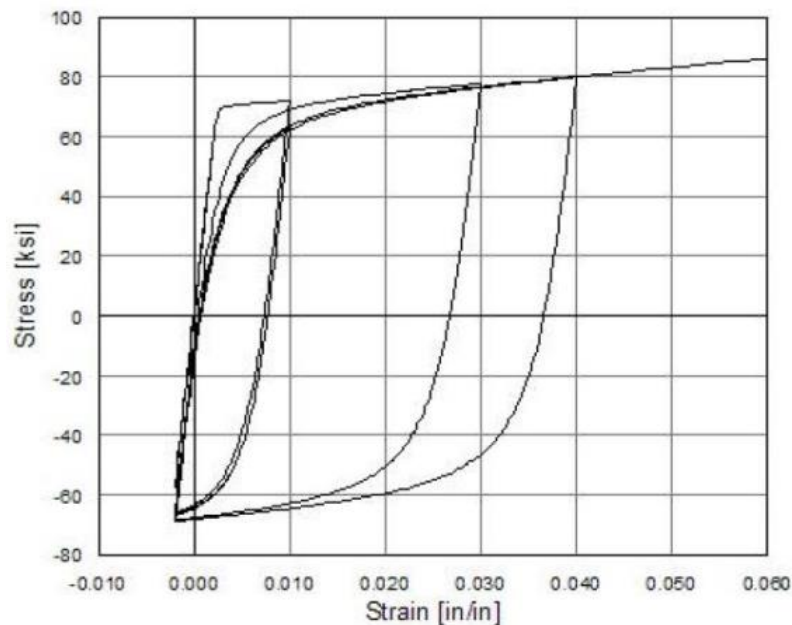


Figure 3-12: Hysteretic Behavior of Steel02 Material with Isotropic Hardening[39]

OpenSees Command: uniaxialMaterial Steel02 \$matTag \$Fy \$E \$b \$R0
\$cR1 \$cR2 <\$a1 \$a2 \$a3 \$a4 \$sigInit>

3.5.2 Modeling of Sections

3.5.2.1 Elastic Section

The modeling of elastic sections is used to perform linear elastic analysis. The required parameters for the modeling of two-dimensional elastic sections are the young's modulus, the cross-sectional area and the area moments of inertia of the section. In addition to the parameters for two-dimensional elastic sections; the shear modulus, the area moments of inertia about the two local axes of the section and the polar moments of inertia are necessary to model the three-dimensional elastic sections.

3.5.2.2 Fiber Section

In the fiber section model, the element is divided into a number of monitored sections represented by the integration points. Each section is further divided into m fibers and each fiber is defined by its centroid area and coordinate location. The inelastic effects were captured by tracing each fiber's uniaxial stress-strain relationship on the cross-sections located along the member length at the selected integration points. A fiber section with quadrilateral elements is used to incorporate the initial residual distribution into the section. The combination of fiber section and corotational transformation enables the analysis to take account for axial-moment interaction.

Fiber sections can be used for advanced analysis and when detailed and more accurate results are required. The geometry of the cross-section was slightly simplified and idealized by removing the fillets on the inner sides of the flanges and at the flange-to-web connections in order to keep the mesh regular (Figure 3-13).

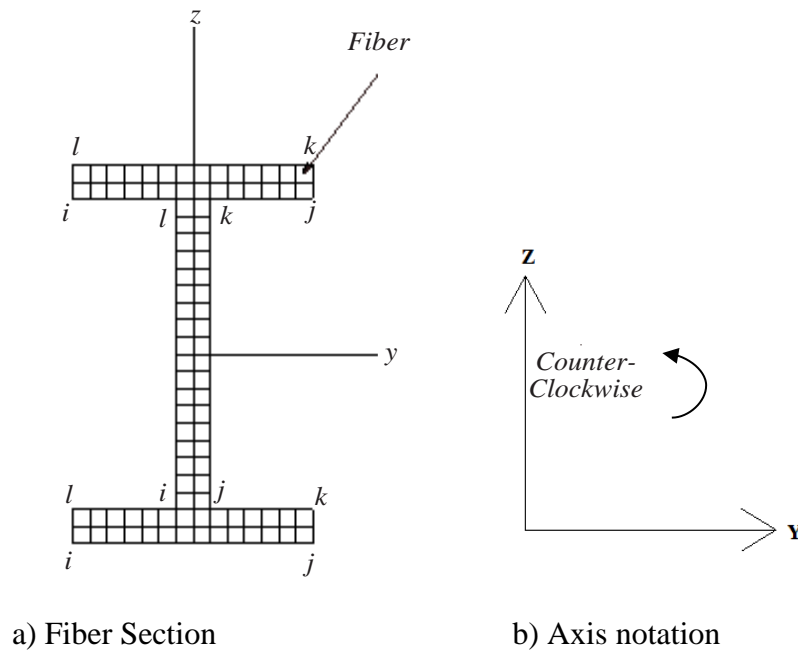


Figure 3-13: Section Discretization

The patch command generates a number of fibers over a cross-sectional area. There are currently three cross-section forms that can produce fibers: quadrilateral, rectangular, and circular. The following is the command to generate a quadrilateral shaped patch (the geometry of the patch is defined by four vertices: I J K L. The coordinates of each of the four vertices is specified in COUNTER CLOCKWISE sequence):

OpenSees Command: patch quad \$matTag \$numSubdivIJ \$numSubdivJK \$yI \$zI \$yJ \$zJ \$yK \$zK \$yL \$zL

\$matTag tag of previously defined material (UniaxialMaterial tag for a FiberSection or NDMaterial tag for use in an NDFiberSection)

\$numSubdivIJ number of subdivisions (fibers) in the IJ direction.

\$numSubdivJK number of subdivisions (fibers) in the JK direction.

\$yI \$zI y & z-coordinates of vertex I (local coordinate system)

- y_J, z_J y & z -coordinates of vertex J (local coordinate system)
- y_K, z_K y & z -coordinates of vertex K (local coordinate system)
- y_L, z_L y & z -coordinates of vertex L (local coordinate system)

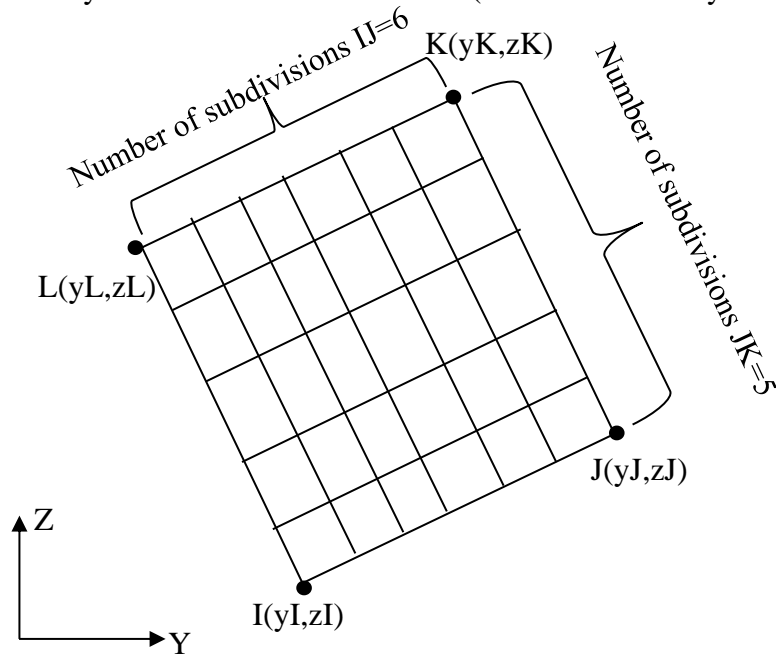


Figure 3-14: Notation on Quadrilateral Patch for Section Discretization[42]

3.5.2.3 Modeling of Residual Stresses

The modeling of residual stresses can be implemented in OpenSees based on the recommendations of ECCS (Figure 2-11). Initial stress values equal to 30% of the yield stress were given for the material **Steel02** and this material was attached to the steel profile.

3.5.3 Modeling of Elements

In structural seismic analysis, the formulation of elements for beam-column elements can be divided into elastic and plastic. Formulation of the elastic beam-column element uses the linear constitutive relation. The plastic beam-column element can further be divided into elements with distributed plasticity and elements with concentrated plasticity [24]. Whereas elements with concentrated plasticity models enable plastic hinges to be formed at the end of the element, distributed plasticity models allow plasticity to be spread along the element causing yield to occur at any position along the element.

The distributed inelasticity elements are modeled as fiber elements displacement-based (DB) or force-based (FB). The DB formulation is based on the assumption of cubic displacement shape functions, section deformations are interpolated from an approximate

displacement field (constant axial deformation and linear curvature distribution are enforced along the element length, exact only for prismatic linear elastic elements) while the FB formulation assume exact force fields in members without rigid body modes. The exactness of the equilibrium between element and section forces holds in the range of constitutive nonlinearity and they have also distributed plasticity with linear curvature distribution.

Because FB elements have no restraints on their displacement fields, they approximate plastic structural response more accurately than DB elements[15]. Moment-axial force interaction effects of columns can be captured by force-based fiber elements.

OpenSees command for FB: `element nonlinearBeamColumn $eletag $ndI $ndJ $numIntgrPts $secTag $transfTag;`

OpenSees command for DB: `element dispBeamColumn $eletag $ndI $ndJ $numIntgrPts $secTag $transfTag;`

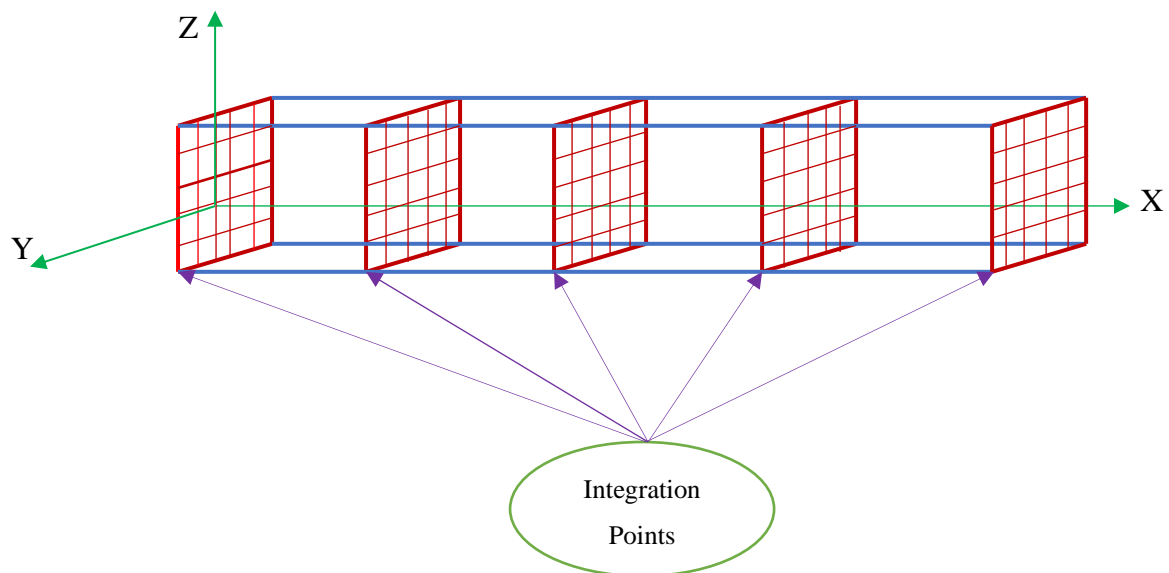


Figure 3-15: Distributed Plasticity Fiber Element

3.5.3.1 Geometric Transformation

Geometric transformation defines the transformation of elemental forces and stiffness from local to global coordinate system. Geometric transformation object's main tasks are 1) transforming global displacements into natural coordinates and 2) transforming natural forces and stiffnesses into global coordinates.

The geometric-transformation command is used to construct a coordinate-transformation (CrdTransf) object, which transforms beam element stiffness and resisting force from the basic system to the global coordinate system. The command has at least one argument, the transformation type.

In OpenSees[38], there are three types of geometric transformations namely Linear, PDelta and Corotational.

Linear performs a linear geometric transformation of beam stiffness and resisting force from the basic system to the global coordinate system, **PDelta** is the transformation with some nonlinearity and **Corotational** is the exact nonlinear transformation with large displacement-small strain problems. For the current version of the software, this transformation does not deal with element loads and will ignore any that are applied to the element.

OpenSees Command for 2D: geomTransf \$TransferType \$transfTag

OpenSees Command for 3D: geomTransf \$TransferType \$transfTag \$vecxzX \$vecxzY \$vecxzZ where

\$TransferType is the type of transformation: Linear,PDelta,Corotational.

\$transfTag is the integer tag identifying transformation

\$vecxzX, \$vecxzY, and \$vecxzZ are the X, Y, and Z components of vecxz, which is the vector used to define the local x-z plane of the local-coordinate system. The vector vecxz is a vector the user specifies that must not be parallel to the x-axis. The local y-axis is defined by taking the cross product of the vecxz vector and the x-axis. For the frame shown in (Figure 3-16) the \$vecxzX \$vecxzY \$vecxzZ components can be 0 0 1 for columns and beams in the X direction, and 1 0 0 for beams in the global Z-direction.

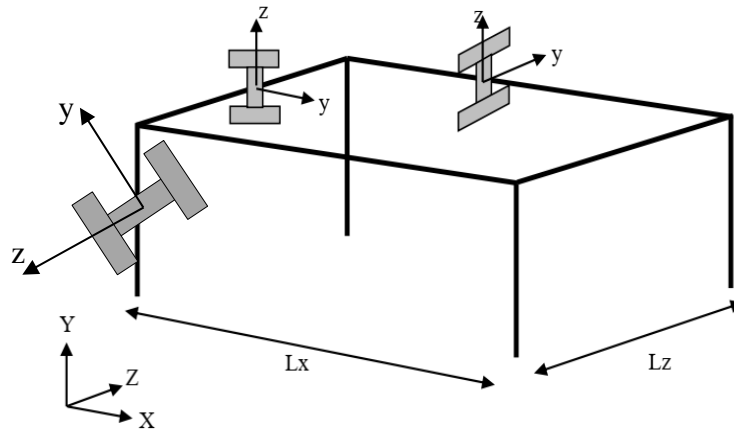


Figure 3-16: Local Coordinates for Beams and Columns

3.5.4 Definition of Loads in OpenSees

3.5.4.1 Gravity Loads in OpenSees

Gravity and/or constant lateral loads can be applied in OpenSees using a load pattern command either as a concentrated joint load or as a uniformly distributed line load. Both types of these loads were applied to the frames used in this research.

3.5.4.2 Imperfection Loads in OpenSees

Two types of geometric imperfections for isolated columns were modeled in OpenSees, these are the initial bow imperfections for an isolated pin ended column and initial out of plumb imperfections for a single cantilever column. The initial out of straightness was assumed as half-sine wave as it is recommended by various literatures. The initial out of plumbness was assumed as a linear function of the length of the member. The initial out of plumbness imperfection of a portal sway frame has also been modeled directly in OpenSees.

Imperfections for the case study building have been incorporated into the global frame in terms of equivalent lateral loads. For the case of a three-dimensional frame, global sway imperfections were considered independently in each orthogonal direction. However initial bow imperfections were ignored in the analysis due to the fact that their significance for unbraced or MRFs is lower than the global sway imperfections. However, initial bow imperfections which have considerable impact on braced frames should be considered for seismic analysis. Initial bow imperfection for a single column was applied to the program

A TCL script that automatically calculates initial out of plumbness imperfections based on the given story height and number of columns in a row was written and implemented into the model.

3.5.4.3 Dynamic Loads in OpenSees

Seven spectrum compatible ground motions were applied to the model and the transient analysis command was selected in OpenSees. Seismic masses were lumped at specified nodes in each orthogonal direction of the frame.

3.5.5 Analysis Procedures

3.5.5.1 Nonlinear Static Analysis in OpenSees

Finite element procedures are employed for the modeling of the structure during the nonlinear static analyses. The geometric transformation commands available in OpenSees have been used to consider the effects of geometric nonlinearity. P-delta transformations were used for the whole columns and beams to account for geometric nonlinearities. The structure is first subjected to gravity loads and seismic masses that are lumped at the nodes. The gravity loads are maintained constant and gradually increasing lateral loads are applied to the structure until the specified target displacement is achieved. The pushover analysis was done by the displacement control method.

Three different lateral load distributions for pushover analysis were considered in this research. These are Uniform pattern, Triangular pattern and Modal pattern. The uniform pattern was based on the mass regardless of the story height. The triangular pattern was based on the height of the story whereas the modal pattern was due to the first mode of vibration after performing linear modal analysis of the structure. The lateral load distribution coefficients for all the three cases are given below.

$$\begin{aligned}\phi &= [1 \ 1 \ 1 \ 1 \ 1 \ 1]^T \text{ Uniform Pattern} \\ \phi &= [1 \ 0.87 \ 0.674 \ 0.512 \ 0.349 \ 0.186]^T \text{ Triangular Pattern} \\ \phi &= [1 \ 0.871 \ 0.695 \ 0.488 \ 0.293 \ 0.131]^T \text{ Modal Pattern for 3D frame}\end{aligned} \tag{3-6}$$

3.5.5.2 Nonlinear Time History Analysis in OpenSees

Nonlinear time-history analyzes are performed on the structure after conducting pushover analyzes. The frame is first subjected to live and dead loads, after which the selected ground motions are added to the prototype and given in the OpenSees command for

transient analysis. The model defined for pushover analyses was used for the time history analyses. The analysis procedures that have been followed in this research can be summarized as in the following chart.

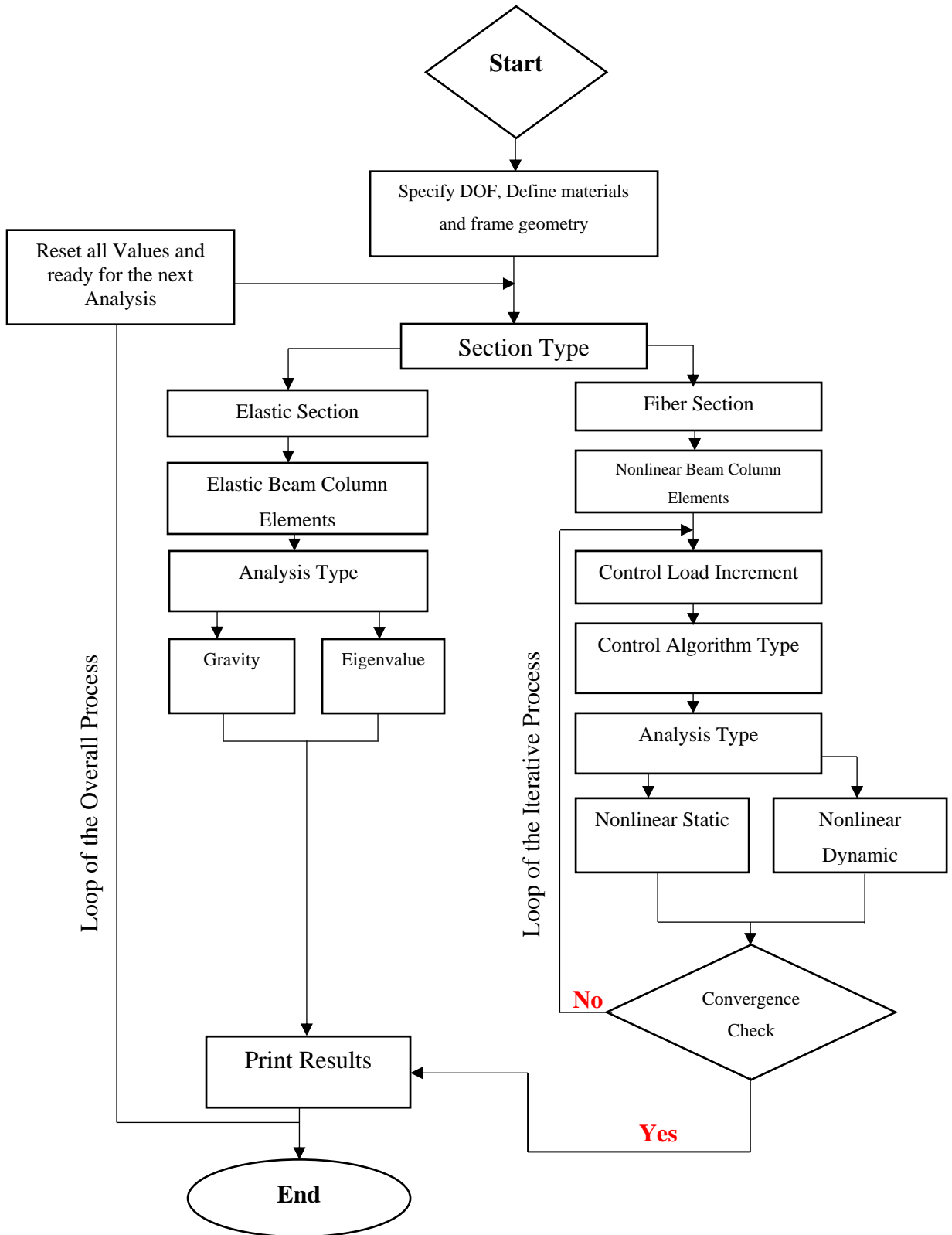


Figure 3-17: Flowchart for Frame Analysis

CHAPTER 4 RESULTS AND DISCUSSION

4.1 Verifications of Single Column Imperfections

To investigate the impact of initial imperfections on single columns, two beam-column elements made of the same material and cross-section with different boundary conditions (one cantilever column and the other pin ended column) have been analyzed by the exact method and by using OpenSees. The results show that for the case of pin ended column with initial bow imperfection, the member has to be subdivided into a sufficient number of elements to converge to the exact or theoretical solution. On the other hand, the analysis of imperfect cantilever column gives fair results even with a small number of element subdivisions per member as compared to the theoretical solution.

Case a) Cantilever column

Figure 4-1 depicts the geometry and loading of a cantilever column with initial sway imperfection. Table 4-1 shows the second-order elastic analysis results for a cantilever column using PDelta transformation to account for the effects of geometric nonlinearity. The exact analysis was done based on equations (2-25) through (2-27).

Table 4-1 Analysis Results for Cantilever Column

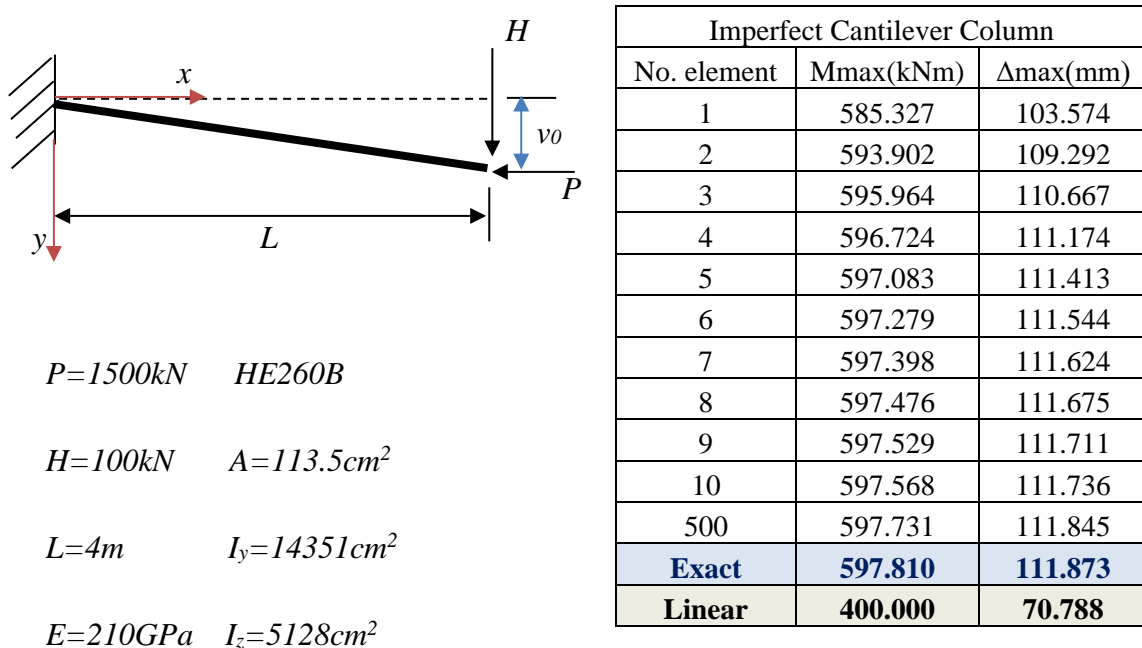


Figure 4-1: Geometry of Imperfect Cantilever Column

Case b) Pin ended column

Figure 4-2 depicts the geometry and loading of a pin ended column with initial bow imperfection.

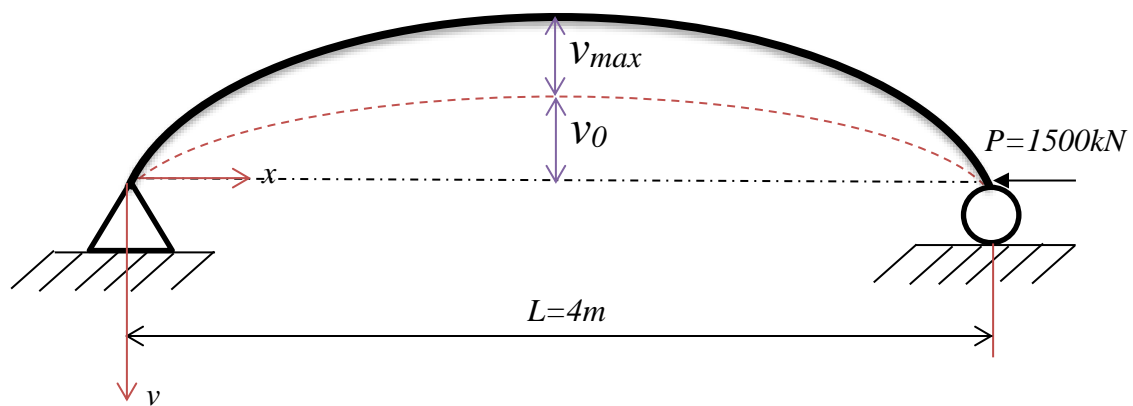


Figure 4-2: Axially Loaded Pin Ended Imperfect Column

The same cross-section as the cantilever column was adopted for this case. Corotational geometric transformation was assumed to account for the effect of geometric nonlinearity. One can observe from Figure 4-3 that the variation of the number of elements per member strongly affects the transversal displacement of a pin ended column, This means that as we increase the number of elements, we can obtain a smooth curve for the displacement of a column along its length. (Table 4-2) and (Figure 4-3) show the second-order elastic analysis results for an imperfect pin ended column. The exact analysis was done based on equations (2-23) and (2-24). For a pin ended column the maximum moment and displacement do not occur at the member end rather they are located at the mid-length of the column. As it can be shown in (Figure 4-3), the second-order elastic analysis results for an imperfect pin ended column highly depends on the number of elements per member. If an odd number of elements are used to subdivide the member, the imperfections will not be assigned correctly to follow the buckling mode which was considered as a half-sine wave.

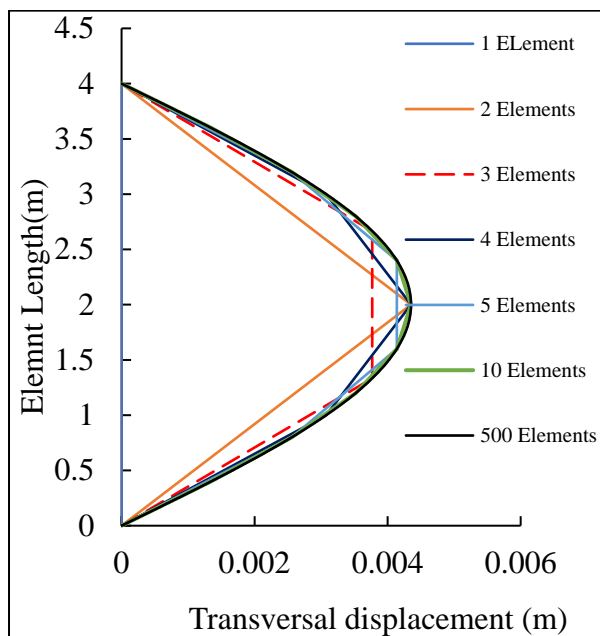


Table 4-2 Pin Ended Column

No element	Mmax(kNm)	Vmax(mm)
1	-	-
2	6.422	4.281
3	5.606	4.273
4	6.494	4.329
5	6.185	4.319
6	6.509	4.340
7	6.349	4.333
8	6.515	4.343
9	6.417	4.339
10	6.517	4.345
500	6.522	4.348
Exact	6.527	4.351

Figure 4-3: Variation of Transversal Displacements for Pin Ended Column

4.2 Verification of Portal Frame Imperfections

The portal frame shown in Figure 2-10 is displayed again for studying the effects of the number of elements per member and modeling imperfections. Two types of modeling imperfections were carried out. These are an explicit modeling of imperfections and modeling of imperfections by replacing with an equivalent lateral load. The results from the two types of models are compared. As it is described in table 4-3, the maximum moment and axial load of elements from elastic second-order analysis was determined, the results show that the modeling of imperfections by equivalent lateral load method gives comparable results with the direct modeling method. The equivalent lateral load method is preferred for its simple procedures to apply imperfections into the structure.

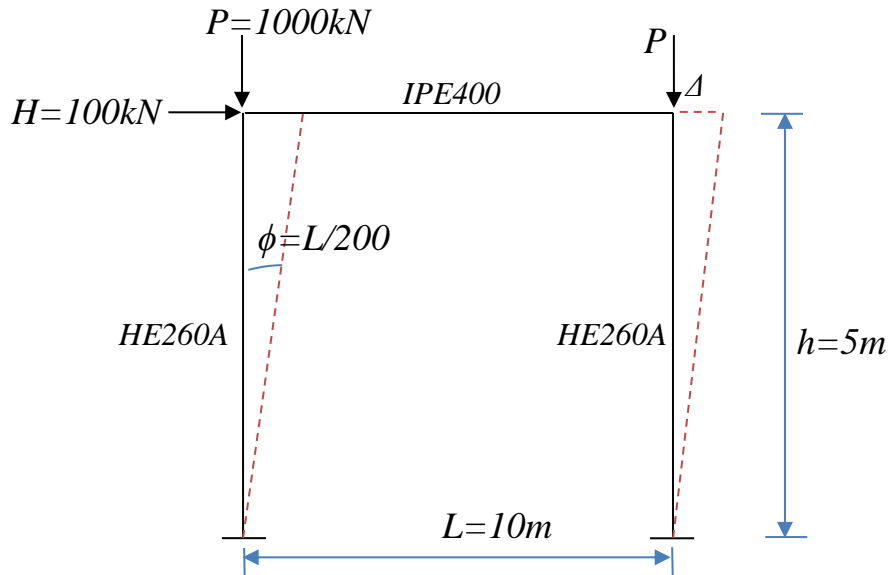


Figure 4-4: Configuration of Typical Portal Frame

Table 4-3 Second-Order Elastic Analysis of Imperfect Portal Frame

No elem	Direct modeling			Equivalent Sway		
	M(kNm)	P(kN)	Δ (m)	M(kNm)	P(kN)	Δ (m)
1	156.046	976.109	0.03651	152.900	976.599	0.03579
2	178.544	972.190	0.04219	174.942	972.759	0.04136
3	178.534	972.110	0.04255	174.931	972.68	0.04171
4	178.547	972.079	0.0427	174.943	972.65	0.04185
5	178.556	972.065	0.04277	174.952	972.636	0.04193
6	178.562	972.057	0.04282	174.957	972.628	0.04197
10	178.571	972.045	0.04288	174.966	972.617	0.04203
100	178.577	972.038	0.04291	174.972	972.61	0.04206
1000	178.577	972.038	0.04291	174.972	972.61	0.04206

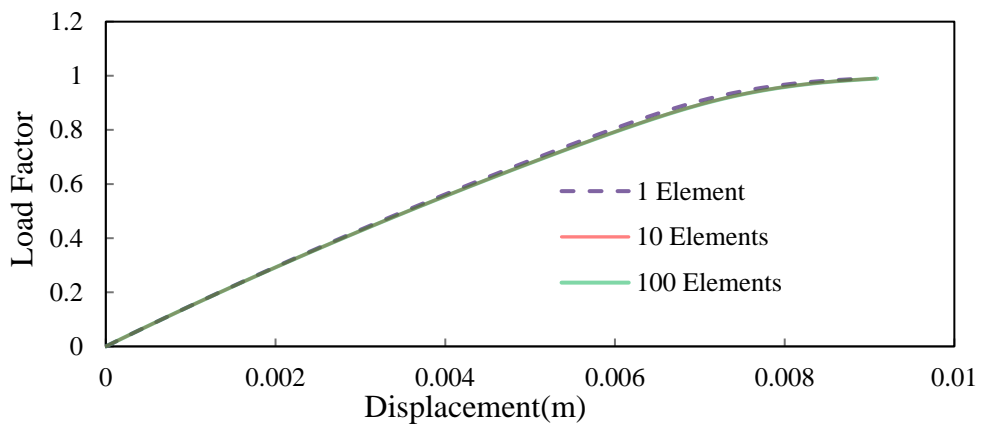


Figure 4-5: Second order Nonlinear Analysis of Imperfect Portal Frame

Figure 4-5 presents the load control nonlinear static analysis results for a typical portal frame by varying the number of elements per member. As it is described in the figure, the number of elements per member has no significance on the lateral displacement of the frame. The load-deflection behavior of sway frames under static loading can be predicted by using a single element per member.

4.3 Linear Elastic Analysis Results

The following section describes the results obtained from linear analysis that has been carried out for the building under consideration. The determination of the first mode shape of the structure is required to distribute the lateral loads along its height for pushover analysis. The linear elastic analysis is therefore performed first, to determine the mode of vibration of the structure and natural periods have also been determined from such analysis.

Table 4-4 presents the fundamental periods of the building frame under consideration; the linear modal analysis was done using three finite element programs and the results for the first mode of vibration from the three programs are almost identical. Particularly, the OpenSees and SeismoStruct results are almost similar, while the ETABS results are a bit larger than the two. Table 4-5 presents the lateral load distribution coefficients along the height of the building. These coefficients have been determined using the formulas presented in section 2.4.2 of chapter 2.

Table 4-4 Fundamental Periods per Mode of Vibration

Mode -	OpenSees Period(sec)	SeismoStruct Period(sec)	ETABSv16.21 Period(sec)
1	1.294	1.302	1.304
2	0.491	0.497	0.542
3	0.447	0.450	0.448
4	0.262	0.264	0.263
5	0.181	0.182	0.184
6	0.170	0.172	0.144

Table 4-5 Lateral Load Patterns for Plane Frames

Story -	mass (tone)	X direction		Y direction		Both directions			
		Modal Pattern		Modal Pattern		Triangular Pattern		Uniform Pattern	
		ϕ_i	Fi(kN)	ϕ_i	Fi(kN)	ϕ_i	Fi(kN)	ϕ_i	Fi(kN)
6	182.550	1	182.550	1	182.550	1	182.550	1	182.550
5	204.704	0.871	178.365	0.853	174.583	0.837	171.380		204.704
4	206.833	0.695	143.802	0.671	138.873	0.674	139.492		206.833
3	206.833	0.488	100.848	0.467	96.620	0.512	105.821		206.833
2	216.172	0.293	63.437	0.270	58.367	0.349	75.409		216.172
1	219.179	0.131	28.696	0.104	22.857	0.186	40.778		219.179

Table 4-6 Distribution of Lateral Loads for 3D Frame

Story -	mass (tone)	Modal Pattern		Triangular Pattern		Uniform Pattern	
		ϕ_i	Fi(kN)	ϕ_i	Fi(kN)	ϕ_i	Fi(kN)
6	365.101	1	365.101	1	365.101	1	365.101
5	409.408	0.871	356.731	0.837	342.674		409.408
4	413.665	0.710	293.702	0.674	278.810		413.665
3	413.665	0.484	200.214	0.512	211.796		413.665
2	432.345	0.290	125.380	0.349	150.888		432.345
1	438.359	0.129	56.548	0.186	81.535		438.359

Table 4-7 Stability Coefficients in X direction

Story	h(mm)	P(kN)	V _x (kN)	U _x (mm)	dr(mm)	Θ_x	α
6	3500	3578.64	568.11	31	26	0.0468	1.0491
5	3500	7596.24	1028.93	27	32.5	0.0686	1.0736
4	3500	11651.04	1389.75	22	45.5	0.1090	1.1223
3	3500	15705.84	1706.86	15	39	0.1025	1.1142
2	3500	19946.64	1999.68	9	32.5	0.0926	1.1021
1	4000	24224.64	2090.22	4	26	0.0753	1.0815

Table 4-8 Stability Coefficients in Y direction

Story	h(mm)	P(kN)	V _y (kN)	U _y (mm)	dr(mm)	Θ_y	α
6	3500	3578.64	423.43	28	13	0.0314	1.0324
5	3500	7596.24	917.58	26	19.5	0.0461	1.0484
4	3500	11651.04	1292.97	23	32.5	0.0837	1.0913
3	3500	15705.84	1577.59	18	32.5	0.0924	1.1019
2	3500	19946.64	1857.49	13	39	0.1197	1.1359
1	4000	24224.64	1947.67	7	45.5	0.1415	1.1648

According to the new seismic code, Since the stability coefficient θ is less than 0.1 for both directions, the second-order effects can be ignored however, the analysis was done by considering the P- Δ effects[4].

Table 4-9 Equivalent Imperfection Loads Per Floor

Story	V _{Ed} (kN)	H _{Edx} (kN)	H _{Edy} (kN)	H _{Edx} /V _{Ed}	H _{Edy} /V _{Ed}	ϕ V _{Ed} (kN)
6	3578.64	568.11	423.43	0.159	0.118	8.57
5	7596.24	1028.93	917.58	0.135	0.121	18.20
4	11651.04	1389.75	1292.97	0.119	0.111	27.92
3	15705.84	1706.86	1577.59	0.109	0.100	37.63
2	19946.64	1999.68	1857.49	0.100	0.093	47.79
1	24224.64	2090.22	1947.67	0.086	0.080	58.04

As per the new steel code[5], the effects of global imperfections for buildings sensitive to buckling in a sway mode can be disregarded if $H_{Ed}/V_{Ed} \geq 0.15$. since the condition is not satisfied the effect of imperfections should be considered.

4.4 Nonlinear Analysis Results of Frames

The following section presents the results of nonlinear analyses of both plane frames extracted from the building described in chapter 3 and the space frame. Basically, two types of seismic analyses have been carried out in this research namely, monotonic pushover analysis and nonlinear time history analysis.

4.4.1 Pushover Analysis Results of Plane Frames

The displacement control nonlinear analysis results for frames extracted from the space frame described in chapter 3 are presented here. The frames were considered in both directions, i.e. the frame in the x-direction is a 5bay 6story MRFs while the frame in the y-direction is a 4 bay 6story frame. The plots of base shear vs top story displacement for frame x and frame y are presented in Figure 4-6 and Figure 4-7 respectively.

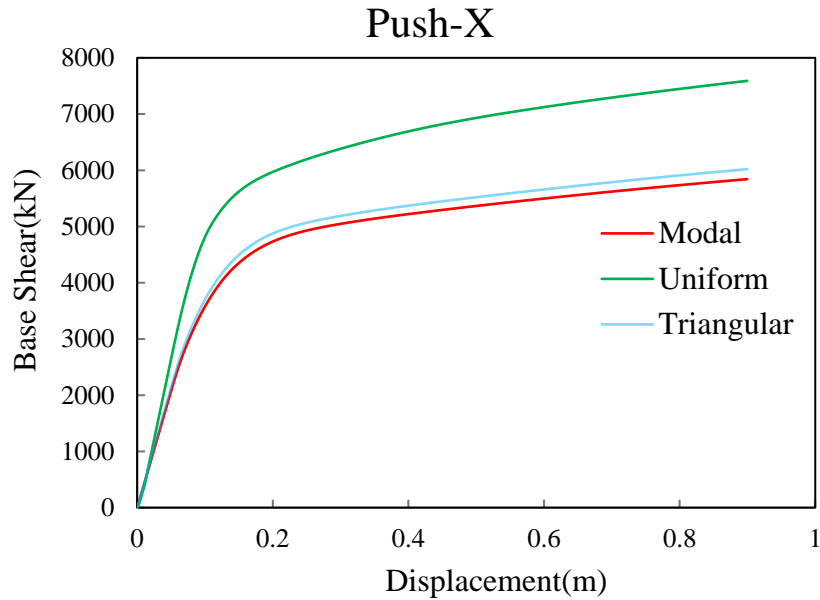


Figure 4-6: Effects of Lateral Load Patterns in Pushover X

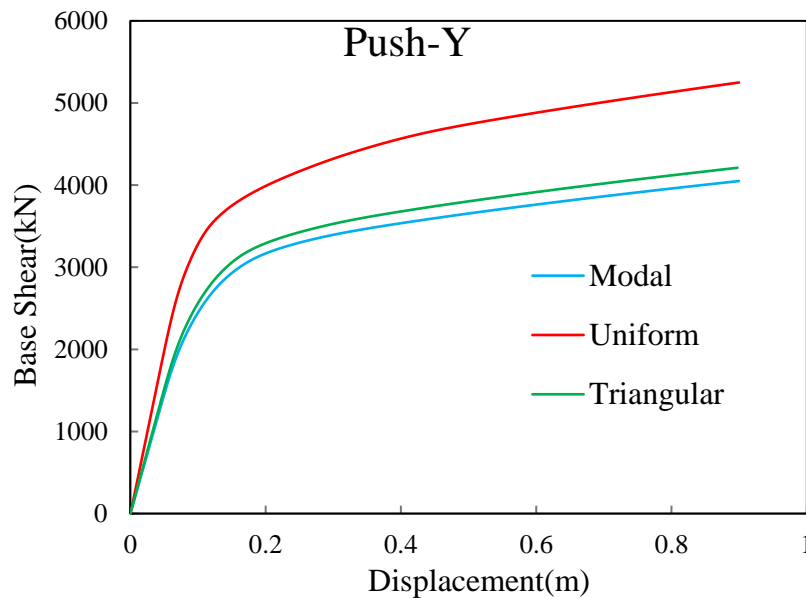


Figure 4-7: Effects of Lateral Load Patterns in Pushover Y

Figure 4-6 and Figure 4-7 describe how the variation of lateral load distribution affects pushover analysis results based on the displacement control technique. The above plots show that the uniform or rectangular lateral load pattern (which is based on mass regardless of the height of the structure) overestimates the base shear comparing to the triangular or modal distribution patterns for the corresponding story displacement. Both the modal and the triangular patterns are almost the same in predicting the base shear vs

roof displacement. However, triangular pattern is best for its simple procedures to estimate the distribution coefficients (which can be obtained by proportioning the height of the structure), while the modal pattern coefficients require the linear modal analysis to determine the first mode of vibration of the structure. In this research, the modal pattern was considered for comparison purposes.

4.4.2 Pushover Analysis Results of 3D Frame

As the case for plane frames, the nonlinear static analysis was performed for the 3D frame in both directions to study the lateral load distributions effects, and the results are presented in figures 4-8 and 4-9 for the x and y directions respectively.

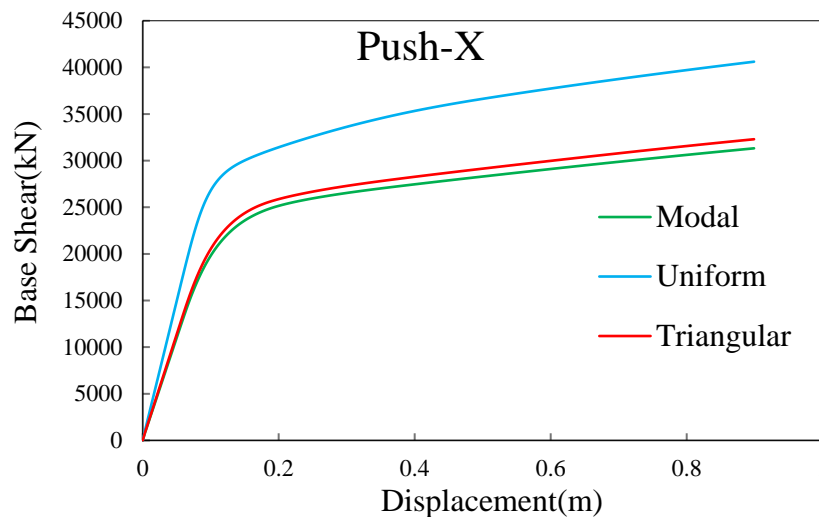


Figure 4-8: Effects of Lateral Load Pattern on 3D Pushover X

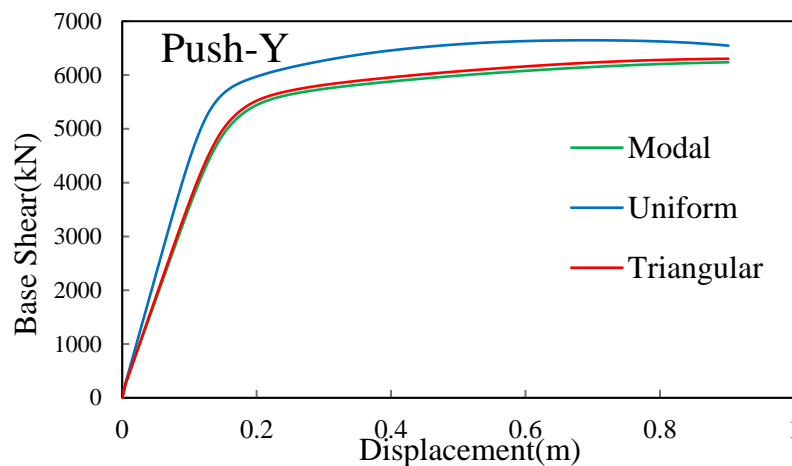


Figure 4-9: Effects of Lateral Load pattern on 3D Pushover Y

As it is presented in figures 4-8 and 4-9, nonlinear static pushover analyses for uniform, triangular and modal load distributions for the 3D frame are compared. The above plots show that the static lateral load analysis strongly depends on the lateral force distribution pattern than the magnitude of the force. Uniform or rectangular distribution always give the higher base shear comparing to other load distributions for the corresponding story displacement.

4.4.3 Imperfections and Second-order Effects in Pushover Analysis Results

After studying the effects of lateral load patterns, the effects of imperfections and geometric nonlinearities were studied for both 2D and 3D frames. The results are presented in the following subsections.

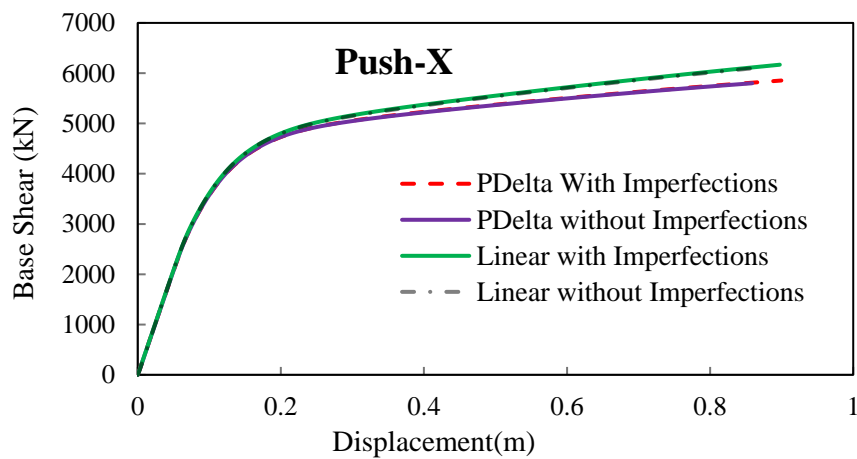


Figure 4-10: Second order effects and Initial Imperfections on Plane Frame X direction

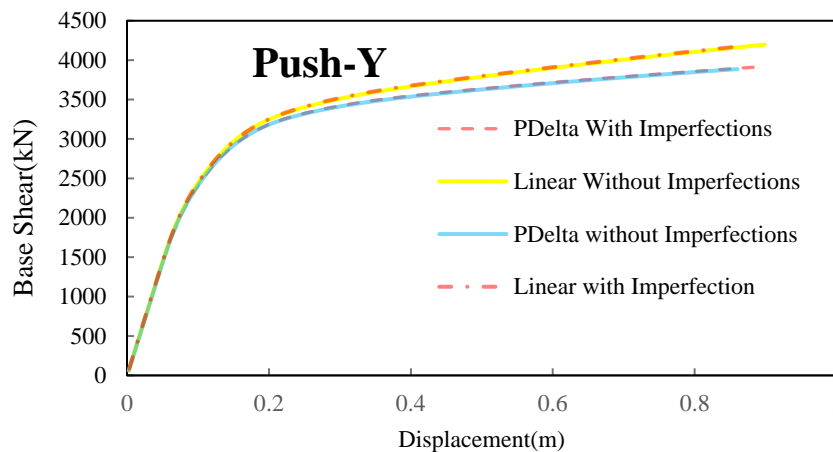


Figure 4-11: Second-Order Effects and Imperfections on Plane Frame Y Direction

Figure 4-10 and Figure 4-11 present the effects of second-order analysis and initial imperfections on the pushover analysis of plane frames along the two orthogonal

directions. It can be observed from these plots that the effects of initial imperfections (global sway and initial residual stress) are small as compared to the second-order analysis which accounts for the geometric nonlinear effects. The first order analysis method overestimates the base shear for a specified roof displacement compared to the geometric nonlinear analysis. The second-order analysis which accounts for global sway and initial residual stress predicts the base shear and roof displacements well than that of the first-order analysis.

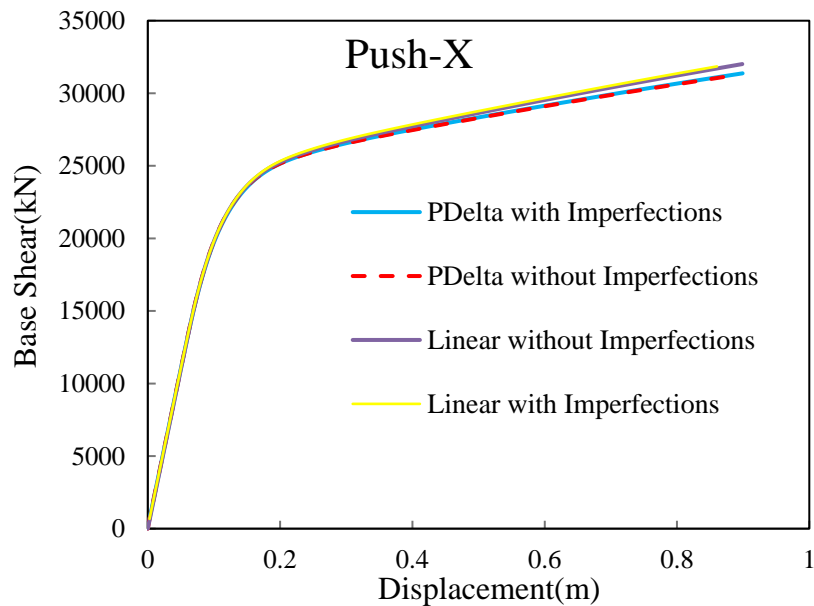


Figure 4-12: Second-Order Effects and Imperfections for 3D Frame X direction

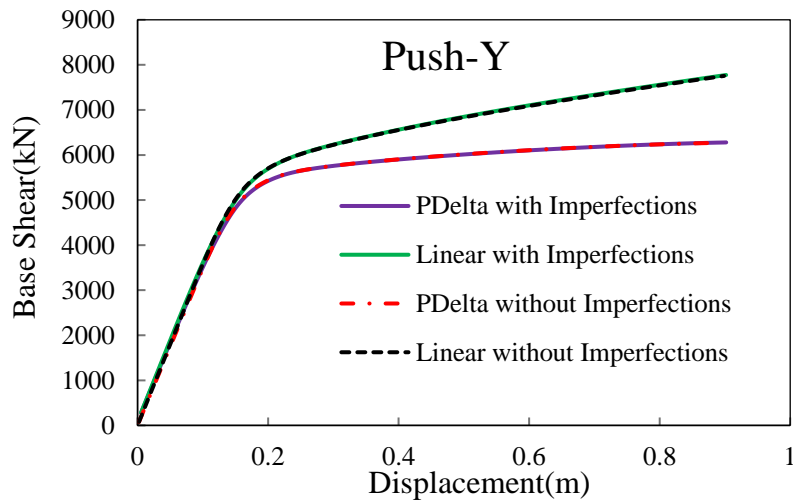


Figure 4-13: Second-Order Effects and Imperfections for 3D Frame Y direction

As it is described in Figure 4-12 Figure 4-13 the nonlinear static analysis of three-dimensional steel frames is affected by several parameters. The plot shows that the effect of initial sway imperfections and residual stresses are negligible as compared to the second-order effects. The pushover analysis of three-dimensional frames indicates that larger forces are required to displace the structure in the x-direction than in the y-direction, the reason behind it is that heavier sections were used for the frames in the x-direction and all of the frames were assumed to be moment-resisting frame.

4.4.4 Nonlinear Dynamic Analysis Results of Plane Frames

The following section describes the effects of imperfections and second-order analysis on plane frames considered in this research.

4.4.4.1 Roof Displacement

The time-history roof displacements for the selected ground motions are presented in figure 4-14. The roof displacement is assessed at the same node as the displacement in the non-linear static analysis. The maximum roof displacements for each analysis case are presented in Table 4-10.

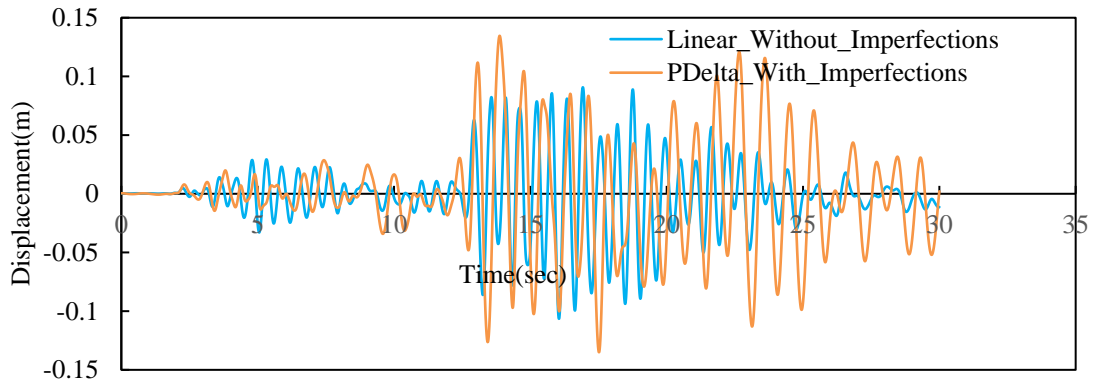
Table 4-10 Maximum Roof Displacements for 2D Analysis

Earthquake	dmax(m)Without Imperfection	dmax(m)With Imperfection
Northern Calif-03	0.107	0.135
Imperial Valley-06	0.111	0.161
Mammoth Lakes-01	0.112	0.253
Victoria_ Mexico	0.099	0.142
Chalfant Valley-02	0.110	0.151
Superstition Hills-02	0.105	0.168
Landers	0.054	0.136

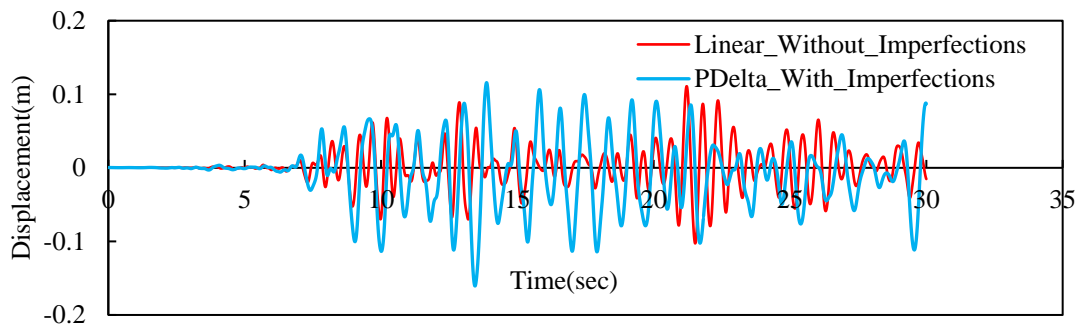
According to section 4.3.3.4.3 of [4], the average response parameter of the seven analysis must be used as the design value. Hence, the expected maximum roof displacements are equal to

$d_{max}=0.100m$ for linear geometric transformation without considering imperfections

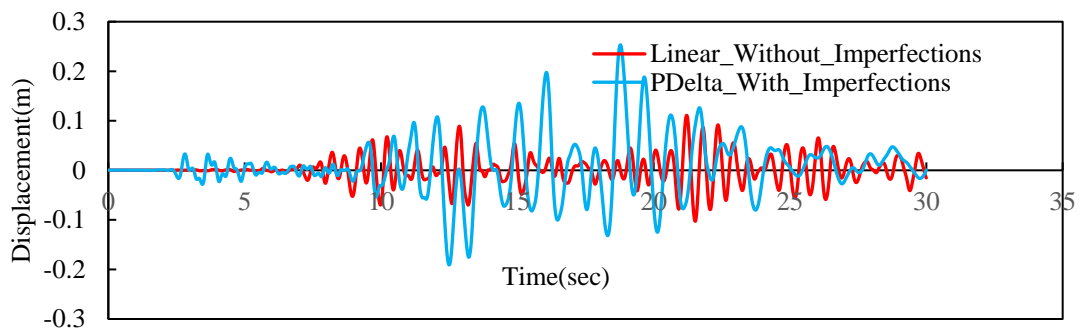
$d_{max}=0.164$ for PDelta geometric transformation with imperfections.



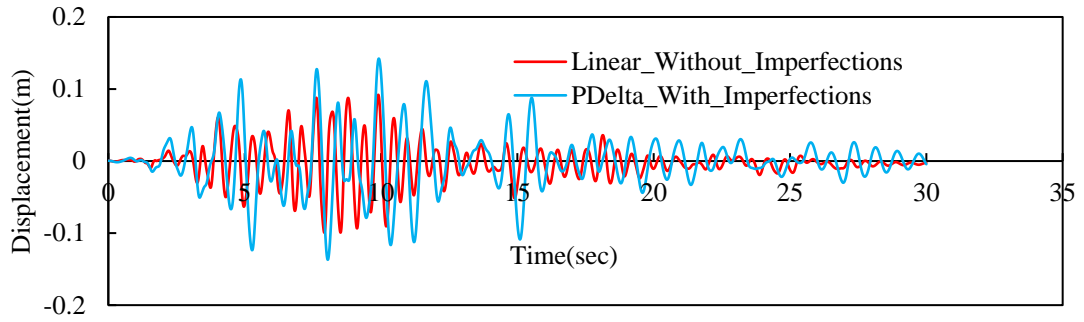
a) Northern Calif-03



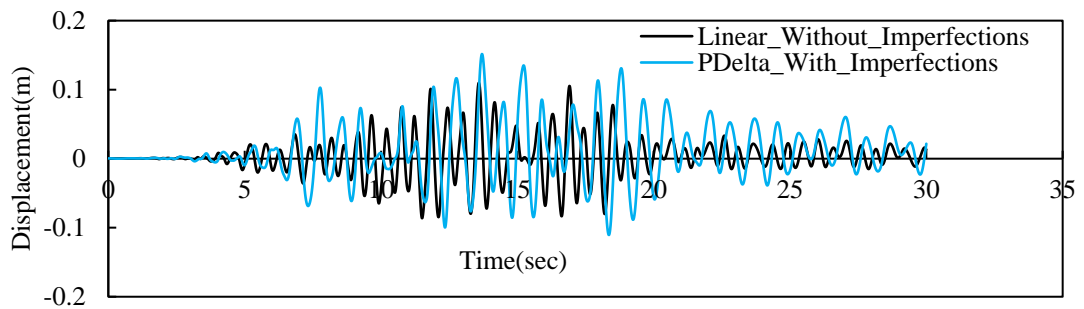
b) Imperial Valley-06



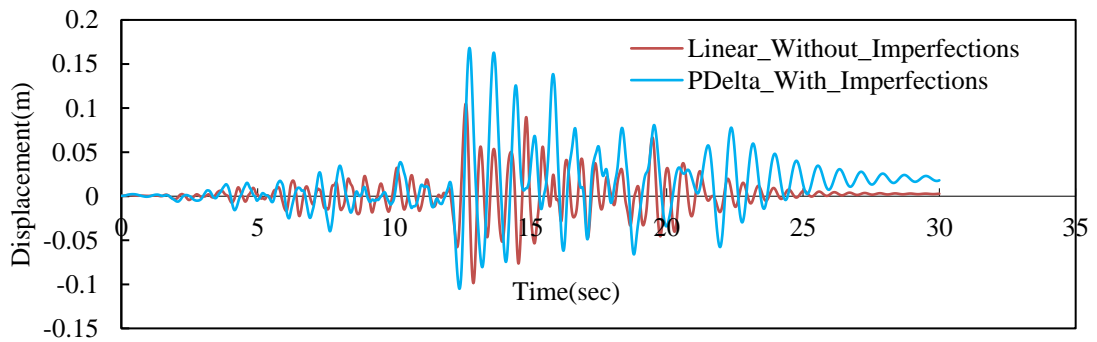
c) Mammoth Lakes-01



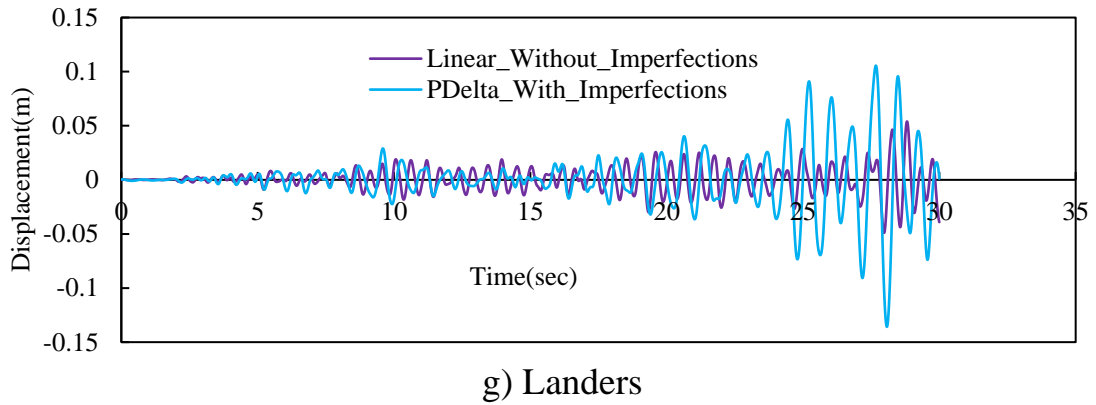
d) Victoria_Mexico



e) Chalfant Valley-02



f) Superstition Hills-02

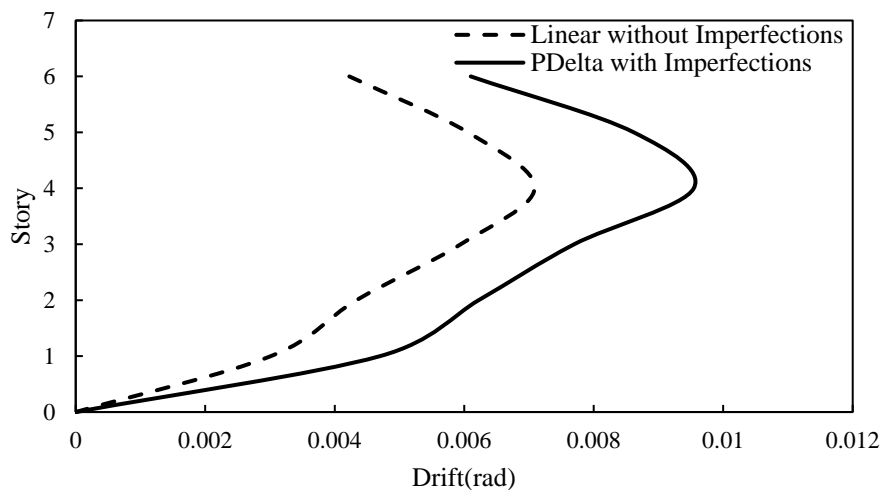


g) Landers

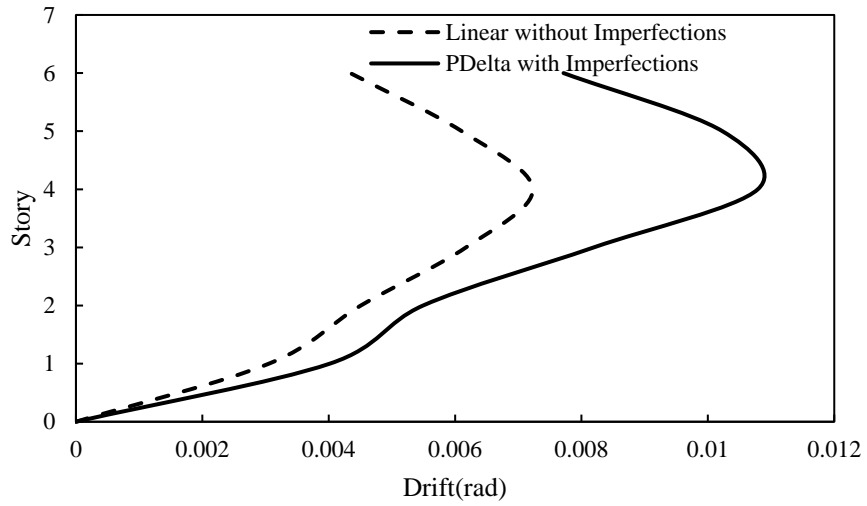
Figure 4-14: Displacement Responses of the Roof

4.4.4.2 Inter Story Drift

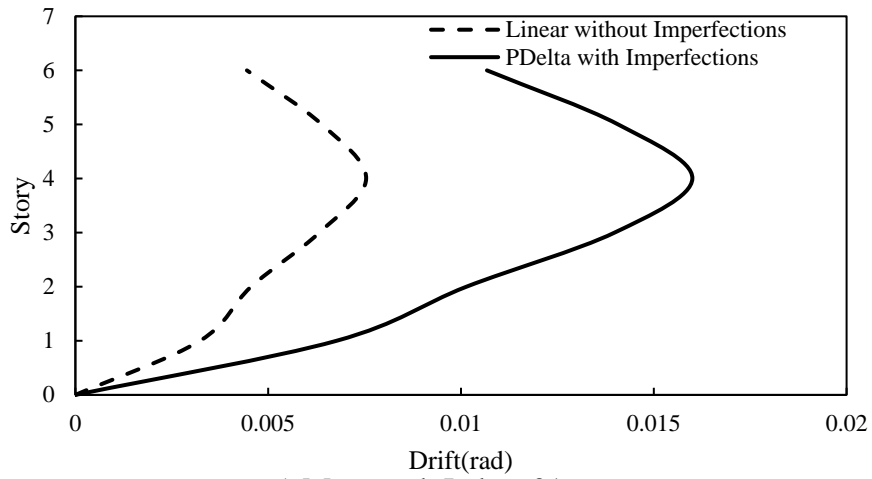
Figure 4-15 presents a comparison between the inter-story drift ratios (IDR) from the seven ground motions for linear geometric transformation and pdelta geometric transformation with imperfections. It should be noticed that the maximum IDRs are not attained simultaneously during the time-history. Drift ratios caused by Northern Calif-03 and Imperial Valley-06 are presented in (figure 4-15 a & b) respectively. Both ground motions induce drift ratios that are nearly similar to each other for first-order and second-order analyses. The drift ratios for the Victoria Mexico earthquake are similar for the first story and slightly different results are obtained for other stories for both types of analyses (figure 4-15 d). Mammoth Lakes-01 and Landers ground motions induce significant variation of drift ratios from both types of analyses.



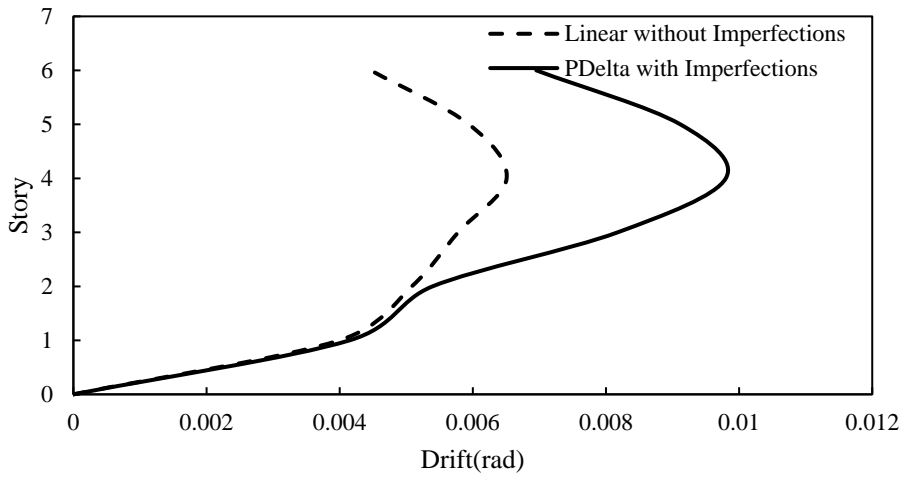
a) Northern Calif-03



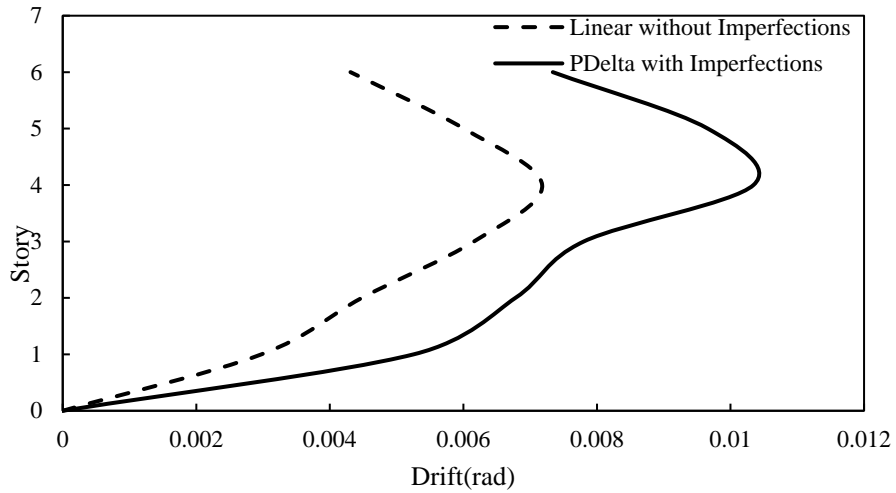
b) ImperialValley-06



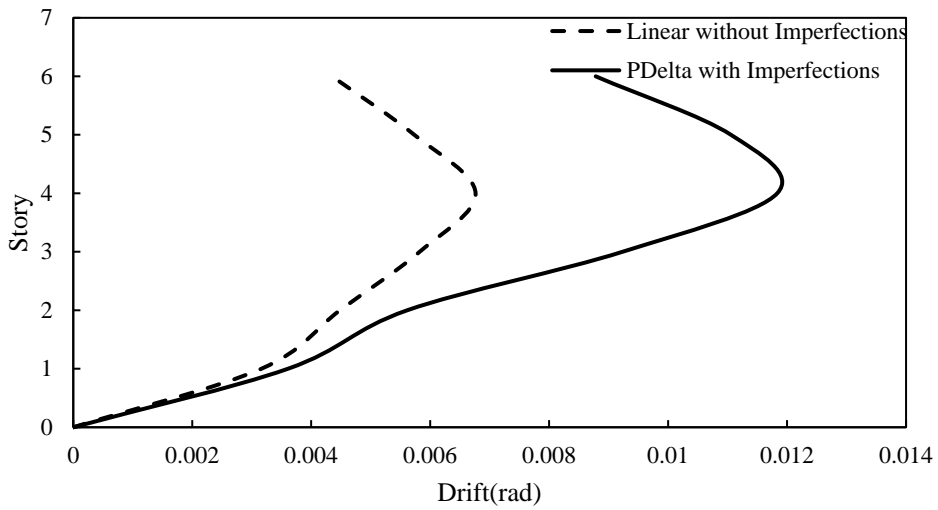
c) Mammoth Lakes-01



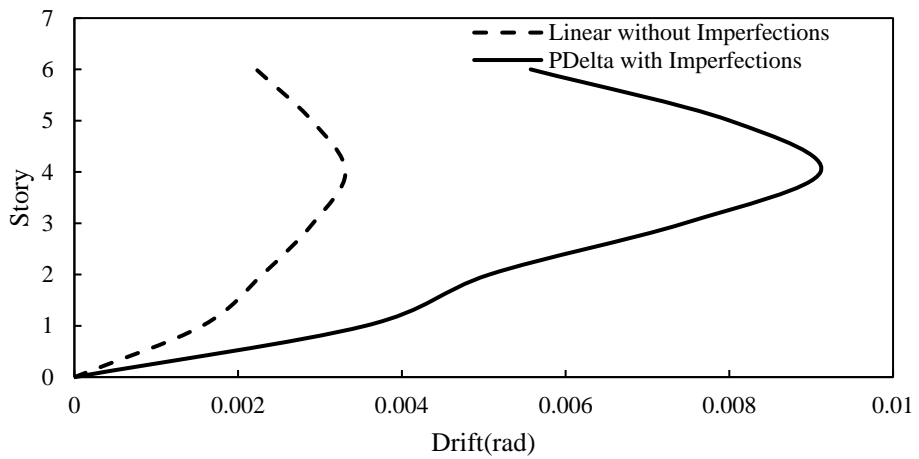
d)Victoria_Mexico



e) Chalfant Valley-02



f) Superstition Hills-02



g) Landers

Figure 4-15: Inter Story Drift Comparison

CHAPTER 5 CONCLUSIONS & RECOMMENDATIONS

5.1 Conclusions

This research is focused mainly on the seismic analysis of MRFs by considering geometric and material nonlinearities and initial imperfections. The following conclusions can be drawn based on the results obtained in chapter 4.

The analysis of isolated columns with different boundary conditions shows that relatively smaller meshes are required for modeling of the cantilever column. For the pin ended column, considering an even number of elements per member can better estimate the maximum responses (i.e. mid-span moment and deflection) as they can follow the pattern of imperfection assumed to be half-sine wave.

A sway portal frame was analyzed by incorporating imperfections into the geometry of the frame as well as replacing imperfections with equivalent lateral loads. The results of linear static analysis show that the modeling by an equivalent lateral load of imperfections gives fair results as that of direct modeling. It can be observed from such analysis that a single portal frame is not mesh sensitive. This means that a relatively small number of elements can be used per member to model the frame by finite element method.

Modeling of the frame by force-based nonlinear beam-column elements using both SeismoStruct and OpenSees shows a good agreement between the two finite element programs. Both the initial sway imperfections that were replaced by a system of equivalent lateral loads and residual stresses were modeled using OpenSees. Results of the pushover analysis show that the effect of initial imperfections on moment-resisting steel frames is less than that of the second-order effects.

The lateral load distribution in nonlinear static analysis strongly affects the analysis results. Uniform lateral load pattern overestimates the base shear. The modal distribution pattern which is based on the first mode of vibration from the linear elastic analysis can better predict structural responses than the uniform pattern.

5.2 Recommendations

Appropriate lateral load distribution pattern should be used for pushover analysis of structures. Modeling of imperfections by equivalent lateral load can be adopted for analysis of steel frames due to its simple modeling assumption and less computational time. Sufficient number of elements should be considered for finite element analysis of members with initial bow imperfections. Care should be taken in dividing a member to elements in assigning imperfections to follow the buckling mode. Relatively smaller meshes can be applied for modeling the cantilever column with imperfection

The work presented in this thesis is based on two-dimensional and three-dimensional frames with steel compact cross-sections. Therefore, the effect of local buckling was not considered. Further work is required to incorporate the effect of local buckling into a beam-column finite-element model and determine the appropriate system resistance factors.

This research is focused on seismic analysis of MRFs only, further investigation is required for seismic analysis of CBFs or EBFs. It is not common to design space frames as moment-resisting frame because of economic constraints, the most feasible construction can be achieved by including leaning columns or $p \Delta$ columns that has no contribution for lateral load resisting system. Moment resisting frames or braced frames are usually placed at the periphery of the structure. Further study can be done by including leaning columns into the space frame structure.

This research assumes that the sway frames have rigid connections that are sufficiently strong and ductile to support the forces and deformation imposed under the loads. In future analysis, it is necessary to consider the effect of connection behaviors (panel-zone modeling) and their uncertainty on system resistance factors.

The work presented assumes that all columns are entirely fixed to the ground, and further study that considers the effect of soil-structure interaction is required. This work also assumes that the floor slabs are infinitely rigid, thus applying the rigid diaphragm principle to the system is possible. It is important to further examine the effect of semi-rigid diaphragms (both vertical and horizontal) and their uncertainties regarding system resistance factors.

REFERENCES

- [1] A. Y. Elghazouli, *Seismic Design of Buildings to Eurocode 8*. London and New York: Spoon Press, 2009.
- [2] Y. Xue, “Capacity Design Optimization of Steel Building Frameworks Using Nonlinear Time-History Analysis,” 2012.
- [3] A. Al-Ali and H. Krawinkler, “Seismic demand evaluation for a 4-story steel frame structure damaged in the Northridge earthquake,” *Struct. Des. Tall Build.*, vol. 5, no. 4, pp. 1–27, 1996.
- [4] ES EN 1998-1, “Design of Structures for Earthquake Resistance Part 1 : General Rules, Seismic Actions and Rules for Buildings,” Addis Ababa, 2015.
- [5] ES EN 1993-1, “Design of steel structures – Part 1-1 : General Rules and Rules for Buildings,” Addis Ababa, 2015.
- [6] AISC, *Specification for Structural Steel Buildings*. Chicago: ANSI/AISC 360-10, 2010.
- [7] Z. Kala, “Sensitivity analysis of steel plane frames with initial imperfections,” *Eng. Struct.*, vol. 33, no. 8, pp. 2342–2349, 2011.
- [8] D. Bernal, “Instability of buildings during seismic response,” *Eng. Struct.*, vol. 20, no. 4, pp. 496–502, 1998.
- [9] G. A. MacRae, “Pdelta effects on SDOF Structures in Earthquakes,” *Earthq. Spectra*, vol. 10, no. 3, pp. 540–568, 1994.
- [10] E. B. Williamson, “Evaluation of Damage and Pdelta Effects for Systems Under Earthquake Excitation,” *Struct. Eng.*, vol. 129, no. 8, pp. 1036–1046, 2003.
- [11] S. Jovašević, “Parametric Study on Seismic Behaviour of Dual-Concentrically Braced Steel Frames,” University of Coimbra, 2015.
- [12] L. F. Ibarra and H. Krawinkler, “Global Collapse of Frame structures under Seismic Excitations,” Stanford, CA, 2005.

- [13] R. Mohshen and H. Krawinkler, “Effects of Soft Soil and Hysteresis model on Seismic Demands,” Stanford, CA, 1993.
- [14] L. Dimitrios, “Sidesway Collapse of Deteriorating Structural Systems Under Seismic Excitations,” Stanford, 2008.
- [15] K. Mathur, “Effects of residual stresses and initial imperfections on Earthquake response of steel moment frames,” University of Illinois at Urbana-Champaign, 2011.
- [16] A. L. Yen-Cheng, “Effects of Member Overstrength And Initial Residual Stresses On the Behaviour of 2D Steel Structure,” University of Canterbury, 2011.
- [17] R. Villaverde, “Methods to Assess the Seismic Collapse Capacity of Building Structures : State of the Art,” *Struct. Eng.*, vol. 133, no. 1, pp. 57–66, 2007.
- [18] S. Shabnam, K. J. Rasmussen, and H. Zhang, “On the modeling of initial geometric imperfections of steel frames in advanced analysis,” *JCSR*, vol. 98, pp. 167–177, 2014.
- [19] FEMA-350, “Recommended Seismic Design Criteria for New Steel Moment Frame Buildings,” Washington DC, 2000.
- [20] K. Lee and D. A. Foutch, “Performance evaluation of new steel frame buildings for seismic loads,” *Earthq. Eng. Struct. Dyn.*, vol. 31, no. 1, pp. 653–670, 2002.
- [21] K. Lee and D. A. Foutch, “Seismic Evaluation of Steel Moment Frame Buildings Designed Using Different R -Values,” *Struct. Eng.*, vol. 132, no. 9, pp. 1461–1472, 2007.
- [22] V. Filip, S. Aurel, and D. Dubina, “Seismic performance of multistorey steel frames with strain hardening friction dampers,” *Proc. Rom. Acad. Ser. A* vol. 15, no. 2, pp. 174–181, 2014.
- [23] A. Henriksson and J. Panarelli, “Initial bow imperfection for flexural buckling of steel members,” Chalmers University of Technology, 2017.
- [24] ECCS, “Eurocode 8: Design of structures for earthquake resistance Part 1-1 –

- General rules, seismic actions, and rules for buildings,” ECCS – European Convention for Constructional Steelwork, 2017.
- [25] G. G. Deierlein, A. M. Reinhorn, and M. R. Willford, “Nonlinear Structural Analysis For Seismic Design A Guide for Practicing Engineers,” U.S. Department of Commerce, 2010.
- [26] M. A. Khan, *Modern Earthquake Engineering. Offshore and Land-based Structures Structures*, 1st ed. Bergen, Norway: Springer, 2017.
- [27] S. Antoniou and R. Pinho, “Advantages and limitations of adaptive and non-adaptive force-based pushover procedures,” *Earthq. Eng.*, vol. 8, no. 4, pp. 497–522, 2004.
- [28] R. D. Ziemian, *Guide to Stability Design Criteria for Metal Structures*, 6th ed. Hoboken, New Jersey: John Wiley & Sons Inc., 2010.
- [29] ECCS, *Design of Steel Structures : ECCS Eurocode design manuals*, U.K. United Kingdom: ECCS – European Convention for Constructional Steelwork, 2014.
- [30] T. V. Galambos and A. E. Surovek, *Structural Stability of Steel: Concepts and Applications for Structural Engineers*. John Wiley & Sons, Ltd, 2008.
- [31] J. D. Aristizabal-Ochoa, “Induced moments and lateral deflections in columns with initial imperfections and semirigid connections: II Verification and examples,” *Theory Dyna*, vol. 172, no. 79, pp. 18–28, 2012.
- [32] W. Liu, J. R. Kim, and H. Zhang, “On the Modelling of Geometric Imperfection in 3D Steel Unbraced Frames,” *EuroSteel*, vol. 1, no. 10, pp. 10–18, 2014.
- [33] ECCS, *Design of Steel Structures*, 2nd ed. ECCS – European Convention for Constructional Steelwork, 2016.
- [34] A. Collow, A. Chand, and G. Macrae, “Axial - moment interaction and load path dependency for steel columns,” 2017.
- [35] SeismoSoft, “SeismoStruct- A Computer Program for Static and Dynamic Nonlinear Analysis of Framed Structures.” SeismoSoft Ltd., Piazza Castelo 19,

Italy, 2018.

- [36] ES EN 1990, “Basis of Design and Actions on Structures,” Addis Ababa, 2015.
- [37] Computers&Structures, “ETABS- Extended Three -Dimensional Analysis of Building Systems.” CSI Inc., California, Berkeley, 2016.
- [38] PEER, “OpenSees: Open System for Earthquake Engineering Simulation.” Pacific Earthquake Engineering Research Center, University of California, Berkeley, CA, 2016.
- [39] G. L. Fenves and F. McKenna, “Open System for Earthquake Engineering Simulation,” 2016. [Online]. Available: <http://opensees.berkeley.edu>. [Accessed: 24-Sep-2019].
- [40] F. McKenna, “OpenSees: A Framework for Earthquake Engineering Simulation,” *California, Berkeley*, 2011.
- [41] F. Fllippou, E. P. Popov, and V. V Bertero, “Effects of bond deterioration on hysteretic behavior of reinforced concrete joints,” Berkeley, California, 1983.
- [42] S. Mazzoni, F. Mckenna, M. H. Scott, and G. L. Fenves, “OpenSees Command Language Manual,” University of California, Berkeley, 2007.
- [43] J. B. Mander, M. J. N. Priestley, and R. Park, “Theoretical Stress-Strain Model for Confined Concrete,” *Struct. Eng.*, vol. 114, no. 8, pp. 1804–1826, 1989.
- [44] F. J. Vecchio and M. B. Emar, “Shear Deformations in Reinforced Concrete Frames,” *ACI Struct. J.*, vol. 6, no. 89, pp. 46–56, 1992.
- [45] S. Güner, “Performance Assessment of Shear Critical Reinforced concrete Plane Frames,” Toronto, 2008.

Appendix A Tables and Equations

Table A--5-1: Recommended Values of Parameters for Type 1 Elastic Response Spectra [4]

Ground-type	S	T_B (s)	T_C (s)	T_D (s)
A	1.0	0.15	0.4	2.0
B	1.2	0.15	0.5	2.0
C	1.15	0.20	0.6	2.0
D	1.35	0.20	0.8	2.0
E	1.4	0.15	0.5	2.0

$$\begin{aligned}
 0 \leq T \leq T_B: S_e(T) &= a_g \cdot S \cdot \left[1 + \frac{T}{T_B} (2.5 \cdot \eta - 1) \right] \\
 T_B \leq T \leq T_C: S_e(T) &= a_g \cdot S \cdot \eta \cdot 2.5 \\
 T_C \leq T \leq T_D: S_e(T) &= a_g \cdot S \cdot \eta \cdot 2.5 \left[\frac{T_C}{T} \right] \\
 T_D \leq T \leq 4s: S_e(T) &= a_g \cdot S \cdot \eta \cdot 2.5 \left[\frac{T_C T_D}{T^2} \right]
 \end{aligned} \tag{A-5-1}$$

$S_e(T)$ is the elastic response spectrum;

T is the vibration period of a linear single-degree-of-freedom system;

a_g is the design ground acceleration on type A ground ($a_g = \gamma I \cdot a_{gR}$);

T_B is the lower limit of the period of the constant spectral acceleration branch;

T_C is the upper limit of the period of the constant spectral acceleration branch;

T_D is the value defining the beginning of the constant displacement response range of the spectrum;

S is the soil factor; η is the damping correction factor with a reference value of $\eta = 1$ for 5% viscous damping.

$$\eta = \sqrt{\frac{10}{5 + \xi}} \geq 0.55 \tag{A-5-2}$$

$$\begin{aligned}
 0 \leq T \leq T_B: S_d(T) &= a_g \cdot S \cdot \left[\frac{2}{3} + \frac{T}{T_B} \left(\frac{2.5}{q} - \frac{2}{3} \right) \right] \\
 T_B \leq T \leq T_C: S_d(T) &= a_g \cdot S \cdot \frac{2.5}{q} \\
 T_C \leq T \leq T_D: S_d(T) &\begin{cases} = a_g \cdot S \cdot \frac{2.5}{q} \left[\frac{T_C}{T} \right] \\ \geq \beta \cdot a_g \end{cases} \\
 T_D \leq T: S_d(T) &\begin{cases} = a_g \cdot S \cdot \frac{2.5}{q} \left[\frac{T_C T_D}{T^2} \right] \\ \geq \beta \cdot a_g \end{cases}
 \end{aligned} \tag{A-5-3}$$

$S_d(T)$ is the design spectrum; q is the behavior factor;

β is the lower bound factor for the horizontal design spectrum.

NOTE The value to be ascribed to β for use in a country can be found in its National Annex. The recommended value for β is 0.2.

Appendix B Software Verification

Three verification examples were presented here for verifying the finite element programs against experimental results.

Verification Example 1: Reinforced Concrete Cantilever Column

The cantilever column tested by Lehman et.al 1998 is presented here for verification of OpenSees and SeismoStruct. The geometry, loading condition and section properties of the column are shown in figure B-5-1.

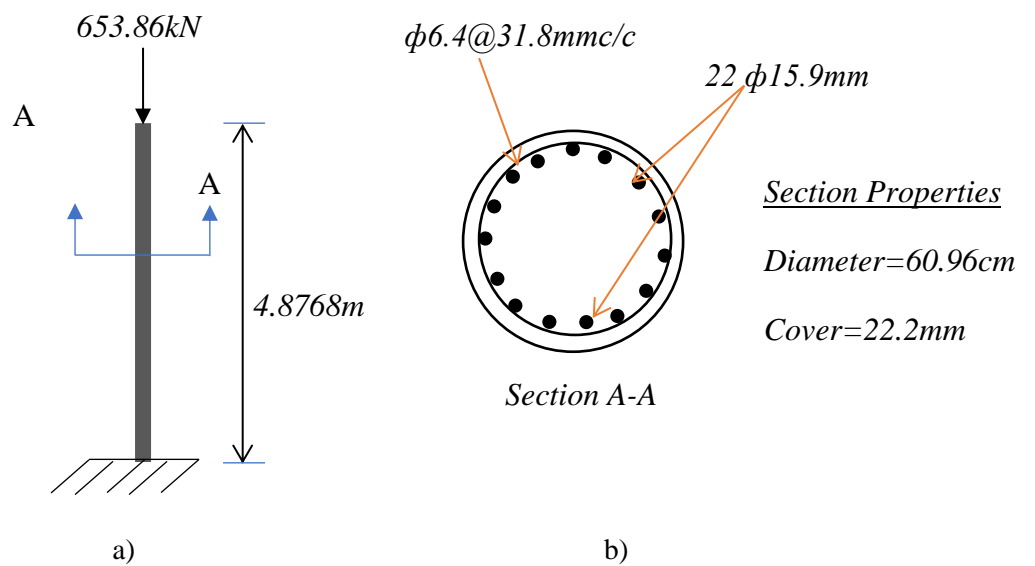


Figure B-5-1: Geometry and loading condition (a) section properties (b) of the column

Table B-5-2 Material properties of Lehman et al.1998 column

Reinforcement						Concrete		
Type	ϕ	f_y	f_u	E_s	ϵ_{sh}	f_c	E_c	ϵ_0
(-)	(mm)	(MPa)	(MPa)	(GPa)	($\times 10^{-3}$)	(MPa)	(GPa)	($\times 10^{-3}$)
Longitudinal	15.9	462	630	200	10	31	26.168	2
Transversal	6.4	606.8	-	200	10			

Concrete02 and Steel02 materials were used for modeling the column in OpenSees. Force-based distributed plasticity with five integration sections were used for modeling the cantilever column. The mander model [43] was implemented for modeling the stress-strain behavior of concrete. number of theta divisions in the core (number of wags) was 20 and the number of radial divisions in the core (number of "rings") was 28. The number of fibers

was assumed to be 12 for both theta and radial divisions for the cover concrete. The corotational geometric transformation was used in OpenSees to account for second-order effects. The figure presents the force deformation relationship of the cantilever column analyzed by OpenSees and SeismoStruct against the experimental results reported by Lehman et.al 1998. As can be shown in figure B-5-2 the results are nearly similar from these finite element programs.

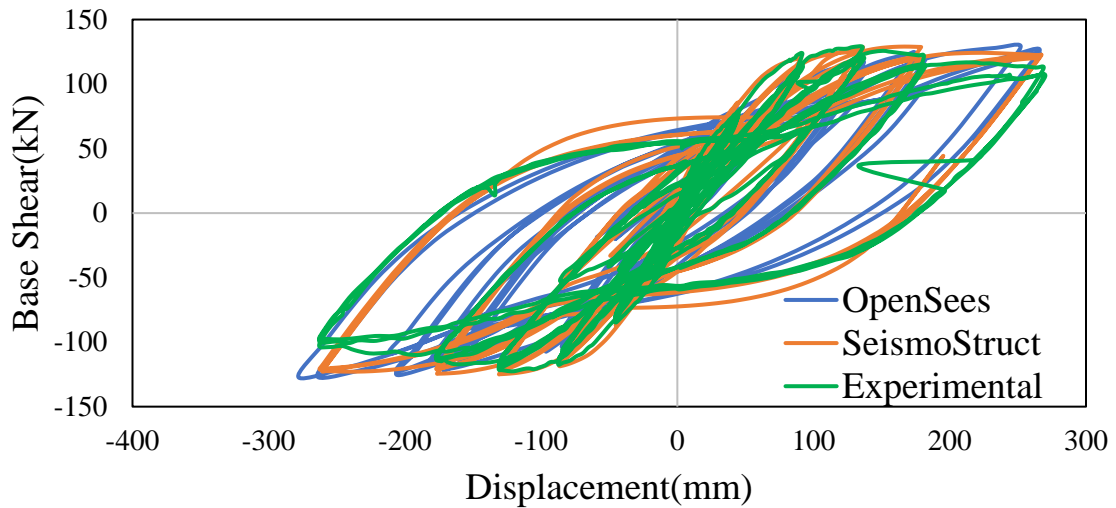


Figure B-5-2: Force deformation relationship of the column tested by Lehman

Verification Example 2: One Bay Two-Story Reinforced Concrete Plane Frame

The frame tested by Vecchio and Emaral[44] was used for verification of OpenSees. The force-based distributed plasticity approach with five integration points were employed for both OpenSees and SeismoStruct. Second-order effects were considered in both of the programs. As can be shown in figure B-5-4 the results are almost similar from the two finite element programs.

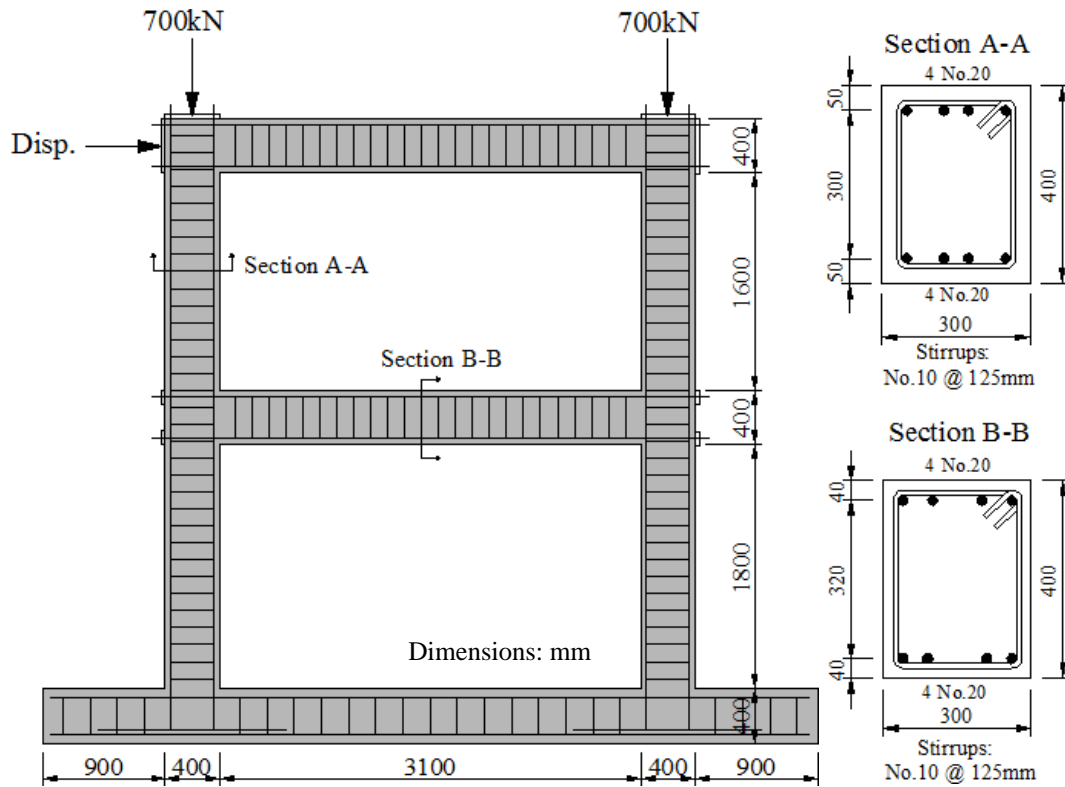


Figure B-5-3: Details of Vecchio and Emara Frame[45]

Table B-5-3: Material Properties of Vecchio and Emara Frame

Bar no.	Reinforcement								Concrete		
	A_s (mm^2)	ϕ (mm)	f_y (MPa)	f_u (MPa)	E_s (GPa)	E_{sh} (MPa)	ϵ_{sh} ($\times 10^{-3}$)	ϵ_u ($\times 10^{-3}$)	f_c (MPa)	E_c (GPa)	ϵ_0 ($\times 10^{-3}$)
20	300	19.5	418	596	192.5	3100	9.5	66.9	30	23.674	1.85
10	100	11.3	454	640	200	3100	9.5	69.5			

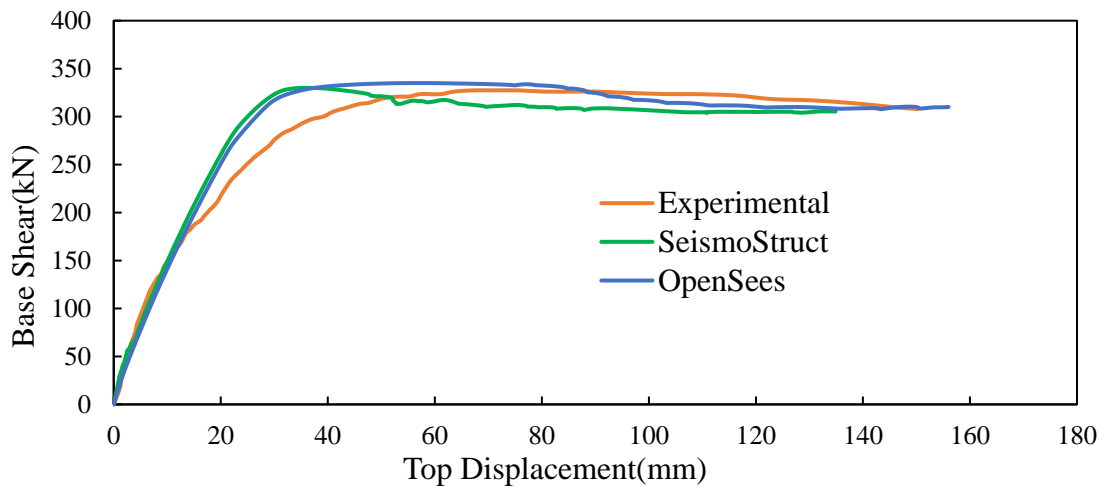
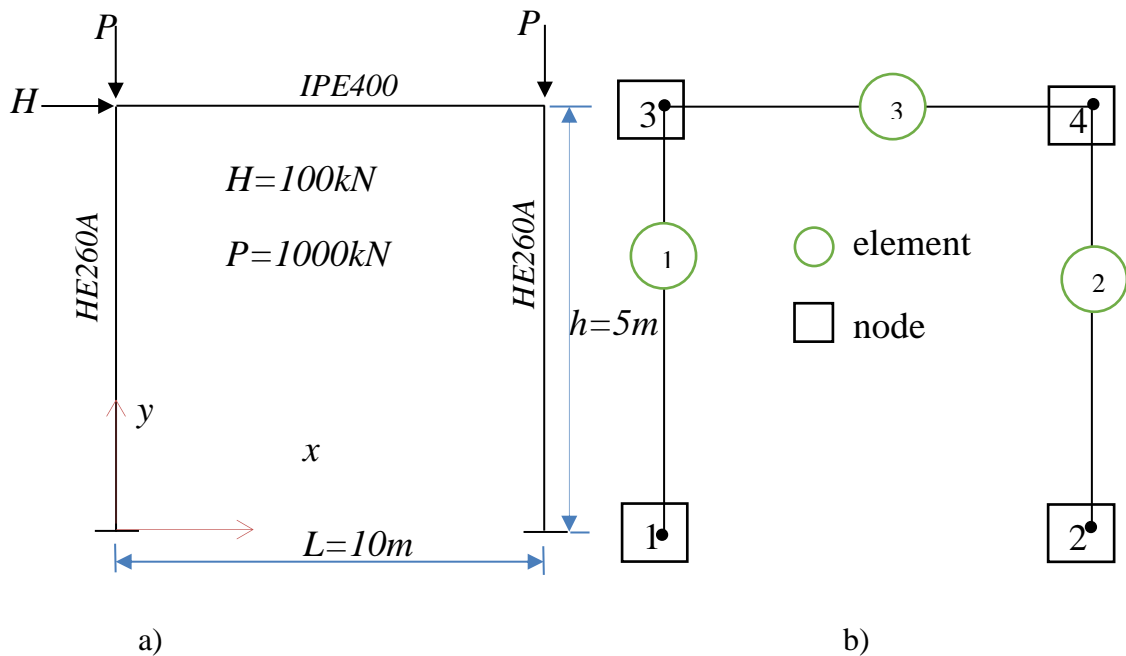


Figure B-5-4: Base shear vs top story displacement of Vecchio & Emara Frame

Verification Example 3: Steel Portal Frame

A single portal frame shown on figure B-5-5 (a) has been analyzed by both MATLAB and OpenSees to compare the second-order elastic analysis results from the two programs. And to check the capability of the software on second-order analysis. The frame was discretized and modeled as 10 elements per member in OpenSees and the notations are as shown in figure B-5-5(b). As is presented in table B-5-4 the elemental forces obtained from the two programs are almost similar. As can be presented on table B-5-5 the nodal displacements for the portal frame analyzed by both programs are nearly identical.


Figure B-5-5: Geometry (a) Node & Element Assignments (b) of Portal Frame
Table B-5-4 Elemental Forces

Elem	OpenSees			MATLAB		
	$N_{Ed}(kN)$	$M_{Ed}(kNm)$		$N_{Ed}(kN)$	$M_{Ed}(kNm)$	
1	974.588	162.414	-127.327	974.582	162.420	-127.357
2	1025.410	161.236	-126.786	1025.417	161.237	-126.814
3	49.659	127.327	-126.786	49.658	127.357	-126.814

Table B-5-5 Nodal Displacements

Node	OpenSees			MATLAB		
	$u_x(m)$	$u_y(m)$	$\Theta(rad)$	$u_x(m)$	$u_y(m)$	$\Theta(rad)$
3	0.0390	-0.0027	-0.0044	0.0391	-0.0027	-0.0044
4	0.0387	-0.0028	-0.0044	0.0388	-0.0028	-0.0044

Appendix C OpenSees Script for Plane Frames

The following tcl files are required to run the model for plane frames in OpenSees.

- a) **UnitsLibrary.tcl**; #Defining systems of units
- b) **Isection.tcl**; # Procedure to create Steel Fiber section
- c) **5bay6StoryMain.tcl**; #The main frame model
- d) **StaticAnalysisParameters.tcl**;**#** set up parameters for static analysis of 2D frame
- e) **PushoverAnalysisCommand.tcl**;**#**Analysis command for static analysis of 2D frame
- f) **DynamicAnalysisParameters.tcl**;**#**set up parameters for dynamic analysis of 2D
- g) **DynamicAnalysisCommand.tcl**;**#**Analysis command for dynamic analysis of 2D frame

The above stated files for a 6-story steel moment resisting plane frame are presented below:

a) UnitsLibrary.tcl

```
#####
# This TCL file is used to define all the units used in the analysis of the frame
# File Name: UnitsLibrary.TCL
# Written by: Mekuriaw Mihrete
# Place: Addis Ababa Institute of Technology
# Date: August, 2019
#####
puts "units Definition started"
set m 1.; # define basic units -- output units
set KN 1.; # define basic units -- output units
set sec 1.; # define basic units -- output units
set rad 1.; # define basic units -- output units
set N [expr $KN/1000]; # 1N=kN/1000
set KNm [expr $KN*$m]; # 1kNm=1000Nm
set LunitTXT "m"; # define basic-unit text for output
set FunitTXT "KN" ; # define basic-unit text for output
set MunitTXT "KNm"; # define basic-unit text for output
set TunitTXT "sec"; # define basic-unit text for output
set mm [expr $m/1000.]; # millimeter 1mm=1m/1000
set cm [expr $m/100.]; # centimeter, 1cm=1m/100
set KNpm [expr $KN/$m]; # KN/m used for uniformly distributed load
set KNpm2 [expr $KN/pow($m,2)]; # KiloNewton per square meter
set KNpm3 [expr $KN/pow($m,3)]; # KiloNewton per cubic meter
set m3 [expr $m*$m*$m]; #cubic meter
set mm2 [expr $mm*$mm]; #square millimeter(mm^2)
set mm3 [expr $mm*$mm*$mm]; #cubic millimeter(mm^3)
set mm4 [expr $mm*$mm*$mm*$mm]; #millimeter to the power 4, (mm^4)
set cm2 [expr $cm*$cm]; #square centimeter, cm^2
set cm3 [expr $cm*$cm*$cm]; #Cubic centimeter,cm^3
set cm4 [expr $cm*$cm*$cm*$cm]; #centimeter to the power 4,cm^4
```

```

set MPa [expr $N/$mm2];      #Mega pascal,Mpa
set GPa [expr $KN/$mm2];    #Giga pascal,Gpa
set Kg [expr $N*$sec*$sec/$m];  #Kilogram,Kg
set Kgpm3 [expr $Kg/$m*$m*$m];  #Kilogram per cubic meter, Kg/m^3
set PI [expr 2*asin(1.0)];    #PI=3.141592653589793 radians
set g [expr 9.81*$m/pow($sec,2)]; #gravitational acceleration
set p [expr 7850*$Kg/$m3];    #density of steel,p=7850Kg/m3
set deg [expr $PI/180];      #conversion factor for degree to radians
set E [expr 210*$GPa];      #young's modulus of steel
set nu 0.3;                  #poison's ratio,v
set Gs [expr $E/2./[expr 1+$nu]]; #shear modulus/ modulus of rigidity
set Ubig 1.e10;              # a really large number
set Usmall [expr 1/$Ubig];   # a really small numberer
#####***Conversion of units from US customary units to SI units #####
set in [expr 2.54*$cm];      #1in =2.54cm
set lbf [expr 4.4482216*$N];  #pound force
set lbm [expr 0.4536*$Kg];   #pound mass
set kip [expr 1000.*$lbf];   #Kilo pounds
set ft [expr 12*$in];       #feet, 1ft =12in
set ksi [expr 1000.*$lbf/pow($in,2)]; #Kilo pounds per square inch
set psi [expr $ksi/1000.];   #pound per square inch
set pcf [expr $lbf/pow($ft,3)]; #pounds per cubic foot
set psf [expr $lbf/pow($ft,3)]; #pounds per square foot
set in2 [expr $in*$in];     #inch^2
set in4 [expr $in*$in*$in*$in]; #inch^4
#set g [expr 32.2*$ft/pow($sec,2)]; #gravitational acceleration g=32.2ft/s2
#set g [expr $lbf/$lbm];    #g can also be expressed as the #ratio of lbf/lbm

```

b) Isection.tcl

```

proc Isection { secID matID h bf tf tw nfdw nftw nfbf nftf } {
#####
# create a standard European I section given the nominal section properties
# written: Mekuriaw Mihrete
# date: 02/10/2019
# input parameters
# secID - section ID number
# matID - material ID number
# h = nominal depth
# tw = web thickness
# bf = flange width
# tf = flange thickness
# nfdw = number of fibers along web depth
# nftw = number of fibers along web thickness
# nfbf = number of fibers along flange width
# nftf = number of fibers along flange thickness

```



```

        set y [expr $Hstory1+($Level-2)*$HstoryTyp]; #levels 3,4,5,6 &7 elevations of other
storey columns
    }
    set NodeID [expr $Dlevel*$Level+$pier]
    node $NodeID $x $y;
    #puts "$NodeID\t$x\t$y\t$Dlevel\t$Level"
    }
}

# determine support nodes where ground motions are input, for multiple-support excitation
set iSupportNode ""
set level 1
for {set pier 1} {$pier <= [expr $NBay+1]} {incr pier 1} {
    set nodeID [expr $level*$Dlevel+$pier]
    lappend iSupportNode $nodeID
    #puts $nodeID; #11 12 13 14 15 16
}
#####
# Define restraints or boundary conditions #
#####
fixY 0.0 1 1 1; #fix all nodes @ y=0
#####
# Define Sections
#####
set SectionType FiberSection ; # options: Elastic FiberSection
# define section tags:
set ColSecTagext 1; #external coumn Elastic section
set ColSecTagint 2; #internal coumn Elastic section
set BeamSecTag2n3 23; #beam elastic section on the 2nd and 3rd floors
set BeamSecTag4n5 45; #beam elastic section on the 4th and 5th floors
set BeamSecTag6n7 67; #beam elastic section on the 6th and 7th floors
set ColSecTagextFiber 11; #Fiber section for external coumn
set ColSecTagintFiber 21; #Fiber section for internal coumn
set BeamSecTag2n3Fiber 231; #beam Fiber section on the 2nd and 3rd floors
set BeamSecTag4n5Fiber 451; #beam Fiber section on the 4th and 5th floors
set BeamSecTag6n7Fiber 671; #beam Fiber section on the 6th and 7th floors
set SecTagTorsion 70; #torsional SectionType

if {$SectionType == "Elastic"} {
    #Define material properties:for linear elastic sections
    set fy [expr 235*$MPa]; #steel yield strength
    set Es [expr 210*$GPa]; #Steel Young's Modulus
    set nu 0.3; #Poisson's ratio
    set Gs [expr $Es/2./[expr 1+$nu]]; #Torsional stiffness Modulus
    set J $Ubig; #set large torsional stiffness
    # Ext column sections: HE600M
    set AgextCol [expr 363.7*$cm2]; # cross-sectional area in (cm2)
    set IyextCol [expr 237400.*$cm4]; # moment of Inertia about the major axis in (cm4)
    set IzextCol [expr 18980.*$cm4]; # moment of Inertia about the minor axis
    # Int column sections: HE700M
    set AgintCol [expr 383*$cm2]; # cross-sectional area in (cm2)
    set IyintCol [expr 329300.*$cm4]; # moment of Inertia about the major axis in (cm4)
    set IzintCol [expr 18800.*$cm4]; # moment of Inertia about the minor axis
    # beam sections: IPE550 for 6th and 7th floors
    set AgBeam6n7 [expr 134.4*$cm2]; #cross-sectional area in (cm2)
    set IyBeam6n7 [expr 67120.*$cm4]; # moment of Inertia about the major axis in (cm4)
    set IzBeam6n7 [expr 2668.*$cm4]; # moment of Inertia about the minor axis in (cm4)
    # beam sections: IPE600 for 4th and 5th floors
    set AgBeam4n5 [expr 156*$cm2]; #cross-sectional area in (cm2)
}

```

```

set IyBeam4n5 [expr 92080.*$cm4]; # moment of Inertia about the major axis in (cm4)
set IzBeam4n5 [expr 3387.*$cm4]; # moment of Inertia about the minor axis in (cm4)
#beam sections: IPE750x196 for 2nd and 3rd floors
set AgBeam2n3 [expr 250.80*$cm2]; #cross-sectional area in (cm2)
set IyBeam2n3 [expr 2.403e5*$cm4]; # moment of Inertia about the major axis in (cm4)
set IzBeam2n3 [expr 8.175e3*$cm4]; # moment of Inertia about the minor axis in (cm4)
set matIDhard 1; # material numbers for recorder (this stressstrain recorder will be
blank, as this is an elastic section)
} elseif {$SectionType == "FiberSection"} {
# Define Material properties
#Method I_____
#steel 01 uniaxial material model/ bi-linear stress strain relationship
set fy [expr 235*$MPa]; #yield stress of steel
set Es [expr 210*$GPa]; # Steel Young's Modulus
set nu 0.3;
set Gs [expr $Es/2./[expr 1+$nu]]; # Torsional stiffness Modulus
set Hiso 0; #isotropic hardening Modulus
set Hkin 1000; #kinematic hardening Modulus
set steel01 1; #unique material object for concentrated plasticity
set b 0.003
#command
#uniaxialMaterial Steel01 $matTag $Fy $E0 $b <$a1 $a2 $a3 $a4>
uniaxialMaterial Steel01 $steel01 $fy $Es $b
#Where
#$matTag integer tag identifying material
#$Fy yield strength
#$E0 initial elastic tangent
#$b strain-hardening ratio (ratio between post-yield tangent and initial elastic tangent)
#$a1 isotropic hardening parameter, increase of compression yield envelope as proportion of yield
strength after a plastic strain of $a2*($Fy/E0). (optional)
#$a2 isotropic hardening parameter (see explanation under $a1). (optional).
#$a3 isotropic hardening parameter, increase of tension yield envelope as proportion of yield strength
after a plastic strain of $a4*($Fy/E0). (optional)
#$a4 isotropic hardening parameter (see explanation under $a3). (optional)
#uniaxialMaterial Hardening $steel01 $Es $Fy $Hiso $Hkin; #considering bilinear stress-strain
condition
#Method II_____
#Giuffre-Monegotto-Pinto Material model/ Steel02 uniaxial material model
# -----
set steel02 2; #unique material object for distributed plasticity
set fy [expr 235*$MPa]; # STEEL yield stress
set Es [expr 210*$GPa]; # modulus of steel
set b 0.01; # strain-hardening ratio
set R0 18; # control the transition from elastic to plastic branches
set cR1 0.925; # control the transition from elastic to plastic branches
set cR2 0.15; # control the transition from elastic to plastic branches
set a1 0.1;
set a2 1.0;
set a3 0.1;
set a4 1.0;#example
# Command:uniaxialMaterial Steel02 $matTag $Fy $E $b $R0 $cR1 $cR2 <$a1 $a2 $a3 $a4 $sigInit>
#where
#$matTag integer tag identifying material
#$Fy,E0and b as previously defined
#$R0 $cR1 $cR2 parameters to control the transition from elastic to plastic branches.
#Recommended values: $R0=between 10 and 20, $cR1=0.925, $cR2=0.15
#$a1 isotropic hardening parameter, increase of compression yield envelope as proportion of yield
strength after a plastic strain of $a2*($Fy/E0). (optional)

```

```

#%a2 isotropic hardening parameter (see explanation under %a1). (optional default = 1.0).
#%a3 isotropic hardening parameter, increase of tension yield envelope as proportion of yield strength
after a plastic strain of %a4*(%Fy/E0). (optional default = 0.0)
#%a4 isotropic hardening parameter (see explanation under %a3). (optional default = 1.0)
#%sigInit Initial Stress Value (optional, default: 0.0) the strain is calculated from epsP=%sigInit/%E
#if (sigInit!= 0.0) { double epsInit = sigInit/E; eps = trialStrain+epsInit; } else eps = trialStrain;
#uniaxialMaterial Steel02 $steel02 $Fy $Es $b $R0 $cR1 $cR2; #considering distributed
plasticity approach
uniaxialMaterial Steel02 $steel02 $fy $Es $b $R0 $cR1 $cR2 $a1 $a2 $a3 $a4;
#####
# ELEMENT properties #
# Structural-Steel I-section properties #
# column sections: HE600M,HE700M external and internal columns resp. #
# Beam Sections:IPE400A #
#####
#column section : HE600M : ExternalColumn
set h [expr 620.*$mm]; #depth
set bf [expr 305.*$mm]; #flange width
set tf [expr 40.*$mm]; #flange thickness
set tw [expr 21.*$mm]; #web thickness
set nfdw 20; #number of fibers along dw
set nftw 2; #number of fibers along tw
set nbf 20; #number of fibers along bf
set nftf 4; #number of fibers along tf
Isection $ColSecTagextFiber $steel02 $h $bf $tf $tw $nfdw $nftw $nbf $nftf
#column section : H700M: Internal Column
set h [expr 716.*$mm]; #depth
set bf [expr 304.*$mm]; #flange width
set tf [expr 40.*$mm]; #flange thickness
set tw [expr 21.*$mm]; #web thickness
set nfdw 20; #number of fibers along dw
set nftw 2; #number of fibers along tw
set nbf 20; #number of fibers along bf
set nftf 4; #number of fibers along tf
Isection $ColSecTagintFiber $steel02 $h $bf $tf $tw $nfdw $nftw $nbf $nftf

#***** Beam sections: IPE550 ***** 6th and 7th floors
set h [expr 550.*$mm]; #depth
set bf [expr 210.*$mm]; #flange width
set tf [expr 17.2*$mm]; #flange thickness
set tw [expr 11.1*$mm]; #web thickness
set nfdw 20; #number of fibers along dw
set nftw 3; #umber of fibers along tw
set nbf 20; #number of fibers along bf
set nftf 4; #number of fibers along tf
Isection $BeamSecTag6n7Fiber $steel02 $h $bf $tf $tw $nfdw $nftw $nbf $nftf
#***** Beam sections: IPE600 ***** 4th and 5th floors
set h [expr 600.*$mm]; #depth
set bf [expr 220.*$mm]; #flange width
set tf [expr 19.*$mm]; #flange thickness
set tw [expr 12.*$mm]; #web thickness
set nfdw 20; #number of fibers along dw
set nftw 3; #umber of fibers along tw
set nbf 20; #number of fibers along bf
set nftf 4; #number of fibers along tf
Isection $BeamSecTag4n5Fiber $steel02 $h $bf $tf $tw $nfdw $nftw $nbf $nftf
#***** Beam sections: IPE750x196 ***** 2nd and 3rd floors
set h [expr 770.*$mm]; #depth

```

```

set bf [expr 268.*$mm]; #flange width
set tf [expr 25.4*$mm]; #flange thickness
set tw [expr 15.6*$mm]; #web thickness
set nfdw 20; #number of fibers along dw
set nftw 2; #umber of fibers along tw
set nbf 20; #number of fibers along bf
set nftf 4; #number of fibers along tf
Isection $BeamSecTag2n3Fiber $steelI02 $h $bf $tf $tw $nfdw $nftw $nbf $nftf
} else {
  puts "No section has been defined"
  return -1
}
#####
# Define Beam-Column Elements #
#####
#set up geometric transformations of element
#separate columns and beams, in case of P-Delta analysis for columns
set IDColTransf 1; # all columns
set IDBeamTransf 2; # all beams
set ColTransfType Linear; #options for columns: Linear, PDelta, Corotational
geomTransf $ColTransfType $IDColTransf; # orientation of column stiffness affects bidirectional
response.
geomTransf Linear $IDBeamTransf;
set numIntgrPts 5; #number of Gauss integration points for nonlinear curvature distribution
# columns parallel to y-axis
set N0col [expr 100-1]; #column element numbers
for {set level 1} {$level <= $NStory} {incr level 1} {
  for {set pier 1} {$pier <= [expr $NBay+1]} {incr pier 1} {
    if {$pier==1 || $pier==6} {
      set HE600M [expr 285.5*$Kg/$m];#For the external columns i.e. 1st and 6th piers or column
lines
      set ColumnIDext [expr $N0col +$level*$Dlevel+$pier]
      set nodeI [expr $level*$Dlevel +$pier]
      set nodeJ [expr ($level+1)*$Dlevel +$pier]
      element nonlinearBeamColumn $ColumnIDext $nodeI $nodeJ $numIntgrPts
$ColSecTagextFiber $IDColTransf; # columns
      #puts "$ColumnIDext $nodeI $nodeJ $numIntgrPts $ColSecTagextFiber $IDColTransf"
    }
    if {$pier>=2&&$pier<=5} {
      set HE700M [expr 300.66*$Kg/$m];#for the internal columns or 2nd,3rd,4th and 5th piers
      set ColumnIDint [expr $N0col +$level*$Dlevel +$pier]
      set nodeI [expr $level*$Dlevel +$pier]
      set nodeJ [expr ($level+1)*$Dlevel +$pier]
      element nonlinearBeamColumn $ColumnIDint $nodeI $nodeJ $numIntgrPts
$ColSecTagintFiber $IDColTransf; # columns
      #puts "$ColumnIDint $nodeI $nodeJ $numIntgrPts $ColSecTagintFiber $IDColTransf"
    }
  }
}
}
# Beams -- parallel to X-axis
#Note the mass can also be applied as the distributed mass per unit length of each member Kg/m
set N0beam 200; # set tag for beam elements
for {set bay 1} {$bay <= $NBay} {incr bay 1} {
  for {set level 2} {$level <=[expr $NStory+1]} {incr level 1} {
    if {$level==2||$level==3} {
      set BeamID23 [expr $N0beam +$level*$Dlevel + $bay]
      set mass23 [expr 196.88*$Kg/$m];#wt. IPE750x196 for the 2nd and 3rd floor beams
      set nodeI [expr $level*$Dlevel + $bay]

```

```

    set nodeJ [expr $level*$Dlevel + $bay+1]
    element nonlinearBeamColumn $BeamID23 $nodeI $nodeJ $numIntgrPts
$BeamSecTag2n3Fiber $IDBeamTransf;# beams
    #puts "$BeamID23 $nodeI $nodeJ $numIntgrPts $BeamSecTag2n3Fiber $IDBeamTransf"
}
if {$level==4||$level==5} {
    set BeamID45 [expr $N0beam + $level*$Dlevel+ $bay]
    set mass45 [expr 122.46*$Kg/$m];#wt. IPE600 for the 4th and 5th floor beams
    set nodeI [expr $level*$Dlevel+ $bay]
    set nodeJ [expr $level*$Dlevel + $bay+1]
    element nonlinearBeamColumn $BeamID45 $nodeI $nodeJ $numIntgrPts
$BeamSecTag4n5Fiber $IDBeamTransf;# beams
    #puts "$BeamID45 $nodeI $nodeJ $numIntgrPts $BeamSecTag4n5Fiber $IDBeamTransf"
}
if {$level==6||$level==7} {
    set mass67 [expr 105.5*$Kg/$m];#wt. IPE550 for the 6th and 7th floor beams
    set BeamID67 [expr $N0beam + $level*$Dlevel + $bay]
    set nodeI [expr $level*$Dlevel + $bay]
    set nodeJ [expr $level*$Dlevel + $bay+1]
    element nonlinearBeamColumn $BeamID67 $nodeI $nodeJ $numIntgrPts
$BeamSecTag6n7Fiber $IDBeamTransf;# beams
    #puts "$BeamID67 $nodeI $nodeJ $numIntgrPts $BeamSecTag6n7Fiber $IDBeamTransf "
}
}
}
#####Assignment of Nodal Masses#####
for {set level 2} {$level <= $NStory+1} {incr level 1} {
    for {set pier 1} {$pier <= [expr ($NBay+1)]} {incr pier 1} {
        set nodeID [expr ($level*$Dlevel)+($pier*$Dpier)]
        if {$level==2} {
            set M2nd [expr 7070*$Kg/$m]
            if {$pier == 1 || $pier == $NBay+1} {
                mass $nodeID [expr $M2nd*3.5] 0 0
            }
            if {$pier==2||$pier==5} {
                mass $nodeID [expr $M2nd*6.5] 0 0
            }
            if {$pier==3||$pier==4} {
                mass $nodeID [expr $M2nd*5.5] 0 0
            }
        }
        if {$level==3} {
            set M3rd [expr 6973*$Kg/$m]
            if {$pier == 1 || $pier == $NBay+1} {
                mass $nodeID [expr $M3rd*3.5] 0 0
            }
            if {$pier==2||$pier==5} {
                mass $nodeID [expr $M3rd*6.5] 0 0
            }
            if {$pier==3||$pier==4} {
                mass $nodeID [expr $M3rd*5.5] 0 0
            }
        }
        if {$level==4||$level==5} {
            set M45th [expr 6672*$Kg/$m]
            if {$pier == 1 || $pier == $NBay+1} {
                mass $nodeID [expr $M45th*3.5] 0 0
            }
        }
    }
}

```

```

    }
    if {$pier==2||$pier==5} {
        mass $nodeID [expr $M45th*6.5] 0 0
    }
    if {$pier==3||$pier==4} {
        mass $nodeID [expr $M45th*5.5] 0 0
    }
}
if {$level==6} {
    set M6th [expr 6603*$Kg/$m]
    if {$pier == 1 || $pier == $NBay+1} {
        mass $nodeID [expr $M6th*3.5] 0 0
    }
    if {$pier==2||$pier==5} {
        mass $nodeID [expr $M6th*6.5] 0 0
    }
    if {$pier==3||$pier==4} {
        mass $nodeID [expr $M6th*5.5] 0 0
    }
}
if {$level==7} {
    set M7th [expr 5889*$Kg/$m]
    if {$pier == 1 || $pier == $NBay+1} {
        mass $nodeID [expr $M7th*3.5] 0 0
    }
    if {$pier==2||$pier==5} {
        mass $nodeID [expr $M7th*6.5] 0 0
    }
    if {$pier==3||$pier==4} {
        mass $nodeID [expr $M7th*5.5] 0 0
    }
}
}
}

set dataDir Modes
file mkdir $dataDir;
set numModes $NStory
for {set k 1} { $k <= $numModes } { incr k } {
    set period "5Baymodes/Periods.txt"
    recorder Node -file [format "modes/mode%i.out" $k] -nodeRange 21 76 -dof 1 "eigen $k"
}

#perform eigen analysis
# Command Example: eigen <$type> <$solver> $numEigenvalues
# $type: optional string detailing type of eigen analysis: -standard or -generalized (default: -
generalized)
# $solver: -genBandArpack, -symmSparseArpack, -symmBandLapack, -fullGenLapack, -
UmfPack, -SuperLU

set lambda [eigen $numModes];#option1
#set lambda [eigen -generalized -SuperLU $numModes]; # option2
# calculate frequencies and periods of the structure
set omega {}
set f {}
set T {}
foreach lam $lambda {
    lappend omega [expr sqrt($lam)]
    lappend F [expr sqrt($lam)/(2*$PI)]
}

```

```

    lappend T [expr (2*$PI)/sqrt($lam)]
  }
  puts "periods are $T"
#write the output file consisting of periods
  set period "Modes/Periods.txt"
  set Periods [open $period "w"]
  foreach t $T {
    puts $Periods " $t"
  }
  close $Periods
  set Frequencies "Modes/Frequencies.out"
set fileID [open $Frequencies "w"];
set temp_i 0;
foreach f $F {
  incr temp_i;
  #puts "Frequency of mode: $temp_i $f Hz"; # Print Period to screen.
  puts $fileID " $f";
}
close $fileID;
#Lateral Load distribution
#Uniform
#set iFj(6) [expr 1*[expr 182.550*$KN]];
#set iFj(5) [expr 1*[expr 204.704*$KN]];
#set iFj(4) [expr 1*[expr 206.833*$KN]];
#set iFj(3) [expr 1*[expr 206.833*$KN]];
#set iFj(2) [expr 1*[expr 216.172*$KN]];
#set iFj(1) [expr 1*[expr 219.179*$KN]];
#Triangular
#set iFj(6) [expr 1.0*[expr 182.550*$KN]];
#set iFj(5) [expr 0.837*[expr 204.704*$KN]];
#set iFj(4) [expr 0.674*[expr 206.833*$KN]];
#set iFj(3) [expr 0.512*[expr 206.833*$KN]];
#set iFj(2) [expr 0.349*[expr 216.172*$KN]];
#set iFj(1) [expr 0.186*[expr 219.179*$KN]];
#Modal
set iFj(6) [expr 1*[expr 182.550*$KN]]; #normalized displacement of roof/eigenvector for mode 1 of
roof
set iFj(5) [expr 0.871*[expr 204.704*$KN]]; #normalized displacement of 5th story /eigenvector for
mode 1 of the 5th story
set iFj(4) [expr 0.695*[expr 206.833*$KN]];
set iFj(3) [expr 0.488*[expr 206.833*$KN]];
set iFj(2) [expr 0.293*[expr 216.172*$KN]];
set iFj(1) [expr 0.131*[expr 219.179*$KN]];
##### create node and load vectors for lateral-load distribution in static analysis
set iFPush ""
set iNodePush ""
for {set level 2} {$level <=[expr $NStory+1]} {incr level 1} {
  set FPush [expr $iFj([expr ($level-1)])]; #totalmass*#lateral load coefficient
  #for {set pier 1} {$pier <= [expr $NBay+1]} {incr pier 1} {
    set nodeID [expr $level*$Dlevel+$Dpier]
    lappend iNodePush $nodeID
    lappend iFPush $FPush
  }
  #puts $FPush
  #puts $nodeID
#}
}
#####
#           Recorders                                     #

```

```
#####
set dataDir 5bay6StoryMain;# Name of dataDirectory
file mkdir $dataDir
set IDctrlDOF 1
set IDctrlNode [expr ($NStory+1)*$Dlevel+$Dpier];
set FreeNodeID $IDctrlNode; # ID: free node
set SupportNodeFirst [lindex $iSupportNode 0]; # ID: first support node
set SupportNodeLast [lindex $iSupportNode [expr [length $iSupportNode]-1]]; # ID: last support
node
set FirstColumn [expr $N0col+1*10+1]; # ID: first column
recorder Node -file $dataDir/DFree.txt -time -node $FreeNodeID -dof 1 disp; # displacements of
free node
recorder Node -file $dataDir/DBase.txt -time -nodeRange $SupportNodeFirst $SupportNodeLast -dof 1 2 3
disp; # displacements of support nodes
recorder Node -file $dataDir/RBase.txt -time -nodeRange $SupportNodeFirst $SupportNodeLast -dof 1
reaction; # support reaction
recorder Drift -file $dataDir/DrNode.txt -time -iNode $SupportNodeFirst -jNode $FreeNodeID -dof 1 -
perpDirn 2; # Maximum lateral drift=(top disp-bot disp)/HBuilding
recorder Drift -file $dataDir/DrNode1.txt -time -iNode $SupportNodeFirst -jNode 21 -dof 1 -perpDirn
2;#lateral drift of story1=(disp floor1-dispground)/Hstory1
recorder Drift -file $dataDir/DrNode2.txt -time -iNode 21 -jNode 31 -dof 1 -perpDirn 2; #lateral drift of
story2=(disp floor2-disp floor1)/HstoryTyp
recorder Drift -file $dataDir/DrNode3.txt -time -iNode 31 -jNode 41 -dof 1 -perpDirn 2; # lateral drift of
story3=(disp floor3-disp floor2)/HstoryTyp
recorder Drift -file $dataDir/DrNode4.txt -time -iNode 41 -jNode 51 -dof 1 -perpDirn 2; #lateral drift of
story4=(disp floor4-disp floor3)/HstoryTyp
recorder Drift -file $dataDir/DrNode5.txt -time -iNode 51 -jNode 61 -dof 1 -perpDirn 2; #lateral drift of
story5=(disp floor5-disp floor4)/HstoryTyp
recorder Drift -file $dataDir/DrNode6.txt -time -iNode 61 -jNode $FreeNodeID -dof 1 -perpDirn 2;#
lateral drift of story6=(disp floor6-disp floor5)/HstoryTyp

recorder Element -file $dataDir/Fel1.txt -time -ele $FirstColumn localForce; # element forces
in local coordinates
recorder Element -file $dataDir/ForceEle1sec1.txt -time -ele $FirstColumn section 1 force; # section
forces, axial and moment, node i
recorder Element -file $dataDir/DefoEle1sec1.txt -time -ele $FirstColumn section 1 deformation; #
section deformations, axial and curvature, node i
recorder Element -file $dataDir/ForceEle1sec$numIntgrPts.txt -time -ele $FirstColumn section
$numIntgrPts force; # section forces, axial and moment, node j
recorder Element -file $dataDir/DefoEle1sec$numIntgrPts.txt -time -ele $FirstColumn section
$numIntgrPts deformation; # section deformations, axial and curvature, node j
recorder Element -file $dataDir/SSEle1sec1.txt -time -ele $FirstColumn section $numIntgrPts fiber 0 0
$steel02 stressStrain; # steel fiber stress-strain, node i
#set ViewScale 5
#DisplayModel2D NodeNumbers $ViewScale; #calling the comand to display the NodeNumbers of a
planar steel frame
#####
# Load Control Gravity Loads & Gravity Analysis
#####
pattern Plain 10 Linear {
  for {set level 2} {$level<=$NStory+1} {incr level 1} {
    for {set pier 1} {$pier<[expr $NBay+1]} {incr pier 1} {
      set elemID [expr $N0beam+$level*$Dlevel+$pier*$Dpier]
      if {$level==2} {
        eleLoad -ele $elemID -type -beamUniform [expr -63.643*$KN/$m]
      }
      if {$level==3} {

```

```

        eleLoad -ele $elemID -type -beamUniform [expr -63.001*$KN/$m]
    }
    if {$level==4} {
        eleLoad -ele $elemID -type -beamUniform [expr -61.006*$KN/$m]
    }
    if {$level==5} {
        eleLoad -ele $elemID -type -beamUniform [expr -61.006*$KN/$m]
    }
    if {$level==6} {
        eleLoad -ele $elemID -type -beamUniform [expr -60.551*$KN/$m]
    }
    if {$level==7} {
        eleLoad -ele $elemID -type -beamUniform [expr -51.854*$KN/$m]
    }
}
##### Define imperfection loads#####
set phi_0 [expr 1/200.];#basic value for global imperfection
if {([expr 2/pow($HBuilding,0.5)]>=[expr 2/3.]&&([expr 2/pow($HBuilding,0.5)]<=1.)) {
set alpha_h [expr 2./pow($HBuilding,0.5)]; #reduction factor for height
} elseif {[expr 2./pow($HBuilding,0.5)]<[expr 2/3.]} {
set alpha_h [expr 2/3.]
} elseif {[expr 2./pow($HBuilding,0.5)]>1. } {
set alpha_h 1.
}
set nColine [expr $NBay+1];#nColine is the number of columns in a row which is m in the code
set alpha_m [expr pow((0.5*(1.+1./$nColine)),0.5)];#reduction factor for number of column
lines
set imperfection [expr $phi_0*$alpha_h*$alpha_m]
#####Apply imperfection loads at each story #####
set nodeID [expr $level*$Dlevel+$Dpier];#Nodes Where global imperfections are applied
if {$level==2} {
load $nodeID [expr $imperfection*63.643*31*$KN] 0 0
} elseif {$level==3} {
load $nodeID [expr $imperfection*63.001*31*$KN] 0 0
} elseif {$level==4||$level==5} {
load $nodeID [expr $imperfection*61.006*31*$KN] 0 0
} elseif {$level==6} {
load $nodeID [expr $imperfection*60.551*31*$KN] 0 0
} elseif {$level==7} {
load $nodeID [expr $imperfection*51.854*31*$KN] 0 0
}
#puts "$nodeID"
}
}
#Gravity-analysis: load-controlled static analysis
set Tol 1.0e-6;          # convergence tolerance for test
constraints Plain;      # how it handles boundary conditions
numberer RCM;          # renumber dof's to minimize band-width (optimization)
system BandGeneral;    # how to store and solve the system of equations in the analysis (large
model: try UmfPack)
test NormDisplIncr $Tol 6;    # determine if convergence has been achieved at the end of an
iteration step
algorithm Newton;        # use Newton's solution algorithm: updates tangent stiffness at every
iteration
set NstepGravity 10;     # apply gravity in 10 steps
set DGravity [expr 1.0/$NstepGravity]; # load increment
integrator LoadControl $DGravity; # determine the next time step for an analysis
analysis Static;        # define type of analysis: static or transient

```

```

analyze $NstepGravity;           # Perform Gravity Analysis
# maintain constant gravity loads and reset time to zero
reactions;
set node1Rxn [nodeReaction 11]; # nodeReaction command returns nodal reactions for specified node
in a list
set node2Rxn [nodeReaction 12]
set node3Rxn [nodeReaction 13]
set node4Rxn [nodeReaction 14]
set node5Rxn [nodeReaction 15]
set node6Rxn [nodeReaction 16]

set inputdFy [expr -11192.922*$KN]
set inputdFx [expr 28.497*$KN]
set computedFx [expr [lindex $node1Rxn 0]+[lindex $node2Rxn 0]+[lindex $node3Rxn 0]+[lindex
$node4Rxn 0]+[lindex $node5Rxn 0]+[lindex $node6Rxn 0]]
set computedFy [expr [lindex $node1Rxn 1]+[lindex $node2Rxn 1]+[lindex $node3Rxn 1]+[lindex
$node4Rxn 1]+[lindex $node5Rxn 1]+[lindex $node6Rxn 1]]
puts "\nEquilibrium Check After analysis of Loads:"
puts "SumX: Inputed: $inputdFx + Computed: $computedFx = [expr $inputdFx+$computedFx]"
puts "SumY: Inputed: $inputdFy + Computed: $computedFy = [expr $inputdFy+$computedFy]"
loadConst -time 0.0
print node 11 12
puts "Running Dynamic..."

```

d) StaticAnalysisParameters

```

variable constraintsTypeStatic Plain; # default;
if { [info exists RigidDiaphragm] == 1 } {
  if {$RigidDiaphragm=="ON"} {
    variable constraintsTypeStatic Lagrange; # for large model, try Transformation
  }; # if rigid diaphragm is on
}; # if rigid diaphragm exists
constraints $constraintsTypeStatic
set numbererTypeStatic RCM
numberer $numbererTypeStatic

set systemTypeStatic SparseSYM; # try UmfPack for large model
system $systemTypeStatic
# determine if convergence has been achieved at the end of an iteration step
# NormUnbalance-- Specifies a tolerance on the norm of the unbalanced load at the current iteration
# NormDispIncr -- Specifies a tolerance on the norm of the displacement increments at the current
iteration
#EnergyIncr-- Specifies a tolerance on the inner product of the unbalanced load and displacement
increments at the current iteration
#RelativeNormUnbalance --
#RelativeNormDispIncr --
#RelativeEnergyIncr --
variable TolStatic 1.e-8; # Convergence Test: tolerance
variable maxNumIterStatic 6; # Convergence Test: maximum
variable printFlagStatic 0; # Convergence Test: flag used
variable testTypeStatic EnergyIncr ; # Convergence-test type
test $testTypeStatic $TolStatic $maxNumIterStatic $printFlagStatic;
# for improved-convergence procedure:
variable maxNumIterConvergeStatic 2000;
variable printFlagConvergeStatic 0;

#Linear -- Uses the solution at the first iteration and continues

```

```

#Newton -- Uses the tangent at the current iteration to iterate to convergence
#ModifiedNewton -- Uses the tangent at the first iteration to iterate to convergence
#NewtonLineSearch --
#KrylovNewton --
#BFGS --
#Broyden --
variable algorithmTypeStatic Newton
algorithm $algorithmTypeStatic;

# Static INTEGRATOR: -- determine the next time step for an analysis
integrator DisplacementControl $IDctrlNode $IDctrlDOF $Dincr

#ANALYSIS -- defines what type of analysis is to be performed
#there are convergence problems with the Transient Analysis object at a peak or when the time step is too
small. The time step in the output is also variable.
set analysisTypeStatic Static
analysis $analysisTypeStatic

```

e) StaticAnalysisCommand

```

#####
#5bay6StoryPushoverAnalysis Static Pushover Analysis #
# execute this file after you have built the model, and after you apply gravity #
#####
source 5bay6StoryMain.tcl; #sourcing the main file
# characteristics of pushover analysis
set Dmax [expr 0.9*$HBuilding/$HBuilding]; # maximum displacement of
set Dincr [expr 0.0001*$HBuilding]; # displacement increment. you want this to be small, but not too
small to slow analysis
# create load pattern for lateral pushover load coefficient when using linear load pattern
pattern Plain 200 Linear {}; # define load pattern
    foreach FPush $iFPush NodePush $iNodePush {}; # these vectors have been defined with the
structure
        load $NodePush $FPush 0.0 0.0
    }
}; # end load pattern
# display deformed shape:
set ViewScale 5;
#DisplayModel2D DeformedShape $ViewScale ; # display deformed shape, the scaling factor needs to
be adjusted for each model
recorder plot $dataDir/DFree.txt ForceDisp 910 10 400 400 -columns 2 1; # a window to plot the load vs.
nodal displacement
# ----- perform Static Pushover Analysis
source StaticAnalysisParameters.tcl; # constraintsHandler,DOFnumberer,system-
ofequations,convergenceTest,solutionAlgorithm,integrator
set fmt1 "%s Pushover analysis: CtrlNode %.3i, dof %.1i, Disp=%.4f %s"; # format for screen/file output
of DONE/PROBLEM analysis
# -----first analyze command-----
set Nsteps [expr int($Dmax/$Dincr)]; # number of pushover analysis steps
set ok [analyze $Nsteps]; # this will return zero if no convergence problems were
encountered
# -----if convergence failure-----
if {$ok != 0} {
    # if analysis fails, we try some other stuff, performance is slower inside this loop
    set Dstep 0.0;
    set ok 0
    while {$Dstep <= 1.0 && $ok == 0} {

```

```

set controlDisp [nodeDisp $IDctrlNode $IDctrlDOF ]
set Dstep [expr $controlDisp/$Dmax]
set ok [analyze 1 ]
# if analysis fails, we try some other stuff
# performance is slower inside this loop  global maxNumIterStatic;      # max no. of iterations
performed before "failure to converge" is ret'd
if {$ok != 0} {
  puts "Trying Newton with Initial Tangent .."
  test NormDispIncr $Tol 2000 0
  algorithm Newton -initial
  set ok [analyze 1]
  test $stestTypeStatic $TolStatic $maxNumIterStatic 0
  algorithm $algorithmTypeStatic
}
if {$ok != 0} {
  puts "Trying Broyden .."
  algorithm Broyden 8
  set ok [analyze 1 ]
  algorithm $algorithmTypeStatic
}
if {$ok != 0} {
  puts "Trying NewtonWithLineSearch .."
  algorithm NewtonLineSearch 0.8
  set ok [analyze 1]
  algorithm $algorithmTypeStatic
}
}; # end while loop
}; # end if ok !0
# -----
if {$ok != 0} {
  puts [format $fmt1 "PROBLEM" $IDctrlNode $IDctrlDOF [nodeDisp $IDctrlNode $IDctrlDOF]
$LunitTXT]
} else {
  puts [format $fmt1 "DONE" $IDctrlNode $IDctrlDOF [nodeDisp $IDctrlNode $IDctrlDOF]
$LunitTXT]
}
#end of Static Pushover Analysis for 2D

```

f) DynamicAnalysisParameters

```

variable constraintsTypeDynamic Transformation;
constraints $constraintsTypeDynamic ;
variable numbererTypeDynamic RCM
numberer $numbererTypeDynamic
variable systemTypeDynamic BandGeneral; # try UmfPack for large problems
system $systemTypeDynamic
variable TolDynamic 1.e-8;           # Convergence Test: tolerance
variable maxNumIterDynamic 1000;    # Convergence Test: maximum number of #iterations that
variable printFlagDynamic 0;        # Convergence Test: flag used to print #information on
variable testTypeDynamic EnergyIncr; # Convergence-test type
test $testTypeDynamic $TolDynamic $maxNumIterDynamic $printFlagDynamic;
# for improved-convergence procedure:
variable maxNumIterConvergeDynamic 2000;
variable printFlagConvergeDynamic 0;
variable algorithmTypeDynamic ModifiedNewton
algorithm $algorithmTypeDynamic;

```

```
variable NewmarkGamma 0.5; # Newmark-integrator gamma parameter (also HHT)
variable NewmarkBeta 0.25; # Newmark-integrator beta parameter
variable integratorTypeDynamic Newmark;
integrator $integratorTypeDynamic $NewmarkGamma $NewmarkBeta
variable analysisTypeDynamic Transient
analysis $analysisTypeDynamic
```

g) DynamicAnalysisCommand.tcl

```
#####
# File Name: DynamicAnalysisCommand.tcl #
# This file can be executed after the model is built and gravity load is applied #
#####
source 5bay6StoryMain.tcl; #source the main Model
source ReadSMDfile.tcl; # procedure for reading GM file and converting it to proper format
# Uniform Earthquake ground motion (uniform acceleration input at all support nodes)
set GMdirection 1; # ground-motion direction
set GMfile "RSN20_NCALIF.FH_H-FRN044"; # sample ground-motion filenames
set GMfact 1.5; # ground-motion scaling factor
# Display deformed shape:
set ViewScale 5; # amplify display of deformed shape
DisplayModel2D DeformedShape $ViewScale; # display deformed shape, the scaling factor needs to be
adjusted for each model
#recorder plot $dataDir/DFree.out Displ 900 700 400 400 -columns 1 2; # a window to plot the nodal
displacements versus time
recorder plot $dataDir/DFree.txt DispTime 910 10 400 400 -columns 1 2;

# ----- set up analysis parameters
source DynamicAnalysisParameters.tcl; # constraintsHandler,DOFnumberer,system-
#ofequations,convergenceTest,solutionAlgorithm,integrator
# ----- Define & apply damping
# RAYLEIGH damping parameters, Where to put M/K-prop damping, switches
(http://opensees.berkeley.edu/OpenSees/manuals/usermanual/1099.htm)
#  $D = \alpha M + \beta_{curr} K_{current} + \beta_{comm} K_{lastCommit} + \beta_{kinit} K_{initial}$ 
set xDamp 0.05; # damping ratio
set MpropSwitch 1.0;
set KcurrSwitch 0.0;
set KcommSwitch 1.0;
set KinitSwitch 0.0;
set nEigenI 1; # mode 1
set nEigenJ 3; # mode 3
set lambdaN [eigen [expr $nEigenJ]]; #eigenvalue analysis for nEigenJ modes
set lambdaI [lindex $lambdaN [expr $nEigenI-1]]; # eigenvalue mode i
set lambdaJ [lindex $lambdaN [expr $nEigenJ-1]]; #eigenvalue mode j
set omegaI [expr pow($lambdaI,0.5)];
set omegaJ [expr pow($lambdaJ,0.5)];
set alphaM [expr $MpropSwitch*$xDamp*(2*$omegaI*$omegaJ)/($omegaI+$omegaJ)]; # M-prop.
damping;  $D = \alpha M + M$ 
set betaKcurr [expr $KcurrSwitch*2.*$xDamp/($omegaI+$omegaJ)]; # current-K;+beatKcurr*KCurrent
set betaKcomm [expr $KcommSwitch*2.*$xDamp/($omegaI+$omegaJ)]; # last-committed
K;+betaKcomm*KlastCommitt
set betaKinit [expr $KinitSwitch*2.*$xDamp/($omegaI+$omegaJ)]; # initial-K;
+beatKinit*Kini
# current, initial & committed stiffness matrices
# define damping
rayleigh $alphaM $betaKcurr $betaKinit $betaKcomm; # RAYLEIGH damping
```

```

# ----- perform Dynamic Ground-Motion Analysis
# the following commands are unique to the Uniform Earthquake excitation
set IDloadTag 400; # for uniformSupport excitation
# Uniform EXCITATION: acceleration input
set dt [expr 0.01*$sec];
#set inFile $GMfile.at2
#set outFile $GMfile.g3; # set variable holding new filename (PEER files have .at2/dt2 extension)
#ReadSMDFile $inFile $outFile dt; # call procedure to convert the ground-motion file
set GMfatt [expr $g*$GMfact]; # data in input file is in g Unifts -- ACCELERATION TH
set AccelSeries "Series -dt $dt -filePath $GMfile.txt -factor $GMfatt"; # time series information
pattern UniformExcitation $IDloadTag $GMdirection -accel $AccelSeries ; # create Uniform
excitation

# set up ground-motion-analysis parameters
set DtAnalysis [expr $dt*$sec]; #time-step Dt for lateral analysis
set TmaxAnalysis [expr 40.*$sec]; # maximum duration of ground-motion analysis -- should be
50*$sec
set Nsteps [expr int($TmaxAnalysis/$DtAnalysis)];
set ok [analyze $Nsteps $DtAnalysis]; # actually perform analysis; returns ok=0 if analysis was
successful

if {$ok != 0} { ; # analysis was not successful.
# -----
# change some analysis parameters to achieve convergence
# performance is slower inside this loop
# Time-controlled analysis
set ok 0;
set controlTime [getTime];
while {$controlTime < $TmaxAnalysis && $ok == 0} {
    set controlTime [getTime]
    set ok [analyze 1 $DtAnalysis]
    if {$ok != 0} {
        puts "Trying Newton with Initial Tangent .."
        test NormDispIncr $Tol 1000 0
        algorithm Newton -initial
        set ok [analyze 1 $DtAnalysis]
        test $stestTypeDynamic $TolDynamic $maxNumIterDynamic 0
        algorithm $algorithmTypeDynamic
    }
    if {$ok != 0} {
        puts "Trying Broyden .."
        algorithm Broyden 8
        set ok [analyze 1 $DtAnalysis]
        algorithm $algorithmTypeDynamic
    }
    if {$ok != 0} {
        puts "Trying NewtonWithLineSearch .."
        algorithm NewtonLineSearch .8
        set ok [analyze 1 $DtAnalysis]
        algorithm $algorithmTypeDynamic
    }
}
}; # end if ok !0
puts "Ground Motion Done. End Time: [getTime]"
#end of Dynamic Analysis for 2D Frame

```

Appendix D OpenSees Script for Space Frames

To run the code of space frame model, the following TCL files and OpenSees.exe should be put into one file directory.

- a) **UnitsLibrary.tcl**
- b) **Isection.tcl**
- c) **6Story3DMain.tcl**; #The main frame model
- d) **StaticAnalysisParameters.tcl** ;#set up parameters for static analysis of 3D frame
- e) **PushoverAnalysisCommand.tcl**
- f) **DynamicAnalysisParameters.tcl**
- g) **DynamicAnalysisCommand.tcl**

```
#####
#   3D Frame Model for Nonlinear Analysis                                     #
#   Written by: Mekuriaw Mihrete                                           #
#   Date: March 7 2019                                                     #
#####
source UnitsLibrary.tcl
#source DisplayModel3D.tcl
#source DisplayPlane.tcl
source Isection.tcl
wipe; #clear all analysis
model BasicBuilder -ndm 3 -ndf 6;
# Define Parameters
#x dxn
set L1 [expr 7*$m];#Length of bay 1 x dxn
set L2 [expr 6*$m];#Length of bay 2 x dxn
set L3 [expr 5*$m];#Length of bay 3 x dxn
set L4 [expr 6*$m];#Length of bay 4 x dxn
set L5 [expr 7*$m];#Length of bay 5 x dxn
#z dxn
set S [expr 6*$m];#uniform spacing of frames 4@6each =24m Length of each bay z dxn
#y dxn
set H1 [expr 4*$m]; #Height of the First story
set H [expr 3.5*$m]; #5@3.5 each=17.5 other story heights

set Alpha 0;#angle of inclination of the local x z axes to the global coordinate x z axes this may be
adjusted from 0-90deg

set ang [expr int($Alpha)];#to convert the input alpha into integer
set FileName "Degree_ $ang";#name the output folder for any value of Alpha
file mkdir $FileName; #directory of the output folder
# Define Nodes
set AlphaRad [expr $Alpha*$PI/180.0]; #Because the value of alpha is recognized in TCL as radian
measures
set Nstory 6; #number of Stories above the ground Level
set NbayX 5; #Number of bays in the X direction
set NbayZ 4; #Number of Bays in the Z direction
set NFrame [expr $NbayZ+1]; #Number of Frames
```



```

fix $MasterNodeID 0 1 0 1 0 1; #constrain other dofs that don't belong to rigid diaphragm control
(x z plane wth perpend 2(y) in this case)
lappend iMasterNode $MasterNodeID
set perpDirn 2; #perpendicular to plane of rigid diaphragm
#puts "perpDirn\t$MasterNodeID $SlaveNodeID"
for {set frame 1} {$frame <=[expr $NFrame]} {incr frame 1} {
for {set pier 1} {$pier <=[expr $NbayX+1]} {incr pier 1} {
set nodeID [expr $level*$Dlevel+$frame*$Dframe+$pier*$Dpier];#slave nodes
rigidDiaphragm $perpDirn $MasterNodeID $nodeID; #Define Rigid Diaphragm, by assigning
master nodes to slave nodes
#puts "$perpDirn\t$MasterNodeID\t$nodeID"
}
}
}
# Determine support nodes where ground motions are input, for multiple-support excitation
set iSupportNode ""
for {set frame 1} {$frame <=[expr $NFrame]} {incr frame 1} {
set level 1
for {set pier 1} {$pier <=[expr $NbayX+1]} {incr pier 1} {
set nodeID [expr $level*$Dlevel+$frame*$Dframe+$pier]
lappend iSupportNode $nodeID
}
}
}
fixY 0.0 1 1 1 1 1 1;#Fix all nodes @ y=0

#####
#####
# DEFINE SECTIONS #
#####
#####
set SectionType FiberSection ; # ptions: Elastic, FiberSection
#define section tags:
set ColSecTagext 1; #external coumn Elastic section
set ColSecTagint 2; #internal coumn Elastic section
set BeamSecTag2n3 23; #beam elastic section on the 2nd and 3rd floors
set BeamSecTag4n5 45; #beam elastic section on the 4th and 5th floors
set BeamSecTag6n7 67; #beam elastic section on the 6th and 7th floors
set ColSecTagextFiber 11; #Fiber section for external coumn
set ColSecTagintFiber 21; #Fiber section for internal coumn
set BeamSecTag2n3Fiber 231; #beam Fiber section on the 2nd and 3rd floors
set BeamSecTag4n5Fiber 451; #beam Fiber section on the 4th and 5th floors
set BeamSecTag6n7Fiber 671; #beam Fiber section on the 6th and 7th floors
set GirdSecTag 500; #Elastic Girder Section
set GirderSecTagbay1n4Fiber 14; #Fiber Section for girder on bays 1&4 of all storreys
set GirderSecTag2n3Fiber 232; #Fiber Section for Girder on level 2 and 3 except bays 1& 4
set GirderSecTag4n5Fiber 452; #Fiber Section for Girder on level 4 and 5 except bays 1& 4
set GirderSecTag6n7Fiber 672; #Fiber Section for Girder on level 6 and 7 except bays 1& 4
set SecTagTorsion 70;

if {$SectionType == "Elastic"} {
#Define material properties:for linear elastic sections
set fy [expr 235*$MPa]; #steel yield strength
set Es [expr 210*$GPa]; #Steel Young's Modulus
set nu 0.3; #Poisson's ratio
set Gs [expr $Es/2./[expr 1+$nu]]; #Torsional stiffness Modulus
set J $Ubig; #set large torsional stiffness
# Ext column sections: HE600M
set AgextCol [expr 363.7*$cm2]; # cross-sectional area in (cm2)

```

```

set IyextCol [expr 237400.*$cm4]; # moment of Inertia about the major axis in (cm4)
set IzextCol [expr 18980.*$cm4]; # moment of Inertia about the minor axis
# Int column sections: HE700M
set AgintCol [expr 383*$cm2]; # cross-sectional area in (cm2)
set IyintCol [expr 329300.*$cm4]; # moment of Inertia about the major axis in (cm4)
set IzintCol [expr 18800.*$cm4]; # moment of Inertia about the minor axis
# girder sections: IPE330A
set AgGird [expr 62.61*$cm2]; # cross-sectional area in (cm2)
set IyGird [expr 11770.*$cm4]; # moment of Inertia about the major axis in (cm4)
set IzGird [expr 788.1*$cm4]; # moment of Inertia about the minor axis in (cm4)

# beam sections: IPE550 for 6th and 7th floors
set AgBeam6n7 [expr 134.4*$cm2]; #cross-sectional area in (cm2)
set IyBeam6n7 [expr 67120.*$cm4]; # moment of Inertia about the major axis in (cm4)
set IzBeam6n7 [expr 2668.*$cm4]; # moment of Inertia about the minor axis in (cm4)
# beam sections: IPE600 for 4th and 5th floors
set AgBeam4n5 [expr 156*$cm2]; #cross-sectional area in (cm2)
set IyBeam4n5 [expr 92080.*$cm4]; # moment of Inertia about the major axis in (cm4)
set IzBeam4n5 [expr 3387.*$cm4]; # moment of Inertia about the minor axis in (cm4)
#beam sections: IPE750x196 for 2nd and 3rd floors
set AgBeam2n3 [expr 250.80*$cm2]; #cross-sectional area in (cm2)
set IyBeam2n3 [expr 240300.*$cm4]; # moment of Inertia about the major axis in (cm4)
set IzBeam2n3 [expr 8175.*$cm4]; # moment of Inertia about the minor axis in (cm4)
#set matIDhard 1; # material numbers for recorder (this stressstrain recorder will be
blank, as this is an elastic section)
section Elastic $ColSecTagext $Es $AgextCol $IyextCol $IzextCol $Gs $J
section Elastic $ColSecTagint $Es $AgintCol $IyintCol $IzintCol $Gs $J
section Elastic $BeamSecTag2n3 $Es $AgBeam2n3 $IyBeam2n3 $IzBeam2n3 $Gs $J
section Elastic $BeamSecTag4n5 $Es $AgBeam4n5 $IyBeam4n5 $IzBeam4n5 $Gs $J
section Elastic $BeamSecTag6n7 $Es $AgBeam6n7 $IyBeam6n7 $IzBeam6n7 $Gs $J
section Elastic $GirdSecTag $Es $AgGird $IyGird $IzGird $Gs $J
#set matIDhard 1; # material numbers for recorder (this stressstrain recorder will be blank, as this
is an elastic section)
} elseif {$SectionType == "FiberSection"} {
# Define Material properties
#Method I_____
#steel 01 uniaxial material model/ bi-linear stress strain relationship
set Fy [expr 235*$MPa]; #yield stress of steel
set Es [expr 210*$GPa]; # Steel Young's Modulus
set nu 0.3;
set Gs [expr $Es/2./[expr 1+$nu]]; # Torsional stiffness Modulus
set Hiso 0; #isotropic hardening Modulus
set Hkin 1000; #kinematic hardening Modulus
set steel01 1; #unique material object for concentrated plasticity
#command
#uniaxialMaterial Steel01 $matTag $Fy $E0 $b <$a1 $a2 $a3 $a4>
#Where
#$matTag integer tag identifying material
#$Fy yield strength
#$E0 initial elastic tangent
#$b strain-hardening ratio (ratio between post-yield tangent and initial elastic tangent)
#$a1 isotropic hardening parameter, increase of compression yield envelope as proportion of yield
strength after a plastic strain of $a2*($Fy/E0). (optional)
#$a2 isotropic hardening parameter (see explanation under $a1). (optional).
#$a3 isotropic hardening parameter, increase of tension yield envelope as proportion of yield
strength after a plastic strain of $a4*($Fy/E0). (optional)
#$a4 isotropic hardening parameter (see explanation under $a3). (optional)

```

```

uniaxialMaterial Hardening $steel01 $Es $Fy $Hiso $Hkin; #considering bilinear stress-strain
condition
#Method II_____
#Giuffre-Monegotto-Pinto Material model/ Steel02 uniaxial material model
# Command:uniaxialMaterial Steel02 $matTag $Fy $E $b $R0 $cR1 $cR2 <$a1 $a2 $a3 $a4
$SIGINIT>
# -----
set steel02 2;          # unique integer tag identifying material object
set Fy [expr 235*$MPa]; # yield strength of Steel
set Es [expr 210*$GPa]; #initial elastic modulus of steel
set b 0.01;           # strain-hardening ratio (ratio between post-yield tangent and initial
elastic tangent)
set R0 18;            # Parameter to control the transition from elastic to plastic branches
set cR1 0.925;        # Parameter to control the transition from elastic to plastic branches
set cR2 0.15;         # Parameter to control the transition from elastic to plastic branches
set a1 0.1;           # $a1 isotropic hardening parameter, increase of compression yield
envelope as proportion of yield strength after a plastic strain of $a2*($Fy/E0). (optional)
set a2 1.0;           # $a2 isotropic hardening parameter (see explanation under $a1).
(optional default = 1.0).
set a3 0.1;           # $a3 isotropic hardening parameter, increase of tension yield envelope
as proportion of yield strength after a plastic strain of $a4*($Fy/E0). (optional default = 0.0)
set a4 1.0; # $a4 isotropic hardening parameter (see explanation under $a3). (optional default =
1.0)
set sigInit 0.3;      # $sigInit Initial Stress Value (optional, default: 0.0) the strain is
calculated from epsP=$sigInit/$E, #if (sigInit!= 0.0) { double epsInit = sigInit/E; eps = trialStrain+epsInit;
} else eps = trialStrain;
uniaxialMaterial Steel02 $steel02 $Fy $Es $b $R0 $cR1 $cR2 $a1 $a2 $a3 $a4; #considering
actual stress strain and ignoring initial residual stress

#To account for initial residual stress
set steel021 3
set steel022 4
set rs 0.3;           # rs = maximum residual stress value for h/b>=1.2
set resc [expr -($rs*$Fy)]; # negative residual stress at tip flange and central of web
set rest [expr $rs*$Fy];   # positive residual stress at flange centre and tip of web
set resab [expr (-$resc)+$rest]; # absolute value between negative and positive

uniaxialMaterial Steel02 $steel021 $Fy $E $b $R0 $cR1 $cR2 $a1 $a2 $a3 $a4 $rest
uniaxialMaterial Steel02 $steel022 $Fy $E $b $R0 $cR1 $cR2 $a1 $a2 $a3 $a4 $resc

#####
#      Element properties                                     #
#      Structural-Steel European I-section properties       #
#      column sections: HE600M,HE700M external and internal columns resp. #
#      Beam Sections:IPE330,IPE550,IPE600,IPE750x196      #
#####
#column section : HE600M : ExternalColumn on the xy plane frame
set h [expr 620.*$mm]; #depth
set bf [expr 305.*$mm]; #flange width
set tf [expr 40.*$mm]; #flange thickness
set tw [expr 21.*$mm]; #web thickness
set nfdw 20;          #number of fibers along dw
set nftw 2;           #number of fibers along tw
set nbf 15;           #number of fibers along bf
set nftf 4;           #number of fibers along tf
Isection $ColSecTagextFiber $steel02 $h $bf $tf $tw $nfdw $nftw $nbf $nftf
#column section : H700M: Internal Column

```

```

set h [expr 716.*$mm]; #depth
set bf [expr 304.*$mm]; #flange width
set tf [expr 40.*$mm]; #flange thickness
set tw [expr 21.*$mm]; #web thickness
set nfdw 20; #number of fibers along dw
set nftw 2; #number of fibers along tw
set nbf 15; #number of fibers along bf
set nftf 4; #number of fibers along tf
Isection $ColSecTagintFiber $steel02 $h $bf $tf $tw $nfdw $nftw $nbf $nftf

##### Beam sections: IPE550 ##### 6th and 7th floors
set h [expr 550.*$mm]; #depth
set bf [expr 210.*$mm]; #flange width
set tf [expr 17.2*$mm]; #flange thickness
set tw [expr 11.1*$mm]; #web thickness
set nfdw 20; #number of fibers along dw
set nftw 3; #umber of fibers along tw
set nbf 16; #number of fibers along bf
set nftf 4; #number of fibers along tf
Isection $BeamSecTag6n7Fiber $steel02 $h $bf $tf $tw $nfdw $nftw $nbf $nftf
##### Beam sections: IPE600 ##### 4th and 5th floors
set h [expr 600.*$mm]; #depth
set bf [expr 220.*$mm]; #flange width
set tf [expr 19.*$mm]; #flange thickness
set tw [expr 12.*$mm]; #web thickness
set nfdw 20; #number of fibers along dw
set nftw 3; #umber of fibers along tw
set nbf 15; #number of fibers along bf
set nftf 4; #number of fibers along tf
Isection $BeamSecTag4n5Fiber $steel02 $h $bf $tf $tw $nfdw $nftw $nbf $nftf
##### Beam sections: IPE750x196 ##### 2nd and 3rd floors
set h [expr 770.*$mm]; #depth
set bf [expr 268.*$mm]; #flange width
set tf [expr 25.4*$mm]; #flange thickness
set tw [expr 15.6*$mm]; #web thickness
set nfdw 30; #number of fibers along dw
set nftw 2; #umber of fibers along tw
set nbf 20; #number of fibers along bf
set nftf 4; #number of fibers along tf
Isection $BeamSecTag2n3Fiber $steel02 $h $bf $tf $tw $nfdw $nftw $nbf $nftf
##### Girder sections: IPE330 #####beams on the 1st and last bay of 3D frame
set h [expr 330.*$mm]; #depth
set bf [expr 160.*$mm]; #flange width
set tf [expr 11.5*$mm]; #flange thickness
set tw [expr 7.5*$mm]; #web thickness
set nfdw 16; #number of fibers along dw
set nftw 2; #umber of fibers along tw
set nbf 16; #number of fibers along bf
set nftf 4; #number of fibers along tf
Isection $GirderSecTagbay1n4Fiber $steel02 $h $bf $tf $tw $nfdw $nftw $nbf $nftf
# assign torsional Stiffness for 3D Model
uniaxialMaterial Elastic $SecTagTorsion $Ubig;#Assign large torsional stiffness
section Aggregator $ColSecTagext $SecTagTorsion T -section $ColSecTagextFiber
section Aggregator $ColSecTagint $SecTagTorsion T -section $ColSecTagintFiber
section Aggregator $BeamSecTag2n3 $SecTagTorsion T -section $BeamSecTag2n3Fiber
section Aggregator $BeamSecTag4n5 $SecTagTorsion T -section $BeamSecTag4n5Fiber
section Aggregator $BeamSecTag6n7 $SecTagTorsion T -section $BeamSecTag6n7Fiber
section Aggregator $GirdSecTag $SecTagTorsion T -section $GirderSecTagbay1n4Fiber

```

```

} else {
  puts "No section has been defined"
  return -1
}
#####
#           Define Elements
#####
#set up geometric transformations of element
#separate columns and beams, in case of P-Delta analysis for columns
set IDColTransf 1; # all columns
set IDBeamTransf 2; # all beams
set IDGirdTransf 3; # all girds
set ColTransfType Linear; # options for columns: Linear, PDelta, Corotational
#vecxzX vecxzY vecxzZ, are the X Y and Z components of the vector vecxz, which is the vector used to
define the local xz plane of the local coordinate system.
#The vector vecxz is a vector the user specifies that must not be parallel to the x-axis
#The local Y-axis can be defined as the cross product of the vector vecxz and the X- axis. i.e. Local Y-
axis=vecxz "X" X-axis
#command: geomtransf $transferType $transferTag $vecxzX $vecxzY $vecxzZ;
geomTransf $ColTransfType $IDColTransf 0 0 1;#[expr -cos($AlphaRad)] [expr -sin($AlphaRad)] 0 ;
# orientation of column stiffness affects bidirectional response.
geomTransf Linear $IDBeamTransf 0 0 1
geomTransf Linear $IDGirdTransf 1 0 0
#####
# Define Beam-Column Elements
#####
set numIntgrPts 5; #number of Gauss integration points for nonlinear curvature distribution i.e.
element subdivision
# columns parallel to y-axis
set N0col [expr 100-1]; #column element numbers
set level 0
#puts "ColumnID nodeI nodeJ AgextCol Es Gs IyextCol IzextCol J IDColTransf"
for {set frame 1} {$frame <=[expr $NbayZ+1]} {incr frame 1} {
  for {set level 1} {$level <=$Nstory} {incr level 1} {
    for {set pier 1} {$pier <=[expr $NbayX+1]} {incr pier 1} {
      if {$pier==1 || $pier==$NbayX+1} {
        set HE600M [expr 285.5*$Kg/$m];
        set ColumnIDext [expr $N0col +$level*$Dlevel + $frame*$Dframe+$pier]
        set nodeI [expr $level*$Dlevel + $frame*$Dframe+$pier]
        set nodeJ [expr ($level+1)*$Dlevel + $frame*$Dframe+$pier]
        element nonlinearBeamColumn $ColumnIDext $nodeI $nodeJ $numIntgrPts
$ColSecTagextFiber $IDColTransf; # columns mass density Kg/m
        #puts "$ColumnIDext $nodeI $nodeJ $AgextCol $Es $Gs $IyextCol $IzextCol $J
$IDColTransf"
      }
      if {$pier>=2 && $pier<=5} {
        set HE700M [expr 300.66*$Kg/$m]
        set ColumnIDint [expr $N0col +$level*$Dlevel + $frame*$Dframe+$pier]
        set nodeI [expr $level*$Dlevel + $frame*$Dframe+$pier]
        set nodeJ [expr ($level+1)*$Dlevel + $frame*$Dframe+$pier]
        element nonlinearBeamColumn $ColumnIDint $nodeI $nodeJ $numIntgrPts
$ColSecTagintFiber $IDColTransf; # columns
        #puts "$ColumnIDint $nodeI $nodeJ $AgintCol $Es $Gs $IyintCol $IzintCol $J
$IDColTransf"
      }
    }
  }
}
}
}

```

```

# Beams -- parallel to X-axis
set N0beam 1000; # beam element numbers
#puts "BeamID nodeI nodeJ AgBeam Es Gs IyBeam IzBeam J IDBeamTransf"
for {set frame 1} {$frame <=[expr $NbayZ+1]} {incr frame 1} {
  for {set bay 1} {$bay <= $NbayX} {incr bay 1} {
    for {set level 2} {$level <=[expr $Nstory+1]} {incr level 1} {
      if {$level==2||$level==3} {
        set mass23 [expr 196.88*$Kg/$m ]
        set BeamID23 [expr $N0beam +$level*$Dlevel + $frame*$Dframe+ $bay]
        set nodeI [expr $level*$Dlevel + $frame*$Dframe+ $bay]
        set nodeJ [expr $level*$Dlevel + $frame*$Dframe+ $bay+1]
        element nonlinearBeamColumn $BeamID23 $nodeI $nodeJ $numIntgrPts
$BeamSecTag2n3Fiber $IDBeamTransf;# beams
        #puts "$BeamID23 $nodeI $nodeJ $AgBeam2n3 $Es $Gs $IyBeam2n3 $IzBeam2n3 $J
$IDBeamTransf"
      }
      if {$level==4|| $level==5} {
        set mass45 [expr 122.46*$Kg/$m ]
        set BeamID45 [expr $N0beam +$level*$Dlevel + $frame*$Dframe+ $bay]
        set nodeI [expr $level*$Dlevel + $frame*$Dframe+ $bay]
        set nodeJ [expr $level*$Dlevel + $frame*$Dframe+ $bay+1]
        element nonlinearBeamColumn $BeamID45 $nodeI $nodeJ $numIntgrPts
$BeamSecTag4n5Fiber $IDBeamTransf;# beams
        #puts "$BeamID45 $nodeI $nodeJ $AgBeam4n5 $Es $Gs $IyBeam4n5 $IzBeam4n5 $J
$IDBeamTransf"
      }
      if {$level==6|| $level==7} {
        set mass67 [expr 105.5*$Kg/$m ]
        set BeamID67 [expr $N0beam +$level*$Dlevel + $frame*$Dframe+ $bay]
        set nodeI [expr $level*$Dlevel + $frame*$Dframe+ $bay]
        set nodeJ [expr $level*$Dlevel + $frame*$Dframe+ $bay+1]
        element nonlinearBeamColumn $BeamID67 $nodeI $nodeJ $numIntgrPts
$BeamSecTag6n7Fiber $IDBeamTransf;# beams
        #puts "$BeamID67 $nodeI $nodeJ $AgBeam6n7 $Es $Gs $IyBeam6n7 $IzBeam6n7 $J
$IDBeamTransf"
      }
    }
  }
}
set N0gird [expr 10000-1];#Girder Label
#puts "GirdID nodeI nodeJ AgGird Es Gs IyGird IzGird J IDGirdTransf"
for {set bay 1} {$bay <=$NbayZ} {incr bay } {
  for {set level 2} {$level <=$Nstory+1} {incr level } {
    for {set pier 1} {$pier <=$NbayX+1} {incr pier } {
      set nodeI [expr $level*$Dlevel + $bay*$Dframe+ $pier]
      set nodeJ [expr $level*$Dlevel + (1+$bay)*$Dframe+ $pier]
      if {($bay ==1 || $bay==4)} {
        set IPE330 [expr 42.97*$Kg/$m]
        set GirdID [expr $N0gird + $level*$Dlevel +$bay*$Dframe + $pier]
        element nonlinearBeamColumn $GirdID $nodeI $nodeJ $numIntgrPts
$GirderSecTagbay1n4Fiber $IDGirdTransf
        #puts "$GirdID $nodeI $nodeJ $AgGird $Es $Gs $IyGird $IzGird $J $IDGirdTransf"
      }
      if {($bay==2 || $bay==3) && ($level==2 || $level==3)} {
        set mass23 [expr 196.88*$Kg/$m ]
        set GirdID23 [expr $N0gird + $level*$Dlevel +$bay*$Dframe+ $pier]
        element nonlinearBeamColumn $GirdID23 $nodeI $nodeJ $numIntgrPts
$BeamSecTag2n3Fiber $IDGirdTransf
      }
    }
  }
}

```

```

#puts "$GirdID23 $nodeI $nodeJ $AgBeam2n3 $Es $Gs $IyBeam2n3 $IzBeam2n3 $J
$IDGirdTransf"
}
if {($bay==2 || $bay==3) && ($level==4 || $level==5)} {
set mass45 [expr 122.46*$Kg/$m ]
set GirdID45 [expr $N0gird + $level*$Dlevel + $bay*$Dframe+ $pier]
element nonlinearBeamColumn $GirdID45 $nodeI $nodeJ $numIntgrPts
$BeamSecTag4n5Fiber $IDGirdTransf;
#puts "$GirdID45 $nodeI $nodeJ $AgBeam4n5 $Es $Gs $IyBeam4n5 $IzBeam4n5 $J
$IDGirdTransf"
}
if {($bay==2 || $bay==3) && ($level==6 || $level==7)} {
set mass67 [expr 105.5*$Kg/$m ]
set GirdID67 [expr $N0gird + $level*$Dlevel + $bay*$Dframe + $pier]
element nonlinearBeamColumn $GirdID67 $nodeI $nodeJ $numIntgrPts
$BeamSecTag6n7Fiber $IDGirdTransf;
##puts "$GirdID67 $nodeI $nodeJ $AgBeam6n7 $Es $Gs $IyBeam6n7 $IzBeam6n7 $J
$IDGirdTransf"
}
}
}
}
puts "End of Define Model Geometry"
##### Assignment of Nodal Masses #####
for {set frame 1} {$frame <= [expr $NbayZ+1]} {incr frame 1} {
for {set level 2} {$level <= [expr $Nstory+1]} {incr level 1} {
for {set pier 1} {$pier <= [expr $NbayX+1]} {incr pier 1} {
set nodeID [expr $frame*$Dframe+$level*$Dlevel+$pier*$Dpier]
if {($level==2) && ($frame==1||$frame==5)} {
set M215 [expr 1767.58*$Kg/$m];#xy frame
if {$pier == 1 || $pier == $NbayX+1} {
mass $nodeID [expr $M215*3.5] 0 [expr $M215*3.5] 0 0 0
}
if {$pier==2||$pier==5} {
mass $nodeID [expr $M215*6.5] 0 [expr $M215*6.5] 0 0 0
}
if {$pier==3||$pier==4} {
mass $nodeID [expr $M215*5.5] 0 [expr $M215*5.5] 0 0 0
}
}
if {($level==3)&&($frame==1||$frame==5)} {
set M315 [expr 1743.33*$Kg/$m]
if {$pier == 1 || $pier == $NbayX+1} {
mass $nodeID [expr $M315*3.5] 0 [expr $M315*3.5] 0 0 0
}
if {$pier==2||$pier==5} {
mass $nodeID [expr $M315*6.5] 0 [expr $M315*6.5] 0 0 0
}
if {$pier==3||$pier==4} {
mass $nodeID [expr $M315*5.5] 0 [expr $M315*5.5] 0 0 0
}
}
if {($level==4||$level==5)&&($frame==1 ||$frame==5)} {
set M45n15 [expr 1668.01*$Kg/$m]
if {$pier == 1 || $pier == $NbayX+1} {
mass $nodeID [expr $M45n15*3.5] 0 [expr $M45n15*3.5] 0 0 0
}
if {$pier==2||$pier==5} {

```

```

mass $nodeID [expr $M45n15*6.5] 0 [expr $M45n15*6.5] 0 0 0
}
if {$pier==3||$pier==4} {
mass $nodeID [expr $M45n15*5.5] 0 [expr $M45n15*5.5] 0 0 0
}
}
if {($level==6)&&($frame==1||$frame==5)} {
set M615 [expr 1650.84*$Kg/$m]
if {$pier == 1 || $pier == $NbayX+1} {
mass $nodeID [expr $M615*3.5] 0 [expr $M615*3.5] 0 0 0
}
if {$pier==2||$pier==5} {
mass $nodeID [expr $M615*6.5] 0 [expr $M615*6.5] 0 0 0
}
if {$pier==3||$pier==4} {
mass $nodeID [expr $M615*5.5] 0 [expr $M615*5.5] 0 0 0
}
}
if {($level==7)&&($frame==1||$frame==5)} {
set M715 [expr 1472.18*$Kg/$m]
if {$pier == 1 || $pier == $NbayX+1} {
mass $nodeID [expr $M715*3.5] 0 [expr $M715*3.5] 0 0 0
}
if {$pier==2||$pier==5} {
mass $nodeID [expr $M715*6.5] 0 [expr $M715*6.5] 0 0 0
}
if {$pier==3||$pier==4} {
mass $nodeID [expr $M715*5.5] 0 [expr $M715*5.5] 0 0 0
}
}
}
if {($level==2)&&($frame>=2&&$frame<=4)} {
set M2nd234 [expr 7070/2.*$Kg/$m]
if {$pier == 1 || $pier == $NbayX+1} {
mass $nodeID [expr $M2nd234*3.5] 0 [expr $M2nd234*3.5] 0 0 0
}
if {$pier==2||$pier==5} {
mass $nodeID [expr $M2nd234*6.5] 0 [expr $M2nd234*6.5] 0 0 0
}
if {$pier==3||$pier==4} {
mass $nodeID [expr $M2nd234*5.5] 0 [expr $M2nd234*5.5] 0 0 0
}
}
}
if {($level==3)&&($frame>=2&&$frame<=4)} {
set M3rd234 [expr 6973/2.*$Kg/$m]
if {$pier == 1 || $pier == $NbayX+1} {
mass $nodeID [expr $M3rd234*3.5] 0 [expr $M3rd234*3.5] 0 0 0
}
if {$pier==2||$pier==5} {
mass $nodeID [expr $M3rd234*6.5] 0 [expr $M3rd234*6.5] 0 0 0
}
if {$pier==3||$pier==4} {
mass $nodeID [expr $M3rd234*5.5] 0 [expr $M3rd234*5.5] 0 0 0
}
}
}
if {($level==4||$level==5)&&($frame>=2&&$frame<=4)} {
set M45th234 [expr 6672/2.*$Kg/$m]
if {$pier == 1 || $pier == $NbayX+1} {
mass $nodeID [expr $M45th234*3.5] 0 [expr $M45th234*3.5] 0 0 0
}
}
}

```

```

    }
    if {$pier==2||$pier==5} {
        mass $nodeID [expr $M45th234*6.5] 0 [expr $M45th234*6.5] 0 0 0
    }
    if {$pier==3||$pier==4} {
        mass $nodeID [expr $M45th234*5.5] 0 [expr $M45th234*5.5] 0 0 0
    }
}
if {($level==6)&&($frame>=2&&$frame<=4)} {
    set M6th234 [expr 6603/2.*$Kg/$m]
    if {$pier == 1 || $pier == $NbayX+1} {
        mass $nodeID [expr $M6th234*3.5] 0 [expr $M6th234*3.5] 0 0 0
    }
    if {$pier==2||$pier==5} {
        mass $nodeID [expr $M6th234*6.5] 0 [expr $M6th234*6.5] 0 0 0
    }
    if {$pier==3||$pier==4} {
        mass $nodeID [expr $M6th234*5.5] 0 [expr $M6th234*5.5] 0 0 0
    }
}
if {($level==7)&&($frame>=2&&$frame<=4)} {
    set M7th234 [expr 5889/2.*$Kg/$m]
    if {$pier == 1 || $pier == $NbayX+1} {
        mass $nodeID [expr $M7th234*3.5] 0 [expr $M7th234*3.5] 0 0 0
    }
    if {$pier==2||$pier==5} {
        mass $nodeID [expr $M7th234*6.5] 0 [expr $M7th234*6.5] 0 0 0
    }
    if {$pier==3||$pier==4} {
        mass $nodeID [expr $M7th234*5.5] 0 [expr $M7th234*5.5] 0 0 0
    }
}
}
}
}
set dataDir modes
file mkdir $dataDir;
set numModes $Nstory
for {set k 1} {$k <= $numModes} {incr k} {
    set period "modes/Periods.txt"
    #recorder Node -file [format "modes/mode%i.out" $k] -nodeRange 211 756 -dof 1 "eigen $k"
}
#perform eigen analysis
set lambda [eigen $numModes];
# calculate frequencies and periods of the structure
set omega {}
set f {}
set T {}

foreach lam $lambda {
    lappend omega [expr sqrt($lam)]
    lappend f [expr sqrt($lam)/(2*$PI)]
    lappend T [expr (2*$PI)/sqrt($lam)]
}

puts "periods are $T"
#write the output file consisting of periods
set period "modes/Periods.txt"

```

```

set Periods [open $period "w"]
foreach t $T {
  puts $Periods " $t"
}
close $Periods

#####
#           Define Recorders                                     #
#####
set FreeNodeID [expr $NFrame*$Dframe+($Nstory+1)*$Dlevel+($NbayX+1)]; # ID: free node
set SupportNodeFirst [lindex $iSupportNode 0]; # ID: first support node
set SupportNodeLast [lindex $iSupportNode [expr [length $iSupportNode]-1]]; # ID: last support
node
set FirstColumn [expr $N0col + 1*$Dframe+1*$Dlevel +1]; # ID: first column
#set dataDir Results
set dataDir 6Story3DPush
file mkdir $dataDir
recorder Node -file $dataDir/DFree.out -time -node $FreeNodeID -dof 3 disp; #
displacements of free node
recorder Node -file $dataDir/DBase.out -time -nodeRange $SupportNodeFirst $SupportNodeLast -dof 1
disp; # displacements of support nodes
recorder Node -file $dataDir/RBase.out -time -nodeRange $SupportNodeFirst $SupportNodeLast -dof 3
reaction; # support reaction
recorder Drift -file $dataDir/DrNode.out -time -iNode $SupportNodeFirst -jNode $FreeNodeID -dof 1 -
perpDirn 2; # lateral drift
recorder Element -file $dataDir/Fel1.out -time -ele $FirstColumn localForce; #
element forces in local coordinates
recorder Element -file $dataDir/ForceEle1sec1.out -time -ele $FirstColumn section 1 force;
# section forces, axial and moment, node i (1st col. is Axial force and 3 columns are moments in Z,X and
Y axes resp.)
recorder Element -file $dataDir/DefoEle1sec1.out -time -ele $FirstColumn section 1 deformation;
# section deformations, axial and curvature, node i
recorder Element -file $dataDir/ForceEle1sec$numIntgrPts.out -time -ele $FirstColumn section
$numIntgrPts force; # section forces, axial and moment, node j
recorder Element -file $dataDir/DefoEle1sec$numIntgrPts.out -time -ele $FirstColumn section
$numIntgrPts deformation; # section deformations, axial and curvature, node j
set yFiber [expr 0.]; # fiber location for stress-
strain recorder, local coords
set zFiber [expr 0.]; # fiber location for stress-
strain recorder, local coords
recorder Element -file $dataDir/SSEle1sec1.out -time -ele $FirstColumn section $numIntgrPts fiber
$yFiber $zFiber stressStrain; # steel fiber stress-strain, node i
# Distribution of Lateral Loads for Pushover Analysis
# Uniform Distribution based on mass regardless of story height and Modal distribution based on first
eigen mode
# calculate distribution of lateral load based on mass/weight distributions along building height
## Fi = (mi)(phi) for both cases
#Lateral Distribution of Mass to each stories
#Uniform Pattern
#set iFj(6) [expr 1*[expr 365.101*$KN]]; #normalized displacement of roof/eigenvector for mode 1
of roof
#set iFj(5) [expr 1*[expr 409.408*$KN]]; #normalized displacement of 5th story /eigenvector for
mode 1 of the 5th story
#set iFj(4) [expr 1*[expr 413.665*$KN]];
#set iFj(3) [expr 1*[expr 413.665*$KN]];
#set iFj(2) [expr 1*[expr 432.345*$KN]];
#set iFj(1) [expr 1*[expr 438.359*$KN]];
#Triangular Pattern
#set iFj(6) [expr 1.000*[expr 365.101*$KN]];

```

```

#set iFj(5) [expr 0.837*[expr 409.408*$KN]];
#set iFj(4) [expr 0.674*[expr 413.665*$KN]];
#set iFj(3) [expr 0.512*[expr 413.665*$KN]];
#set iFj(2) [expr 0.349*[expr 432.345*$KN]];
#set iFj(1) [expr 0.186*[expr 438.359*$KN]];
##Modal Pattern
set iFj(6) [expr 1.000*[expr 365.101*$KN]]; #normalized displacement of roof/eigenvector for mode 1
of roof
set iFj(5) [expr 0.871*[expr 409.408*$KN]]; #normalized displacement of 5th story /eigenvector for
mode 1 of the 5th story
set iFj(4) [expr 0.710*[expr 413.665*$KN]];
set iFj(3) [expr 0.484*[expr 413.665*$KN]];
set iFj(2) [expr 0.290*[expr 432.345*$KN]];
set iFj(1) [expr 0.129*[expr 438.359*$KN]];
## create node and load vectors for lateral-load distribution in static analysis
set iFPush ""
set iNodePush ""
for {set level 2} {$level <=[expr $Nstory+1]} {incr level 1} {
    set FPush [expr $iFj([expr ($level-1)])]; #totalmass*#lateral load coefficient
    set MasterNodeID [expr 9900+$level]; #lateral loads need to be applied only to the master nodes
of the rigid diaphragm at each floor
    lappend iNodePush $MasterNodeID
    lappend iFPush $FPush
    #puts $FPush
    #puts $MasterNodeID
}
#####
#####
# Define Gravity load applied to beams -- eleLoad applies loads in local coordinate axis #
#####
#####
pattern Plain 22 Linear {
    for {set level 2} {$level <=[expr $Nstory]} {incr level 1} {
set MasterNodeID [expr 9900+$level];
#####Define imperfection loads #####
        set phi_0 [expr 1/200.];#basic value for global imperfection
        if {[expr 2/pow($HBuilding,0.5)]>=[expr 2/3.]}&&([expr 2/pow($HBuilding,0.5)]<=1.) {
            set alpha_h [expr 2./pow($HBuilding,0.5)]; #reduction factor for height
        } elseif {[expr 2./pow($HBuilding,0.5)]<[expr 2/3.]} {
            set alpha_h [expr 2/3.]
        } elseif {[expr 2./pow($HBuilding,0.5)]>1. } {
            set alpha_h 1.
        }
        set nColineX [expr ($NbayX+1)];#nColine is the number of columns in a row to X direction
which is m in the code
        set alpha_mX [expr pow((0.5*(1.+1./$nColineX)),0.5)];#reduction factor for number of column
lines
        set imperfectionX [expr $phi_0*$alpha_h*$alpha_mX]
        set nColineZ [expr ($NbayZ+1)];#nColine is the number of columns in a row which is m in the
code
        set alpha_mZ [expr pow((0.5*(1.+1./$nColineZ)),0.5)];#reduction factor for number of column
lines
        set imperfectionZ [expr $phi_0*$alpha_h*$alpha_mZ]
#####Apply imperfection loads at each story #####
        #Apply Equivalent geometric imperfections to each orthogonal directions independently
        #Global Sway imperfections to the X direction
        if {$level==2} {

```

```

load $MasterNodeID [expr $ImperfectionX*24224.64*$KN] 0 0 0 0 0;#imperfection to the x
direction
} elseif {$level==3} {
load $MasterNodeID [expr $ImperfectionX*19946.64*$KN] 0 0 0 0 0;#imperfection to the x
direction
} elseif {$level==4} {
load $MasterNodeID [expr $ImperfectionX*15705.84*$KN] 0 0 0 0 0;#imperfection to the x
direction
} elseif {$level==5} {
load $MasterNodeID [expr $ImperfectionX*11651.04*$KN] 0 0 0 0 0;#imperfection to the x
direction
} elseif {$level==6} {
load $MasterNodeID [expr $ImperfectionX*7596.24*$KN] 0 0 0 0 0;#imperfection to the x direction
} elseif {$level==7} {
load $MasterNodeID [expr $ImperfectionX*3578.64*$KN] 0 0 0 0 0;#imperfection to the x direction
}
#Global Sway imperfections to the Z direction
#if {$level==2} {
#load $MasterNodeID 0 0 [expr $ImperfectionZ*24224.64*$KN] 0 0 0;#imperfection to the z
direction
#} elseif {$level==3} {
#load $MasterNodeID 0 0 [expr $ImperfectionZ*19946.64*$KN] 0 0 0;#imperfection to the z
direction
#} elseif {$level==4} {
#load $MasterNodeID 0 0 [expr $ImperfectionZ*15705.84*$KN] 0 0 0;#imperfection to the z
direction
#} elseif {$level==5} {
#load $MasterNodeID 0 0 [expr $ImperfectionZ*11651.04*$KN] 0 0 0;#imperfection to the z
direction
#} elseif {$level==6} {
#load $MasterNodeID 0 0 [expr $ImperfectionZ*7596.24*$KN] 0 0 0;#imperfection to the z
direction
#} elseif {$level==7} {
#load $MasterNodeID 0 0 [expr $ImperfectionZ*3578.64*$KN] 0 0 0;#imperfection to the z
direction
#}
}
# Gravity Loads Assigned to beams on each floor
for {set frame 1} {$frame <=[expr $NbayZ+1]} {incr frame 1} {
for {set level 2} {$level <=[expr $Nstory+1]} {incr level 1} {
for {set bay 1} {$bay <= $NbayX} {incr bay 1} {
set elemID [expr $NObeam + $level*$Dlevel + $frame*$Dframe+ $bay]
if {$level==2 && ($frame==1 || $frame==5)} {
set Wt2 [expr 17.3399*$KN/$m ];#self weight (N/m)
eleLoad -ele $elemID -type -beamUniform -$Wt2 0; # UDL on BEAMS
}
if {$level==2 && ($frame>=2 && $frame<=4)} {
set Wt2 [expr 34.6799*$KN/$m ]
eleLoad -ele $elemID -type -beamUniform -$Wt2 0;
}
if {$level==3 && ($frame==1 || $frame==5)} {
set Wt3 [expr 17.102*$KN/$m ];#self weight (N/m)
eleLoad -ele $elemID -type -beamUniform -$Wt3 0;
}
if {$level==3 && ($frame>=2 && $frame<=4)} {
set Wt3 [expr 34.2041*$KN/$m ]
eleLoad -ele $elemID -type -beamUniform -$Wt3 0;
}
}
}
}

```

```

if {($level==4||$level==5) && ($frame==1 || $frame==5)} {
set Wt45 [expr 16.3631*$KN/$m ];
eleLoad -ele $elemID -type -beamUniform -$Wt45 0;
}
if {($level==4||$level==5) && ($frame>=2 && $frame<=4)} {
set Wt45 [expr 32.7263*$KN/$m ]
eleLoad -ele $elemID -type -beamUniform -$Wt45 0;
}
if {($level==6) && ($frame==1 || $frame==5)} {
set Wt6 [expr 16.1947*$KN/$m ];
eleLoad -ele $elemID -type -beamUniform -$Wt6 0;
}
if {($level==6) && ($frame>=2 && $frame<=4)} {
set Wt6 [expr 32.3895*$KN/$m ]
eleLoad -ele $elemID -type -beamUniform -$Wt6 0;
}
if {$level==7 && ($frame==1 || $frame==5)} {
set Wt7 [expr 14.4421*$KN/$m ];
eleLoad -ele $elemID -type -beamUniform -$Wt7 0;
}
if {$level==7 && ($frame>=2 && $frame<=4)} {
set Wt5 [expr 28.8842*$KN/$m ]
eleLoad -ele $elemID -type -beamUniform -$Wt5 0;
#puts $Wt5
}
}
}
}
}

#Apply gravity load, set it constant and reset time to zero, load pattern has already been defined
#Gravity-analysis parameters -- load-controlled static analysis
variable constraintsTypeGravity Plain; #default;
if {[info exists RigidDiaphragm] == 1} {
if {$RigidDiaphragm=="ON"} {
variable constraintsTypeGravity Transformation; #large model: try Transformation,small model try
Lagrange
}; #if rigid diaphragm is on
}; #if rigid diaphragm exists
constraints $constraintsTypeGravity; #how it handles boundary conditions
numberer RCM; #renumber dof's to minimize band-width (optimization), if
you want to
set Tol 1.0e-8; #convergence tolerance for test
system BandGeneral; #how to store and solve the system of equations in the
analysis (large model: try UmfPack)
test EnergyIncr $Tol 10; #determine if convergence has been achieved at the end of
an iteration step
algorithm Newton; #use Newton's solution algorithm: updates tangent stiffness at
every iteration
set NstepGravity 10; #apply gravity in 10 steps
set DGravity [expr 1./$NstepGravity]; #first load increment;
integrator LoadControl $DGravity; #determine the next time step for an analysis
analysis Static; #define type of analysis static or transient
analyze $NstepGravity; #apply gravity
# ----- maintain constant gravity loads and reset time to zero-----
loadConst -time 0.0
# -----
puts "Model Built"

```